

Southern Methodist University

SMU Scholar

Economics Theses and Dissertations

Economics

Spring 5-11-2024

Essays on the Application and Improvement of the Geographical Economics Models to Policy Analysis: The Case of Road Infrastructure in Central America

Ignacio Penagos

Southern Methodist University, ipenagos@smu.edu

Follow this and additional works at: https://scholar.smu.edu/hum_sci_economics_etds



Part of the [Central American Studies Commons](#), [Economic Policy Commons](#), [Economics Commons](#), and the [Other Geography Commons](#)

Recommended Citation

Penagos, Ignacio, "Essays on the Application and Improvement of the Geographical Economics Models to Policy Analysis: The Case of Road Infrastructure in Central America" (2024). *Economics Theses and Dissertations*. 22.

https://scholar.smu.edu/hum_sci_economics_etds/22

This Thesis is brought to you for free and open access by the Economics at SMU Scholar. It has been accepted for inclusion in Economics Theses and Dissertations by an authorized administrator of SMU Scholar. For more information, please visit <http://digitalrepository.smu.edu>.

ESSAYS ON THE APPLICATION AND IMPROVEMENT OF THE GEOGRAPHICAL
ECONOMICS MODELS TO POLICY ANALYSIS: THE CASE OF ROAD
INFRASTRUCTURE IN CENTRAL AMERICA

Approved by:

Dr. Omer Ozak
Associate Professor

Dr. Klaus Desmet
Professor

Dr. Rocío Madera
Assistant Professor

ESSAYS ON THE APPLICATION AND IMPROVEMENT OF THE GEOGRAPHICAL
ECONOMICS MODELS TO POLICY ANALYSIS: THE CASE OF ROAD
INFRASTRUCTURE IN CENTRAL AMERICA

A Dissertation Presented to the Graduate Faculty of the
Dedman College
Southern Methodist University
in
Partial Fulfillment of the Requirements
for the degree of
Doctor of Philosophy
with a
Major in Economics
by
Ignacio Penagos Montoya

B.S., Economics, Pontificia Universidad Javeriana
M.A., Economics, Pontificia Universidad Javeriana
M.A., Economics, Southern Methodist University

May 11, 2024

Copyright (2024)

Ignacio Penagos Montoya

All Rights Reserved

ACKNOWLEDGMENTS

Several persons and institutions made this research and the whole Ph.D. experience possible. I'm deeply grateful to my wife, Juliana, who chose to join me during all this time. None of this could have been possible without her emotional support, patience, and love in the challenging and happy moments. I'm grateful to my mom, who always believed in me and supported the early stages of the path that has come to this end. I'm thankful to my friends and family, who offered constant emotional and financial support. Sergio, Astrid, Ariana, Agustin, Luis, Karen, and Juanita are among them. Also, I'm grateful to my former students who became family, Sofía, María Sofía, Laura, Anita, and María. I'm also obligated to my new Dallas family, Omer, Judith, Andres, Diana, and Alejandro. I'm thankful to my advisors, Omer, Klaus, and Rocío, who had the patience to guide me during this project and managed to make me give the best I could. I'm thankful to all my fellow Ph.D. students, the SMU economics department faculty, and collaborators for all their comments and support during this time that contributed to the quality of this research. Regarding institutions, I must thank the Pontificia Universidad Javeriana for allowing me to come to the USA and pursue a Ph.D. To all the PUJ Economics Department faculty, Andres, Andres Felipe, Gonzalo, Luz Karime, Silvia, and many others who supported this plan. Finally, I'm obligated to the Inter-American Development Bank transportation and integration group, Mauro Alem and Julio Elías, who provided crucial time, data, comments, and funding to this research. Lastly, I want to thank Colfuturo, who provided financial support during the first years of this endeavor.

Penagos Montoya, Ignacio

B.S., Economics, Pontificia Universidad Javeriana
M.A., Economics, Pontificia Universidad Javeriana
M.A., Economics, Southern Methodist University

Essays on the Application and Improvement of the Geographical
Economics Models to Policy Analysis: The Case of Road
Infrastructure in Central America

Advisor: Dr. Omer Ozak

Doctor of Philosophy degree conferred May 11, 2024

Dissertation completed April 15, 2024

The novel models of Geographical Economy have analyzed the effects on the distribution of economic activity over the area of a given region, generated by different socio-economic shocks. For example, the costs of migrating from one place to another, as shown in Desmet et al. (2018). A key advantage of such models is that, given the structural definition of the market interactions, they can first create counterfactual scenarios based on the economic fundamentals. And second, a broad set of variables can account for that impact. These dynamic spatial general equilibrium models embody features such as measures for amenities, trade and transportation costs, productivity, and GDP that allow for multiple applications and uses. One of those is the design and evaluation of specific policies, such as the investment in infrastructure. This dissertation analyzes the application of the model to the case of the Pacific Corridor. It is a highway from Mexico City to Panamá City, passing through six countries over 1.300 miles. This corridor is critical to the economic integration of that region. Desmet et al. (2018) model can account for the potential benefits of improving such infrastructure. In the first chapter, I show how to adapt the model to create the necessary counterfactuals. The benefits are favorable for the locations near the project. In the second chapter, I introduce an improvement to the model's transportation costs matrix. It consists of the possibility to account for the effects of the administrative border controls (customs)

on transportation costs. I used data on travel times in five regional countries to calibrate the model's matrix. It matches the observed increase in transportation time cost due to border delays. The impact of removing such delay is more significant than the effect of the corridor on economic activity. Finally, I provide policy recommendations and the future steps of this research.

TABLE OF CONTENTS

LIST OF FIGURES	ix
LIST OF TABLES	xi
CHAPTER	
1 A Complementary Methodology to Perform Project Evaluations in Latin America	1
1.1. Introduction	1
1.2. Central America and The Pacific Corridor	7
1.3. The Model	11
1.3.1. Location of Each Economy	13
1.3.2. Preferences and Consumer's Choices	13
1.3.3. Technology and Firms	15
1.3.4. Prices, Export Probability, and Trade Balance	17
1.3.5. Equilibrium	18
1.4. Calibration, Data, and Counterfactuals	18
1.4.1. Data and Calibration	19
1.4.2. Counterfactuals	25
1.5. Results	28
1.5.1. Stage I: Using the World, Analyzing the Region	30
1.5.1.1. Growth and Income Distribution	35
1.5.2. Stage II: Restricted Simulations	38
1.5.2.1. Robustness check: Increasing the Cost of Water Transport	41
1.5.2.2. Welfare and Annualized Returns	44
1.6. Conclusions	46

2	Quantifying the Border Effect: A Simulation Approach	48
2.1.	Introduction	48
2.2.	Transport Costs and Border Effect: Theory	54
2.2.1.	The Iceberg Costs.....	54
2.2.2.	Iceberg Costs and The Border Effect.....	55
2.2.3.	From Allen & Arkolakis (2014) to Desmet et al. (2018)	58
2.2.4.	Adding the Border Effect in the Instantaneous Trade Costs	62
2.3.	Calibrating The Border Effect	64
2.4.	Results	76
2.5.	Conclusions	89
APPENDIX		
A	Additional Parameters of the Model	91

LIST OF FIGURES

Figure	Page
1.1 Pacific Corridor Approximate Project Location	7
1.2 The Current Pacific Corridor Reality	11
1.3 Cells of Central America	24
1.4 Chosen Cells to Treatment	25
1.5 Instantaneous Costs Comparison Across Counterfactuals	26
1.6 Sub-cell Example: Crossing the cell.....	27
1.7 Initial Distribution of Population in Central America	29
1.8 Impact on Productivity	30
1.9 Impact on Population	31
1.10 Impact on Total Trade Shares	32
1.11 Impact on GDP per capita	32
1.12 Impact on Utility	33
1.13 Comparative Effects of the Project Cells.....	34
1.14 GDP per capita distribution After 100 Years.....	36
1.15 GDP Geographic Distribution Impact	37
1.16 Economic Growth effects	38
1.17 Productivity and Population, Stage II	39
1.18 GDP per capita and Trade Shares, Stage II.....	40
1.19 Impact on Utility, Stage II	40

1.20	Productivity and Population, Stage III	42
1.21	Trade Shares and GDP per capita, Stage III	43
1.22	Impact on Utility, Stage III	44
2.1	Location of the Included Border Crossing Controls	67
2.2	Benchmark Observed Travel Time Reduction When Removing Borders	68
2.3	Benchmark Observed Travel Time Chart	70
2.4	First Calibration Exercise	72
2.5	Second Calibration Exercise	73
2.6	Third Calibration Exercise	74
2.7	Fourth Calibration Exercise	75
2.8	Productivity Under the Three Counterfactuals	80
2.9	Population Net Flows Under the Three Counterfactuals	82
2.10	Trade Shares Under the Three Counterfactuals	84
2.11	Real GDP per Capita index Under the Three Counterfactuals	85
2.12	Utility Under the Three Counterfactuals	87

LIST OF TABLES

Table		Page
1.1	Trade Value Comparison	8
1.2	Total Trade Change Between 2000 and 2022	9
1.3	Intra-Regional Trade Share Comparison	10
1.4	Allen and Arkolakis (2014) Parameters	22
1.5	Country Welfare Impact.....	45
1.6	Costs, Investment and Annualized Returns	46
2.1	Average Border Time Delay Freight (Hours)	49
2.2	Border Time Delay Freight (Hours).....	50
2.3	Calibration Exercise Output Summary	76
2.4	Calibration Exercise Correlations	76
2.5	Aggregate Impact	88
A.1	Parameters from Desmet et al. (2018)	91

To my wife and mom, there is always time to pursue our dreams.

CHAPTER 1

A Complementary Methodology to Perform Project Evaluations in Latin America

1.1. Introduction

When a significant infrastructure project is presented, for example, a new highway connecting a pair of remote cities, the discussion of its convenience typically involves rates of return, engineering concerns, national or regional debt, and the effect on economic aggregates. For example, The Pacific Corridor in Central America is a project that upgrades an existing road to US interstate highway standards to improve the travel time between Mexico City and Panama City. It has been planned since the onset of the twenty-first century, and currently, only 30% of it has been executed. The main difficulties regarding the execution of this project are the fiscal restrictions, financing, and debt of each country in the region. That discussion usually ignores a fundamental consequence of those big projects, the possible responses of the inhabitants of a region due to the shift in geography, and the accessibility to transportation methods and markets. An agent's decision of where to reside depends on a location's productivity, amenities, and market access. How do infrastructure projects affect individuals' choices of where to live and work? In particular, how does the Pacific Corridor affect individual's decisions of where to live and work in Central America, impacting the distribution of economic activity across the space?

To answer these questions there exist a set of methods and techniques. Following [Davis \(1990\)](#) and [Bernal and Peña \(2011\)](#), those methods can be divided into two main categories: the project or ex-ante evaluation and the impact or ex-post evaluation. The first category refers to models, methods, or techniques that attempt to address the impact of a given project or policy before it is constructed or implemented. The second category explores

the impact of a project or a policy in the aftermath of its construction or execution. In summary, while the first tries to forecast the impact of some variable of interest reasonably, the second attempts to set the best measurements of the observed effects. Both categories use counterfactuals to compare against a baseline and then derive a measurement of the impact. Establishing or selecting a reasonable counterfactual and baseline is fundamental to obtaining accurate impact measures in both cases. Such counterfactuals and baselines regarding big infrastructure projects involving multiple countries are difficult to find. Therefore, this research contributes to proposing a novel application to the impact evaluation of infrastructure using the spatial dynamic general equilibrium model of [Desmet et al. \(2018\)](#), which can analyze counterfactuals given its detailed geographical information.

The geographic economic model of [Desmet et al. \(2018\)](#) is characterized by its ability to account for economic activity's spatial distribution. It also embeds a detailed geographic representation of the world that permits the creation of reasonable baselines and counterfactuals for infrastructure projects of considerable size. These characteristics are central to performing any impact or project evaluation. In addition, its dynamic representation of technology and its diffusion allows the simulation of a set of output variables, such as the GDP, into long time horizons. One of the key advantages of this framework is its exogenous modeling of trade costs. It comprises a multimodal trade costs matrix based on accessibility to different transportation modes. That feature permits the recreation of counterfactuals regarding transportation infrastructure by altering the accessibility of a particular transportation mode. Thus, this model provides an excellent framework to evaluate the impacts of the Pacific Corridor and give answers to the questions posted above.

The Pacific Corridor is a highway that connects Puebla in the south of Mexico with Panama City in Panama, with an approximate distance of eighteen hundred miles. This highway is a section of the Pan-American Highway and passes through five countries in Central America. It is vital to the logistics and commerce integration for those countries.

At the beginning of the 2000's decade, Mexico, Guatemala, Belize, Honduras, El Salvador, Nicaragua, Costa Rica, and Panama created the Meso-America Plan. This project considered updating the Pacific Corridor to a US-standard highway with two lanes in each direction, expecting to boost the regional economy by integrating market accessibility. According to the Inter-American Development Bank (IADB), the total investment amount to build the project is about \$5.3 billion US dollars. However, only Mexico and Panama have built their sections of the highway. Other countries have to pay for the maintenance of the old road. Therefore, most of the project is still on paper. Given its size, it is a large-scale infrastructure project, and will make a good fit for the proposed methodology.

The effects of large-scale infrastructure projects are commonly related to economic integration of regions by connecting markets and increasing trade. For example, [Donaldson \(2018\)](#) examined the effect of an extensive railroad system built up by the British colonial government across the Indian subcontinent. This project connected today's Pakistan, India, and Bangladesh. The historical evidence shows that it boosted trade and welfare gains related to improvements in commerce. The accessibility to roads and markets has heterogeneous effects depending on income levels of each location, as suggested by [Jedwab and Storeygard \(2022\)](#). They show that in Sub-Saharan Africa, distant road construction's impact on market access is stronger for small and remote cities than politically favored regions. According to this evidence, it is expected that the Pacific Corridor could increase regional integration, access to the markets, and, ultimately, increase trade. However, as suggested by [Jedwab and Storeygard \(2022\)](#), the increase in trade could also incentivize migration to more productive areas, which means urban areas. As shown below, Central America is characterized by a high concentration of its population in urban areas, mainly in the capital cities. Then, this project could potentially move population towards such regions, increasing the demand for amenities and generating congestion. This aspect is not considered in the "Puebla-Panama Plan," and is central to the population's welfare.

Assuming that the totality of the Pacific Corridor is still to be built, and using [Desmet et al. \(2018\)](#) model, I find a positive but limited effect of this infrastructure. The reduction in trade costs across the locations in the project’s neighborhood drives these benefits. Such a reduction incentivizes the agglomeration forces of productivity, particularly in locations such as Mexico City’s neighboring areas, where productivity was initially high. This agglomeration force attracts the population and increases the trade shares, positively affecting GDP per capita. The long-run trends of the region, like economic growth and income distribution, are not significantly affected by this project. After running some robustness checks, the simulations suggest that the positive effect of the Pacific Corridor is partially due to its connections to essential transportation networks in the south of Mexico. Finally, following [Allen and Arkolakis \(2014\)](#) welfare calculation, the annualized returns of the Pacific Corridor are approximately 4.8%, which is around two times bigger than a comparable measure using cost-benefit analysis, according to the Inter-American Development Bank (IADB).

This research is related to the extensive literature that performs infrastructure project evaluations. Many economic-based models, accounting techniques, or methodologies incorporating different disciplines attempt to measure the impact of infrastructure projects. Regarding economic-based models, the usual objective is calculating the impact over some macroeconomic aggregate. For example, [Andrade Hernández and Lugo Delgadillo \(2018\)](#) use a structural dynamic general equilibrium model of an economy with government. They find that investment in infrastructure projects benefits growth, productivity, competitiveness, and the creation of new businesses. [Perkins et al. \(2005\)](#) find a positive impact of infrastructure on growth, although the causal relationship between them is unclear. [McCarthy and Zhai \(2019\)](#) use input-output analysis to assess the economic impact of a new light rail in Georgia, US. Importantly, these methods and models do not take into account the spatial effects or nature of the projects.

Another common approach is engineering techniques complemented by basic economic notions like the Highway Development and Management Model Four (HDM-4). This model can simulate several variables, including travel times, travel costs, congestion, and expected demand for transportation. The HDM-4 is embedded into its software and requires a set of inputs, including distance, geographic characteristics, and engineering specifications of a road. The World Bank developed this software, and it is expected to be updated to include environmental, social, and economic impact variables. The HDM-4 is widely used. For example, [Wardman et al. \(2023\)](#) revisits the values of the travel time savings depending on the transportation mode. There are other similar tools for commercial use, such as the Transportation Planning Software Visum, which works similarly. Usually, the outcomes of this method become inputs to perform cost-benefit analyses.

The most common, accepted, and used tool in the cost-benefit analysis (CBA). According to [Jones et al. \(2014\)](#), CBA evolved from the economic constructs of consumer surplus and externality to a regulated process performed by economists and governmental agencies that seek project approval. Its goal is to improve the efficient allocation of public resources. Governments, public and private agencies, and multilateral banks use this tool as a common practice. For example, [Hallegatte et al. \(2019\)](#) conducts a CBA to analyze the investment in resilient infrastructure capable of lasting longer with less maintenance, finding it profitable in most of the tested scenarios. However, [Vickerman \(2007\)](#) points out the limitations of the CBA for large-scale infrastructure projects. He argues that the main difficulty is forecasting over long periods and the imperfections of the transport sector, suggesting the complementary role of the general equilibrium models on extensive network projects.

This research also relates to the growing geographical and economic literature that performs impact evaluation. For instance, [Sánchez and Méndez \(2000\)](#), in the case of Colombia or [Hong et al. \(2011\)](#) for China, studied this empirical relationship and found a positive relationship between transportation infrastructure and growth, mainly for poor municipalities.

[Maparu and Mazumder \(2017\)](#) find similar results for India. They discuss the direction of causality, concluding that it primarily goes from development to infrastructure. Similarly, [Hong et al. \(2011\)](#) find that economic development could lead to further infrastructure development. Likewise, [Banerjee et al. \(2020\)](#) examine whether proximity to transportation networks affects the regional economic outputs in China. They found a small positive causal effect on the GDP level but no impact on economic growth. Using a Diff-in-Diff approach to quantify the impact of the Chinese program on the construction of highways on the Yangtze River Delta, [Zhang et al. \(2020\)](#) found positive effects on several economic outputs using a time series of ten years.

Finally, this chapter closely relates to the recent literature using the Spatial Dynamic General Equilibrium Models (SDGEM) framework to evaluate infrastructure impact. There are multiple examples of this methodology. [Allen and Arkolakis \(2014\)](#) measure the benefit of building the U.S. highway system, finding a positive effect on well-being measured by income. [Allen and Arkolakis \(2022\)](#) extend their previous findings to account for the quality of the highways, endogenizing transportation costs. [Asturias \(2020\)](#) measures the impact of India's golden quadrilateral, a modern highway system connecting four major cities on well-being. They use a model of endogenous transport costs and the difference in price levels by region to estimate the effect on real income. [Fajgelbaum and Redding \(2022\)](#) examine Argentina's internal and external trade integration. They found a positive impact of a railroad (internal integration) on the GDP, population density, and welfare.

This chapter is organized as follows: Section 1.2 introduces the Pacific Corridor. Section 1.3 presents a summary of [Desmet et al. \(2018\)](#) model. Section 1.4 discusses the counterfactual exercise. Section 1.5 discusses the results. Section 1.6 concludes.

1.2. Central America and The Pacific Corridor

The Pacific Corridor is a highway built with US financial funding as a part of the ambitious Pan-American highway conceived in 1923. The construction of the road was different depending on the country, but the earliest implementation dates back to the 1950s. Therefore, it is a sequence of segments built by each country, and its name comes from the location of the road along the Central American Pacific Coast. The Pacific Corridor takes different names depending on the country it passes. For example, it is known as the Federal Highway 200 in Mexico. The road's original features consist of lanes, one in each direction. Figure 1.1 shows the approximate location of the road. This is because, in Mexico, it has several ramifications nowadays. The approximate longitude of the highway is around 2.103 miles.

Figure 1.1: Pacific Corridor Approximate Project Location



Source: IADB.

The upgrade of the Pacific Corridor was initially proposed as an integration project in the early 2000's decade. It consists mainly of implementing two additional lanes in each direction. The project also includes other investments, such as moving some road segments to the most convenient locations, building safety crossings in urban areas, and building specific lanes for bikes and pedestrians. According to [Infante \(2012\)](#), the expected output is to reduce the time travel from Mexico to Panama from 190 to 54 hours and to increase

the speed from an average of 10 to 40 miles per hour. According to the IADB, the expected investment amount to build such a project is around \$5.3 billion US dollars. The project also contemplates updating and improving the border’s customs checkpoints along the six borders on the route. This feature will be discussed in Chapter II.

Table 1.1: Trade Value Comparison

Region	Exports	Imports	Total	GDP	Exports %	Imports %	Total %
US - Canada	427.7	481.2	908.9	22690	1.88%	2.12%	4.01%
US - Mexico	362	493.1	855.1	22210	1.63%	2.22%	3.85%
Central America	20.8	26.4	47.2	286	7.28%	9.24%	16.51%

Source: US Trade Representative Office, World Bank, Inter American Development Bank and Author’s Calculations.
Notes: Columns 1-4 in US billion dollars. GDP 2022 in constant 2015 US dollars. Columns 5-7 are percentages of the GDP.
Central America is the aggregation of Guatemala, Belize, Honduras, El Salvador, Nicaragua, Costa Rica and Panama.

Due to its strategic importance in logistics and integration, the region’s governments agreed to include the Pacific Corridor in the “Puebla-Panama” plan. Its importance relies on commerce because approximately 95% of regional trade passes through this road. Therefore, the ultimate goal of this project is to boost Central America’s regional trade by improving the region’s integration and increasing access to their markets. Table 1.1 shows the value of regional trade in Central America compared to the regional trade between the US-Canada and the US-Mexico in 2022. The US-Canada and US-Mexico trade value is around 19 and 18 times, respectively, the one in Central America. These comparisons against significative markets such as the US, Mexico, or Canada may be inappropriate due to the evident differences in the economic size. The US-Canada economy is around 79 times the Central American economy, a similar number if found when comparing Central America to the US-Mexico economy. However, those countries are the closest neighbors of this region, connected by roads, which is not the case with South America.

Table 1.2: Total Trade Change Between 2000 and 2022

Country	Change in Exports	Change in Imports
Mexico	138.4%	124.1%
Belize	124.9%	90.4%
Guatemala	98.7%	160.1%
Honduras	71.1%	129.8%
El Salvador	32.1%	104.1%
Nicaragua	-18.8%	219.4%
Costa Rica	141.5%	105.0%
Panama*	115.1%	102.0%
Central America	94.4%	123.4%

Source: World Bank and Author's Calculations.

Notes: The percentage variation is calculated between 2000 and 2022 values. Data for Panama corresponds to the year 2017. Central America is Guatemala, Honduras, El Salvador, Nicaragua, Costa Rica, and Panama.

Since 2000, total trade has grown for all the countries in the region except Nicaragua, but this is not the case for regional trade. Table 1.2 shows the percentage difference in export and import values between 2000 and 2022 for each country in the region. Central America has experienced a positive trade increase, almost duplicating exports and imports. Nevertheless, that is not the case for intra-regional trade. According to the IADB, the shares of regional trade have not changed much. Table 1.3 shows the IADB's most recent calculations of those shares for a subset of countries of the region. Except for El Salvador exports, these shares remain relatively stable. Even with the tables' different periods, this data suggests that the trade gains over the last 22 years are not from regional trade. It also implies that integration plans like Puebla-Panama are still not impacting the region.

Table 1.3: Intra-Regional Trade Share Comparison

Country	Exports 2017	Imports 2017	Exports 2022	Imports 2022
Guatemala	28%	14%	34%	13%
Honduras	17%	22%	20%	22%
El Salvador	39%	24%	56%	24%
Nicaragua	15%	28%	16%	27%
Costa Rica	19%	8%	17%	13%
Panama	16%	30%	14%	30%

Source: Inter American Development Bank, Transportation Unit.

Notes: Exports and Imports columns refer to the percentage share of the total exports and imports traded with countries of Central America: Guatemala, Honduras, El Salvador, Nicaragua, Costa Rica and Panama.

A simple fact can explain the possible failure of the integration plans: those plans have not yet been executed. The construction of the Pacific Corridor started in 2009, and currently, only 30% of it is finished, mainly in Panama and Mexico. The advance is similar regarding the optimization of border and customs controls. The main drawback is that the implementation of such plans relies on each country. Each has to build its part of the project and find the resources to do so. Most countries fell on administrative and legal issues, preventing or delaying the execution of the project. Figure 1.2 illustrates some locations where the project is executed and locations that are not.

Figure 1.2: The Current Pacific Corridor Reality



Source: Inter American Development Bank.

Notes: Pictures on the left and center-down show segments where the Pacific Corridor is built. The up-right picture shows a segment without any intervention. The down-right picture shows a segment where the project is being constructed.

Given the characteristics of the Pacific Corridor summarized above, it is a convenient project to apply [Desmet et al. \(2018\)](#). The Pacific Corridor affects the geography of seven countries. Due to such extension, it can be considered a large-scale infrastructure project according to [Vickerman \(2007\)](#). Therefore, the use of spatial general equilibrium models is valid in this case. Given that, currently, there is no access to data regarding the specific locations where the Pacific Corridor was built, and considering that it only represents 30% of the total project; for the rest of this chapter, I will assume that the project wasn't executed.

1.3. The Model

In this section, I summarize the model of [Desmet et al. \(2018\)](#), emphasizing the relevant parts to understand the counterfactual exercise and the intuition of the results below. Suppose the world is divided into a continuum of two-dimensional locations; each location is identified with a latitude and a longitude. The agents have to choose their preferred location to live and work. An idiosyncratic utility function determines those choices depending on the level of consumption and amenities available at each location. Access to amenities is

negatively related to the population density in a given location. Thus, the effect of population density over amenities is a fundamental dispersion force, resulting in less concentration of economic activity. The agent can move or stay every period, but moving (migrating) is costly. The more the agent moves, the less utility she gets. The agent obtains income from wages, providing one unit of work inelastically, and from land rent paid by firms.

The firms optimally allocate resources (workers) for goods production and innovation. The firm's technology employs workers to produce consumption varieties, whose prices are given in a Bertrand price competition. Firms also invest in innovation by employing workers to improve the quality of their products. This innovation process determines the productivity of a location. Specifically, productivity depends on former innovation investments, the nearby location's innovation investment, and the location's past productivity values. Then, the firm pays similar wages to all the workers and land rent to the agents. Each firm sells its products locally and abroad. The price of a local good sold in a remote location depends on the firm's marginal product; productivity draws in the location, and trade costs. Intuitively, such costs are defined in terms of the accessibility and relevance of transportation modes. The accessibility measurement is central to setting the counterfactuals discussed below. Then, the more accessibility to a mode in a particular location, the less costly it is to pass by it. The set of prices, productivities, and trade costs determine a firm's export probability.

Given a set of initial values of population, land, amenities, migration costs, trade costs, and productivity, a unique equilibrium for wages, utility, and population density is reached. The agglomeration and the congestion forces generate a distribution of population where the goods, labor, and land markets clear. People choose where to live, generating a spatial distribution of economic activity. This implies the possibility of obtaining simulated productivity measurements, such as net population flows, trade shares, GDP per capita, and utility. Now, I turn to introduce a formal representation of this intuition. It's important to

note that I am not introducing any variation or modification to the model in this chapter. Therefore, the following paragraphs summarize [Desmet et al. \(2018\)](#) model.

1.3.1. Location of Each Economy

Suppose an economy that occupies a space defined by the subset S over a two-dimensional surface. A location is defined as point $r \in S$. Each location has a land density $H(r) > 0$, where $H(\cdot)$ is exogenously normalized so that $\int_S H(r) dr = 1$. Therefore, a country C is defined as the collection of points r that belong to C . Then, the set S is constituted by the partition $S : (S_1, S_2 \dots S_C)$ of the world's countries. Assume that \bar{L} agents are endowed inelastically with one unit of labor each. The initial distribution of population is represented by $L(\bar{r})$.

1.3.2. Preferences and Consumer's Choices

The agent i who lives in r in the period t , and lived in a series of locations $\bar{r}_- = (r_0, \dots, r_{t-1})$ obtains utility from consuming different goods in a bundle represented by a CES utility function and the amenities of each location r . Preferences are governed by:

$$U_t^i(\bar{r}_-, r) = a_t(r) \left[\int_0^1 c_t^\omega(r)^\rho d\omega \right]^{\frac{1}{\rho}} \varepsilon_t^i(r) \prod_{s=1}^t m(r_{s-1}, r_s)^{-1} \quad (1.1)$$

Where, $a_t(r)$ is the initial amenity endowment in location r at time t . $c_t^\omega(r)$ is the consumption of the good ω in r at time t . The consumption bundle is aggregated using a CES function with $0 < \rho < 1$, so that the elasticity of substitution is $[11 - \rho]$. $\varepsilon_t^i(r)$ is a preference shock that follows a Frechet distribution with parameter $\frac{1}{\Omega}$. The agent loses utility by moving across locations, $m(r_{s-1}, r_s)$ represents the permanent flow-utility cost for moving from r_{s-1} in period $s-1$ to r_s in period s . Put differently, every period after observing

$\varepsilon_t^i(r)$, agents decide where to live subject to a permanent flow-utility bilateral mobility costs $m(r_{s-1}, r_s)$. These costs are paid in terms of a permanent percentage decline in utility. The amenities are given by $a_t(r) = \bar{a}(r)\bar{L}_t(r)^{-\lambda}$ where $\bar{a}(r) > 0$ is a continuous and given exogenous function, $\bar{L}_t(r)$ is population per unit of land, and $\lambda \geq 0$ is fixed and represents the elasticity of amenities with respect to population. A greater value of λ implies a higher effect of population due to congestion, therefore acting as a dispersion force. A higher value of Ω implies more dispersion in the agent's preferences across locations; thus, it acts as a second dispersion force.

The agents obtain income from wages $w_t(r)$, and land rent $R_t(r)$ per unit of land. All the inhabitants of location r are assumed to obtain homogeneous income. Therefore, total per capita income in location r is given by $w_t(r) + R_t(r)\bar{L}_t(r)$. Then, if the consumer's budget constraint is binding, the utility function can be expressed as:

$$U_t^i(\bar{r}_-, r) = \frac{a_t(r) \left[\frac{w_t(r) + R_t(r)\bar{L}_t(r)}{P_t(r)} \right] \varepsilon_t^i(r)}{\prod_{s=1}^t m(r_{s-1}, r_s)}$$

Assuming $P_t(r)$ as the ideal price index, and setting $\frac{w_t(r) + R_t(r)\bar{L}_t(r)}{P_t(r)} = y_t(r)$, where $y_t(r)$ is the per capita real income. Then, the utility can be defined as¹:

$$U_t^i(\bar{r}_-, r) = \frac{a_t(r)y_t(r)\varepsilon_t^i(r)}{\prod_{s=1}^t m(r_{s-1}, r_s)} \quad (1.2)$$

Assume that $m(r, s)$ is the product of an origin-specific cost $m_1(s)$ and a destination-specific cost $m_2(r)$. In addition, if staying in the same location is costless, This means that $m(r, s) = m_1(s)m_2(r)$ with $m(r, r) = 1$ for all $r \in S$. As proven in [Desmet et al. \(2018\)](#), this assumption implies that if the agent chooses to migrate, the cost depends on the specific origin and destination. In addition, it also implies that $m_2(r) = m_1(r)^{-1}$, the permanent

¹See [Eaton and Kortum \(2002\)](#) for details

flow of entering a location is compensated by a permanent flow of benefit when leaving the location. These assumptions imply that the dynamic agent's decision choice is simplified to a sequence of static decisions, as shown in [Desmet et al. \(2018\)](#).

From the assumptions regarding migration costs, two results can be obtained. First, as shown in [Desmet et al. \(2018\)](#) the probability that an agent located in s prefers r over all the possible locations v is:

$$Pr(\tilde{u}_t(s, r) \geq \tilde{u}_t(s, v) \forall v \in S) = \frac{l_t(s, r)}{H(s)\bar{L}_{t-1}(s)} \quad (1.3)$$

Where $l_t(s, r)$ denotes the number of people moving from s to r in period t . Second, as shown in [Desmet et al. \(2018\)](#), equation (1.4) establishes a relationship between utility, amenities, and income level. Therefore, the utility becomes a measurement of a location's desirability.

$$u_t(r) = a_t(r)y_t(r) \quad (1.4)$$

1.3.3. Technology and Firms

There exists a continuum of firms in Bertrand price competition that produce local goods and invest in innovation of their product quality. The technology to produce the consumption bundle ω is given by:

$$q_t^\omega(r) = \phi_t^\omega(r)^{\gamma_1} z_t^\omega(r) L_t^\omega(r)^\mu \quad (1.5)$$

Where $L_t^\omega(r)$ is the labor force devoted to the production of ω . Two factors give the total factor productivity; $\phi_t^\omega(r)^{\gamma_1}$ that represents the quality or technology innovation of the firm and, $z_t^\omega(r)$ which is a drawn of random variable following a Frechet distribution reflecting specific exogenous shocks to location r and good ω . Then, using the Frechet distribution's definition, $F(z, r) = e^{-T_t(r)z^{-\theta}}$ it is assumed that $T_t(r) = \tau_t(r)\bar{L}_t(r)^\alpha$ is the total productivity. It can be interpreted as an average draw, positively related to population density $\bar{L}_t(r)$, and the fundamental productivity $\tau_t(r)$. Equation (1.6) shows that $\tau_t(r)$ is exogenously determined by a dynamic process that depends on past innovations $(\phi_{t-1}(r)^{\theta\gamma_1})$, and past realizations of $\tau_t(r)$ in the own and nearby locations. Given that the innovation process is local, it creates scale advantages, constituting an agglomeration force.

$$\tau_t(r) = \phi_{t-1}(r)^{\theta\gamma_1} \left[\int_s \eta(r, s) \tau_{t-1}(s) ds \right]^{1-\gamma_2} \tau_{t-1}(r)^{\gamma_2} \quad (1.6)$$

After learning the productivity draw, a firm in r maximizes its profits per unit of land, choosing labor to produce and innovate, and bidding for land until reaching zero benefits:

$$\underset{L_t^\omega(r), \phi_t^\omega(r)}{Max} \quad p_t^\omega(r, r) \phi_t^\omega(r)^{\gamma_1} Z_t^\omega(r) L_t^\omega(r)^\mu - w_t(r) L_t^\omega(r) - w_t(r) v \phi_t^\omega(r)^\xi - R_t(r) \quad (1.7)$$

Where, p_t^ω is the price of good ω in location r , the cost of devoting workers to innovating is given by $v \phi_t^\omega(r)^\xi$ and, $w_t(r)$ is the wage paid to workers. After solving the maximization problem, the price of the good ω in location r is given by:

$$p_t^\omega(r, r) = \left[\frac{1}{\mu} \right]^\mu \left[\frac{v\xi}{\gamma_1} \right]^{1-\mu} \left[\frac{\gamma_1 R_t(r)}{w_t(r) v (\xi(1-\mu) - \gamma_1)} \right]^{(1-\mu) - (\gamma_1 \xi)} \frac{w_t(r)}{z_t^\omega(r)} \quad (1.8)$$

with $p_t^\omega(r, r) = \frac{mc_t(r)}{z_t^\omega(r)}$, where:

$$mc_t(r) = \left[\frac{1}{\mu} \right]^\mu \left[\frac{v\xi}{\gamma_1} \right]^{1-\mu} \left[\frac{\gamma_1 R_t(r)}{w_t(r)v(\xi(1-\mu) - \gamma_1)} \right]^{(1-\mu) - (\gamma_1 \xi)} w_t(r)$$

1.3.4. Prices, Export Probability, and Trade Balance

Suppose $\varsigma(s, r) \geq 1$ is the iceberg transportation cost of shipping goods from r to s . Assume that the function $\varsigma(\cdot, \cdot) : S \times S \rightarrow \mathbb{R}$ is symmetric and given exogenously. Then the price of the good ω produced in r and sold in s , $p_t^\omega(s, r)$ is equal to the price in r times the transportation cost. This result is central to the analysis below. A reduction in $\varsigma(s, r)$ will reduce the prices $p_t^\omega(s, r)$.

$$p_t^\omega(s, r) = p_t^\omega(r, r)\varsigma(s, r) = \frac{mc_t(r)}{z_t^\omega(r)}\varsigma(s, r) \quad (1.9)$$

This price setting is similar to the one in [Eaton and Kortum \(2002\)](#), with the realizations of $z_t^\omega(r)$ inversely related to the price. As in [Eaton and Kortum \(2002\)](#), the probability that certain goods produced in r are sold in s is given by $\pi_t(s, r)$, with $r, s \in S$. Intuitively, the probability that a good produced in r could be sold in s depends on the comparison of the determinants of such price ($mc_t(r)$, $\varsigma(s, r)$, and $T_t(r)$) in r with the correspondent ones in all the other locations u in S that also produces that good. Furthermore, reducing trade costs or increasing total productivity positively relates to such probability. As shown in [Desmet et al. \(2018\)](#), $\pi_t(s, r)$ can be interpreted as the export share from r to s .

$$\pi_t(s, r) = \frac{T_t(r) [mc_t(r)\varsigma(s, r)]^{-\theta}}{\int_s T_t(u) [mc_t(u)\varsigma(u, r)]^{-\theta} du} \quad (1.10)$$

Finally, it is assumed that trade is balanced in each location r , and markets clear. Therefore, each location's income is equal to its expenditure. Thus,

$$w_t(r)H(r) [L_t(r) + v\phi_t^\omega(r)^\xi] + H(r)R_t(r) = \frac{1}{\mu}w_t(r)H(r)L_t(r) \quad (1.11)$$

The left-hand side shows the total revenue in location r from labor income plus the total land rent. The right-hand side shows the total expenditure on goods produced in r .

1.3.5. Equilibrium

All the conditions above define a dynamic competitive equilibrium where firms optimize and goods markets clear, trade balance conditions are met, land markets are in equilibrium so that the land is assigned to the higher bidder. Given the migration costs and the idiosyncratic preferences, people choose where to live. Labor markets clear. Therefore, for any t and all $r, s \in S$, given $\bar{a}(\cdot)$, $\tau_t(\cdot)$, $\bar{L}_{t-1}(\cdot)$, $\varsigma(\cdot, \cdot)$, $m(\cdot, \cdot)$, and $H(\cdot)$, the model generates a reduced system of equations that determines the equilibrium wage $w_t(\cdot)$, population density $\bar{L}_t(\cdot)$ and the utility $u_t(\cdot)$, and a set of initial values for technology, amenities, and population for every location S . As shown by [Desmet et al. \(2018\)](#), the existence and unicity of the equilibrium requires:

$$\frac{\alpha}{\delta} + \frac{\gamma_1}{\xi} < \lambda + 1 - \mu + \Omega \quad (1.12)$$

Intuitively, the agglomeration forces of better productivity draw in dense locations $\frac{\alpha}{\delta}$ and the spread of innovation costs over more units in dense locations $\frac{\gamma_1}{\xi}$ on the left-hand side should be less strong than the congestion forces over amenities λ , land $1 - \mu$, and the taste for heterogeneity Ω .

1.4. Calibration, Data, and Counterfactuals

This section will discuss the relevant calibration and data for this chapter. I use the same data and parameters as in [Desmet et al. \(2018\)](#). In the next chapter, I will adjust some calibration features to enhance the realism of the trade cost matrix for the region. Here, I focus on the transportation cost matrix, the critical element of the model, to create the counterfactuals in the context of this research.

1.4.1. Data and Calibration

The following exercise exploits the possibility of modifying the geography information used to compute the trade costs matrix $\varsigma(r, s)$ in [Desmet et al. \(2018\)](#). This trade costs matrix follows a standard iceberg form that quantifies the accessibility to a set of transportation modes and the relative participation of each transportation mode in the computation of the cost². Those participations are taken from the parameters estimated by [Allen and Arkolakis \(2014\)](#). The geography information measures accessibility to the transportation modes for each location r .

Following [Desmet et al. \(2018\)](#), each location r is represented by a cell of $1^\circ \times 1^\circ$ resolution. Then, the world's surface corresponds to $360 \times 180 = 64,800$ cells. Each cell size is $62mi \times 62mi = 3844mi^2$ in the equator. From those, only cells with a positive emerged land mass are used; this means a total of 17,048. For each cell, the accessibility to the transportation mode is accounted for. Assume that *mode* is a set of transportation modes that could be available or not at each location r . Then:

²In chapter II, I will discuss the advantages and consequences of such assumption.

$$mode(r) = \left\{ \begin{array}{c} rail(r) \\ no_rail(r) \\ major_road(r) \\ other_road(r) \\ no_road(r) \\ water(r) \\ no_water(r) \end{array} \right\}$$

Where *rail* stands for railroad transportation (trains), *road* stands for road transportation (trucks, cars), and *water* for waterways transportation (Ships, boats). *major* stands for main road similar to a US interstate highway, and *other* accounts for any road that does not satisfy US interstate highway standards.

Initially, this framework uses categories to account for accessibility. This means that if it is observed that the cell r has access to major roads, other roads, and no access to rail and water, then the modes in r are given by $mode(r)$:

$$mode(r) = \begin{cases} rail(r) = 0 \\ no_rail(r) = 1 \\ major_road(r) = 1 \\ other_road(r) = 1 \\ no_road(r) = 0 \\ water(r) = 0 \\ no_water(r) = 1 \end{cases}$$

However, these observations are measured using information from www.naturalearthdata.com at a higher resolution of $0.1^\circ \times 0.1^\circ$. To accommodate this data into the bigger cells, define $mode(r_i)$ as the proportion of smaller cells of size $0.1^\circ \times 0.1^\circ$ with access to a given transportation mode. Knowing that each cell contains 100 sub cells, and replicating the same accounting method for the sub-cells:

$$mode(r) = \frac{\sum_{i=1}^{100} mode(r_i)}{100}$$

For example, if in a certain location, 86 of the subcells have access to railroads, then $rail(r) = \frac{86}{100} = 0.86$. Using this accessibility measurement, following [Desmet et al. \(2018\)](#), the instantaneous cost of passing through location r is given by $\varsigma(r)$. Specifically, a log-linearization of $\varsigma(r)$ implies:

$$\begin{aligned}
\log \varsigma(r) = & \log \varsigma_{rail} [rail(r)] + \log \varsigma_{no_rail} [1 - rail(r)] \\
& + \log \varsigma_{major_road} [major_road(r)] + \log \varsigma_{other_road} [other_road(r)] \\
& + \log \varsigma_{no_road} [1 - major_road(r) - other_road(r)] \\
& + \log \varsigma_{water} [water(r)] + \log \varsigma_{no_water} [1 - water(r)]
\end{aligned} \tag{1.13}$$

With ς_{mode} standing for the parameters from [Allen and Arkolakis \(2014\)](#) summarized in Table 1.4. If the accessibility of rails increases for location r , given the parameters ς_{rail} and ς_{no_rail} , everything else constant, the instantaneous cost of passing through r should fall. I discuss the features of this iceberg transportation function in Chapter II. Intuitively, suppose a location exogenously increases its access to transportation because its government places a train connecting it to other remote locations. In that case, the costs of passing through it should fall, as stated by [Allen and Arkolakis \(2014\)](#). This feature allows us to perform the counterfactual exercise explained below.

Table 1.4: Allen and Arkolakis (2014) Parameters

Parameter	ς_{rail}	ς_{no_rail}	ς_{major_road}	ς_{other_road}	ς_{no_road}	ς_{water}	ς_{no_water}
Estimated Value	0.1434	0.4302	0.5636	1.1272	1.9726	0.0779	0.779

Source: taken from [Desmet et al. \(2018\)](#), based on [Allen and Arkolakis \(2014\)](#)

One may be concerned that the parameters estimated by [Allen and Arkolakis \(2014\)](#) are not relevant to my analysis. A first concern would suggest they are not because the estimation uses data from the US, and the characteristics of Central America could be different. However, the proportions of transportation modes used in the estimation of [Allen and Arkolakis \(2014\)](#) show a striking dominance of freight shipments using roads, with a proportion of 90%. Similarly, the ones in Central America are above 95% according to [Infante \(2012\)](#). One could argue that trade volume within the region is a fraction compared to the US, as shown in Table 1.1, and that could be a reason to discard these parameters.

Nevertheless, the similarity of the proportions seems a good reason to use them. In addition, at the time of the elaboration of this research, the exact data to replicate [Allen and Arkolakis \(2014\)](#) is not available. A forthcoming dataset of the IADB will provide the necessary information to validate the fit of the actual ς_{mode} parameters for the region.

Once $\varsigma(r)$ is calculated for every cell, the Fast Marching Algorithm is applied to compute the lowest cost between two cells. Equation (1.14) shows the general setup of the algorithm, $\int_{g(r,s)} \varsigma(u) du$ is the line integral of $\varsigma(\cdot)$ along the path $g(r, s)$.

$$\varsigma(r, s) = \left[\inf_{g(r,s)} \int_{g(r,s)} \varsigma(u) du \right]^{\tau} \quad (1.14)$$

The counterfactual exercise consists of modifying the accessibility to transportation modes data, specifically those corresponding to major roads. That modification is arbitrary, but it focuses on the best way to incorporate the Pacific Corridor into the geographical data. Below, I explain the alternatives considered and the reasons for choosing two.

There are two ways to perform this exercise: by using the model as it is, running the simulations for the world, or limiting the simulations to the region's area. The advantage of the first is that it allows for interactions of the agglomeration and congestion forces across all the cells representing the world. This also implies trade across the whole set of cells in the model. However, that could potentially reduce or attenuate the effects on the area of interest, Central America. The second way to reduce the number of cells in the simulation to those belonging to the region is a subsample of 302 cells, as shown in Figure 1.3, corresponding to seven countries from Mexico to Panama. The argument here is the opposite; given the reduction of the cells, the interactions with other cells worldwide are ignored, increasing the local effects of the agglomeration and congestion forces. Therefore, I use both specifications to explore if there are any differences. In stage one, simulate all the cells and extract and discuss the results for the subsample of 302. Then, in stage two, I shut down the cells that

don't belong to the subsample of Central America, running the simulation only for the 302 cells of the region. Then, to add some characteristics of the region, I ran some robustness checks on stage three, using only the 302 cells of the region.

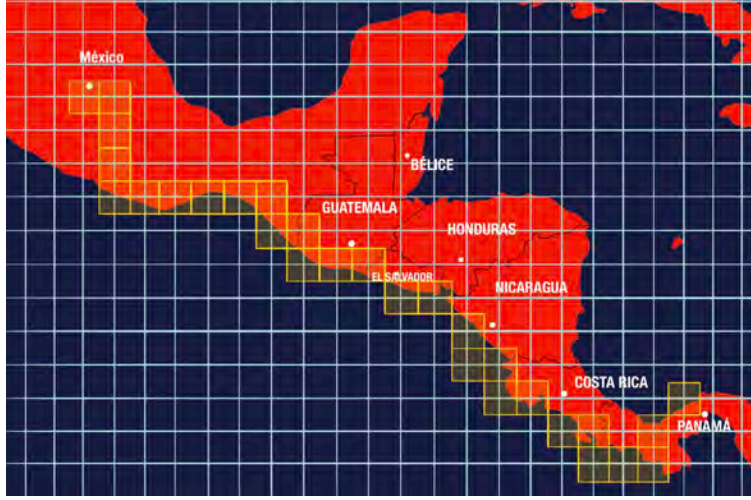
Figure 1.3: Cells of Central America



Source: Authors calculations based on the trade cost matrix in [Desmet et al. \(2018\)](#). Processed in QGIS using Open Street Maps.

The Pacific Corridor approximate location shown in Figure 1 is adapted to the cell location in Figure 1.4. These 29 cells are chosen given the approximate location of the project. It is important to note that the exact location of the Pacific Corridor in some countries is uncertain, and in other cases, it is still to be determined. Given the cell size and the nature of the project of building two additional lanes and upgrading the road to US interstate highway standards, I assume the 29 cells contain the whole project, from Mexico to Panama City. Therefore, to perform the counterfactuals, the information regarding main road accessibility in those cells is modified as discussed below. Finally, it is essential to remark that all the other calibration features remain as in [Desmet et al. \(2018\)](#) and are taken as given for this research.

Figure 1.4: Chosen Cells to Treatment



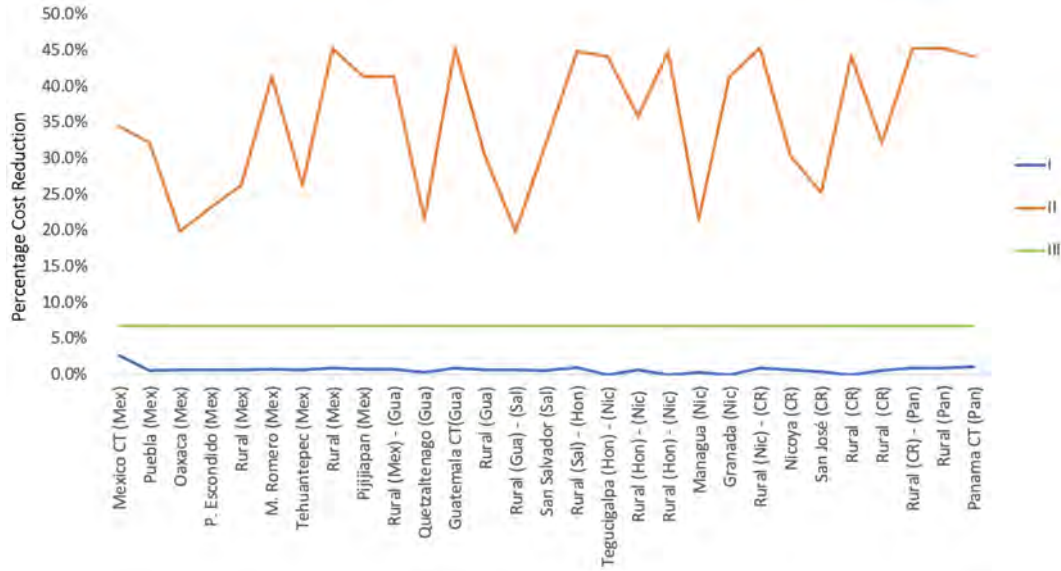
Source: IADB

1.4.2. Counterfactuals

To perform the counterfactual exercise, I modified the data on the accessibility of major roads. Suppose that \tilde{r} represents the 29 treated cells containing the Pacific Corridor with $\tilde{r} \in \tilde{S}$ the sample of 302 cells of the region, and $\tilde{S} \subset S$. Then, the treated access to major roads is defined as before as $major_road(\tilde{r}) = \frac{\sum_{i=1}^{100} major_road(\tilde{r}_i)}{100}$, where the number of sub-cells with access to major roads \tilde{r}_i increases with respect to the baseline (e.g., with PC construction). Counterfactual I consists of increasing the proportion of major roads on each cell by a fixed proportion of 10%. This number was consulted with the IADB transportation officials and seemed reasonable according to their experience in the field. However, the road infrastructure density is heterogeneous in the region. There are areas with higher major road accessibility (like Mexico City) compared to regions with lower ones (like Guatemala's rural area). In addition, some of the 29 cells treated have no access to major roads. Those cells were imputed with an accessibility of 10 smaller cells to eliminate the zero, reducing the likeliness of the exercise. The computation of the instantaneous costs of this counterfactual in Figure 1.5 shows that the reduction in costs is minimal. On average, the reduction in the

instantaneous costs is 0.68%. Dense areas like Mexico City or Panama City get higher cost reductions under this scenario. Then, given the above reasons, this counterfactual was not used for this exercise.

Figure 1.5: Instantaneous Costs Comparison Across Counterfactuals

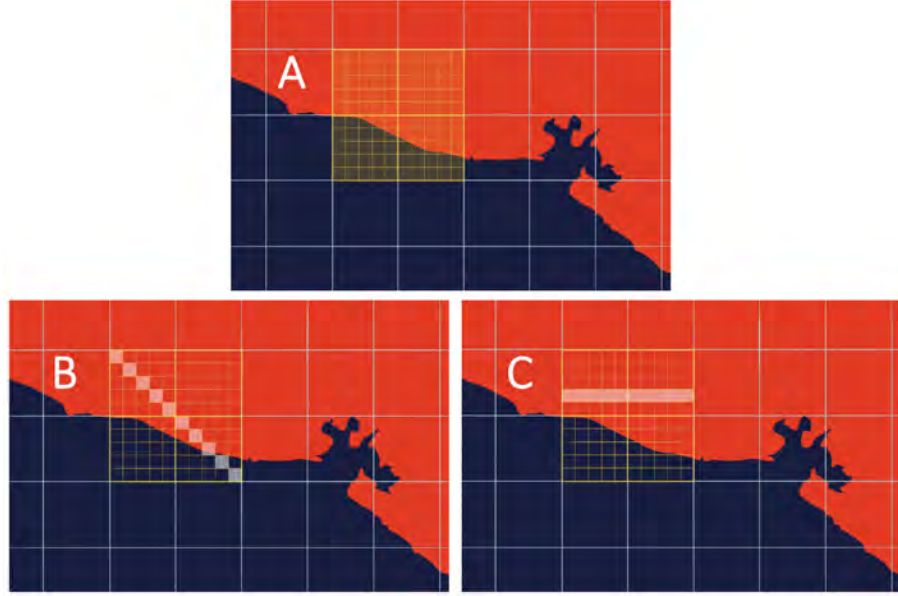


Source: Author's calculations.

Notes: Vertical axis: percentage reduction in the instantaneous trade costs per cell of the three counterfactuals with respect to the baseline. Horizontal axis, cell location by name of the main urban area, or "rural." Country name initials are in parentheses. Counterfactual I (blue), Counterfactual II (orange), Counterfactual III (green)

Counterfactual II consists of increasing the accessibility of major roads by a fixed amount rather than using a proportion. Figure 1.6 illustrates the intuition of this counterfactual. Suppose that there is no access to main roads in a given cell. That cell and subcells look like the yellow cell in panel A. Then, if a government decides to build a major road across this cell, assuming that this road passes the cell in a straight line, ten sub-cells will have access to major roads, $\Delta \tilde{r} = 0.1$. Therefore, that cell could look like panel B or C. This assumption simplifies the specific layout of the road. Areas with mountains would show a different pattern, adding more subcells with accessibility. However, the advantage of this setup is that it generates the same reduction in instantaneous trade costs for all cells regarding road density, as shown in Figure 1.5. The average cost reduction in this scenario is 6.7%

Figure 1.6: Sub-cell Example: Crossing the cell



Counterfactual III adjusts the accessibility information of major roads to target an external infrastructure feature. According to the IADB transportation unit's engineering calculations, the Pacific Corridor could reduce travel time costs by around 35%. Using this feature, I adjusted the instantaneous costs matrix of the project's cells \tilde{r} to target such cost reduction on average. An important characteristic of this exercise is the irrelevance of the internal adjustment of $\varsigma(r)$, as long as $\Delta\varsigma(\tilde{r}) \approx -0.35$. Therefore, I adjusted the accessibility to major roads on each project's cell, computing the average reduction in $\varsigma(\tilde{r})$ until the target reduction is reached. Given that this time cost reduction was estimated only for the Pacific Corridor, it is possible that it may not be the case for the entire road network of the region. Figure 1.5 shows that this counterfactual generates cost reductions between 45% to 20%, with an average reduction of 35.35%

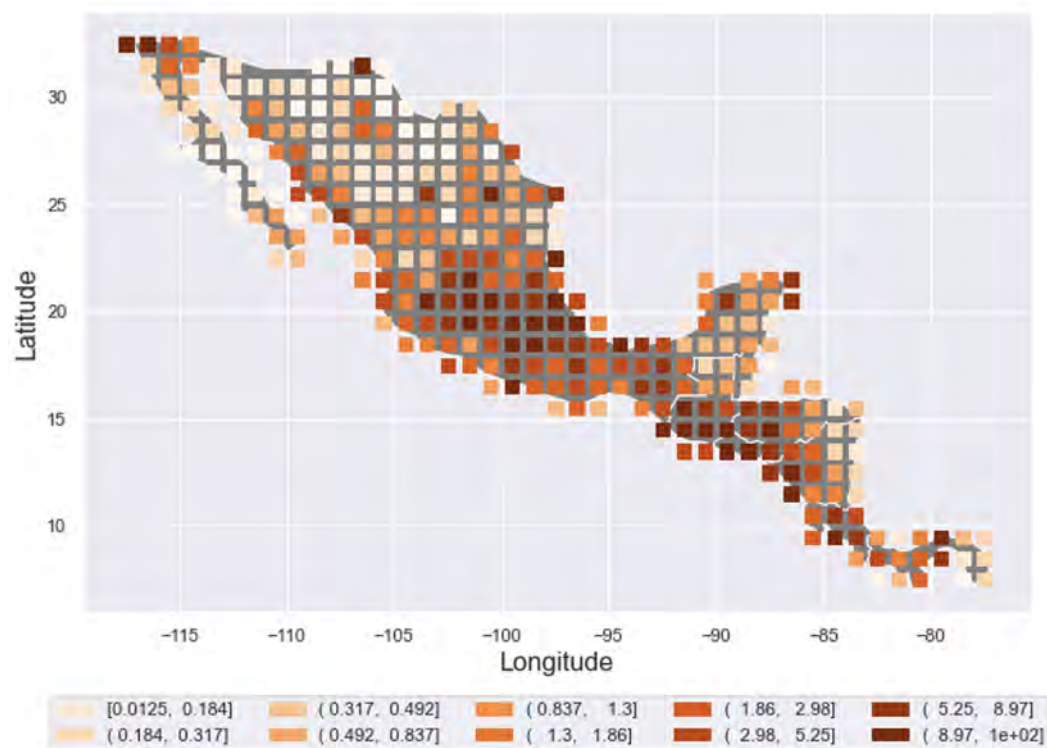
The baseline scenario corresponds to the model simulations when the Pacific Corridor is not introduced in the geography. The baseline scenario is simulated for stages one and two according to the cell sample size. Stage three uses the same baseline as stage two. It can be interpreted as the path each variable follows in the absence of the project.

The set of results I show below to understand the effect of the Pacific Corridor over the distribution of economic activity and the choices of individuals is population (net population flows). GDP per capita normalized with $GDP_{princeton} = 100$, utility as a measure of the attractiveness of a given location. Productivity, interpreted as an agglomeration force as shown in equation (1.6), and the total sum of trade shares corresponding to the total summation of all the bilateral trade shares of cell r with all cells $s \in S$, calculated by the model but not solved sequentially. For every stage and counterfactual, the results are shown as the percentage change in the 100-year average cell value for a given variable between the baseline scenario and the counterfactual, except for trade shares, which is not an average, as explained before. There's not much variation in these results for a shorter period, only the magnitude but not the sign of the effect.

1.5. Results

Before proceeding to discuss the results, it is worth recalling the intuition of the model, which is the basis for analyzing the results shown in section 1.3. An exogenous shock such as the Pacific Corridor directly affects the prices of the goods produced by a firm in a specific location and sold abroad by reducing trade costs. The firm will face better prices (less distorted by the trade costs), thus increasing its profits and participation in trade. Such an increase in profits can change the firm's optimal allocation of inputs, generating an additional allocation of workers to produce goods and innovate, increasing the demand for workers and productivity. This effect also increases the GDP per capita of the location, ultimately growing its attractiveness in terms of utility. The shift in productivity works as an agglomeration force, attracting agents to the most productive locations. The congestion effects over the amenities offset agglomeration effects; the more population in a particular location, the less access to amenities. All these effects reach an equilibrium, generating a new distribution of the population, productivity, GDP per capita, utility, and trade shares across the space.

Figure 1.7: Initial Distribution of Population in Central America



Source: [Desmet et al. \(2018\)](#)

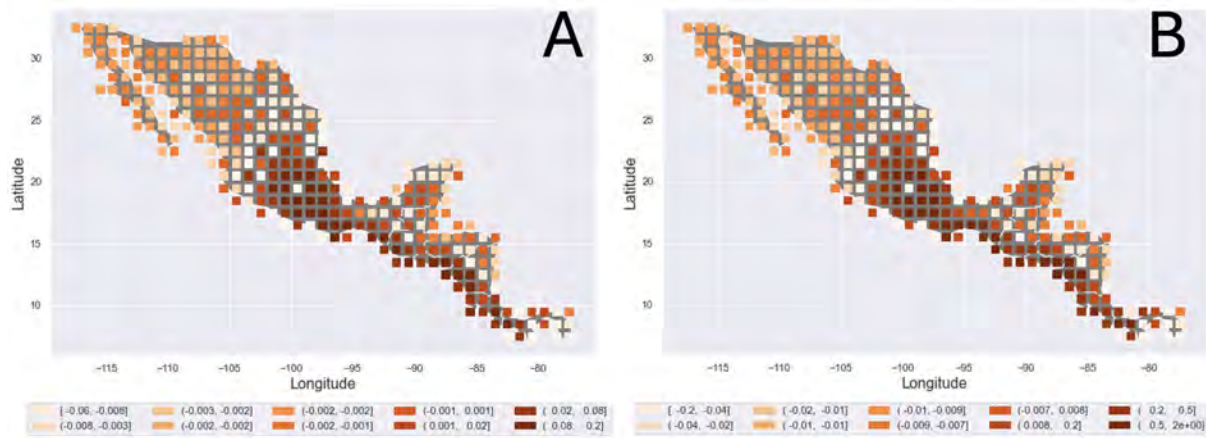
Notes: Population per cell. Color scale in deciles. High decile values are darker.

A driving force to explain the results below is the initial population distribution across the region. Figure 1.7 shows population density in each cell by deciles. Dark blue cells are the most populated, and light green ones are the least populated. For example, in Tijuana, on the border with the US, the neighborhoods of Mexico City, San Salvador, El Salvador, and Tegucigalpa, Honduras, are among the most populated. Given their population density, these areas, in terms of the model, are also initially more productive. The less populated areas are Baja California and the north of Mexico, and the area from the Yucatan peninsula to the south, mainly on the Caribbean coastline, thus endowed with less initial productivity.

1.5.1. Stage I: Using the World, Analyzing the Region

As stated above, stage one uses the whole sample of cells representing the world in the model. Intuitively, the new infrastructure increases the region's connectivity, facilitating technology spillovers and increasing productivity along the Pacific Corridor path. In Figure 1.8, both counterfactuals show a similar direction and spatial distribution of impact measured by deciles, but with higher numbers for counterfactual III. On average, counterfactual II shows an impact of 0.68% compared with an average of 4.35% for counterfactual III. The positive impact is concentrated in two areas: in Mexico City's neighborhood and along the PC path. Then, the agglomeration generated by the initial higher productivity values tends to boost South Mexico's productivity. Along the PC's path, several cells show positive impacts, fueled by the fact that most of the capital cities are near the Pacific coast, thus increasing population density. The small or null effect occurs in remote cells mainly situated along the Caribbean coast and northern Mexico.

Figure 1.8: Impact on Productivity



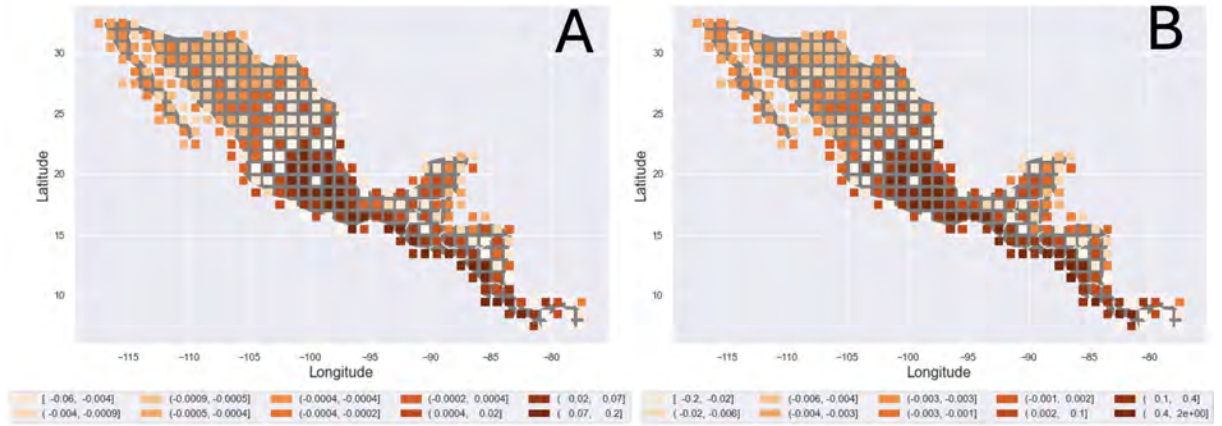
Source: Author's Calculations.

Notes: Cell 100-year mean percentage difference between Counterfactual II (A) or Counterfactual III (B) with respect to the baseline. Color scale in deciles. High decile values are darker.

Figure 1.9 shows the impact of population flows. Intuitively, the productivity boost attracts the population due to increasing jobs and better wage opportunities in such areas, regardless of the congestion effects over amenities. In the middle of the observed clustered

results of Mexico, the only cell with negative population flows is Mexico City. Given its initial population density, the congestion effects over amenities offset the agglomeration effects. As before, the magnitude of the impact in Counterfactual III is higher, but the direction and spatial distribution of the impact are preserved. On average, counterfactual II shows an effect of 1.35% and 9.63% for counterfactual III.

Figure 1.9: Impact on Population



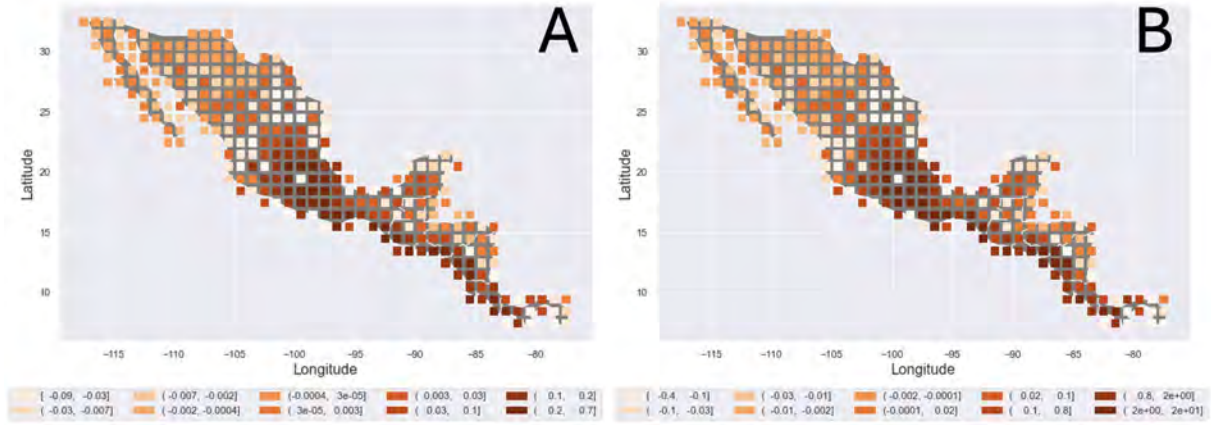
Source: Author's Calculations.

Notes: Cell 100-year mean percentage difference between Counterfactual II (A) or Counterfactual III (B) with respect to the baseline. Color scale in deciles. High decile values are darker.

Following the same pattern and spatial distribution, there is a positive impact on trade shares in the same area in Figures 1.8 and 1.9. Counterfactual III showed a higher effect (Figure 1.10) than counterfactual II, with an average of 5.3% and 66.6%, respectively. Intuitively, the increase in productivity will reduce firms' prices, as shown in section 1.3. In addition, the reduced transportation costs will also reduce the prices of goods produced in such areas and sold worldwide. This shift in trade shares is concentrated in Mexico City's cluster. The initial population density in that area benefits the agglomeration forces of productivity.

Mexico City's productivity spillovers attract the population to its neighbor cells, as well as the Pacific Corridor path. Higher productivity and population induce a higher GPD, as shown in Figure 1.11. On average, counterfactual II and counterfactual III show an impact

Figure 1.10: Impact on Total Trade Shares

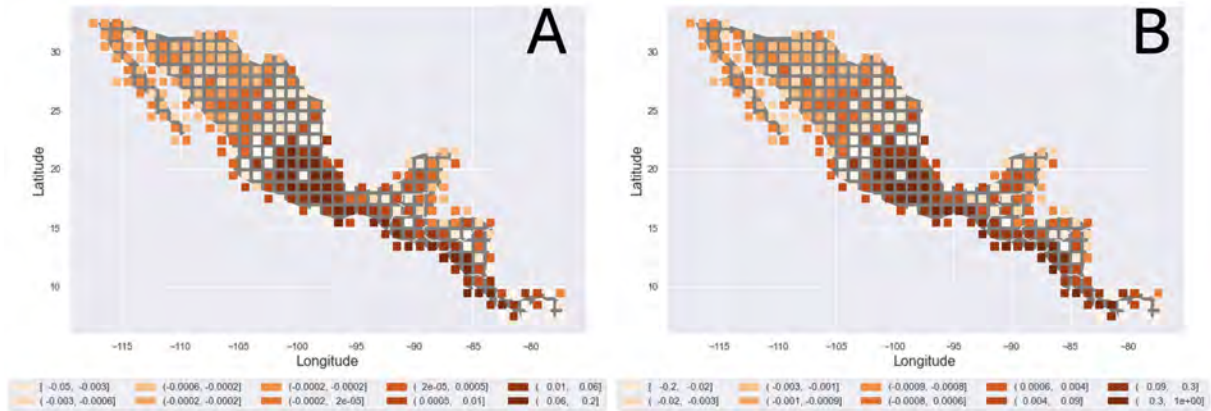


Source: Author's Calculations.

Notes: Cell 100-year mean percentage difference between Counterfactual II (A) or Counterfactual III (B) and the baseline. Color scale in deciles. High decile values are darker.

of 1.12% and 7.68, respectively. Figure 1.12 shows that given the amenities value, such cells with a positive effect on GDP will also become more attractive in terms of utility. However, the agglomeration forces of productivity generate congestion on such cells, which explains a lower average change in utility compared to the GDP in both counterfactuals.

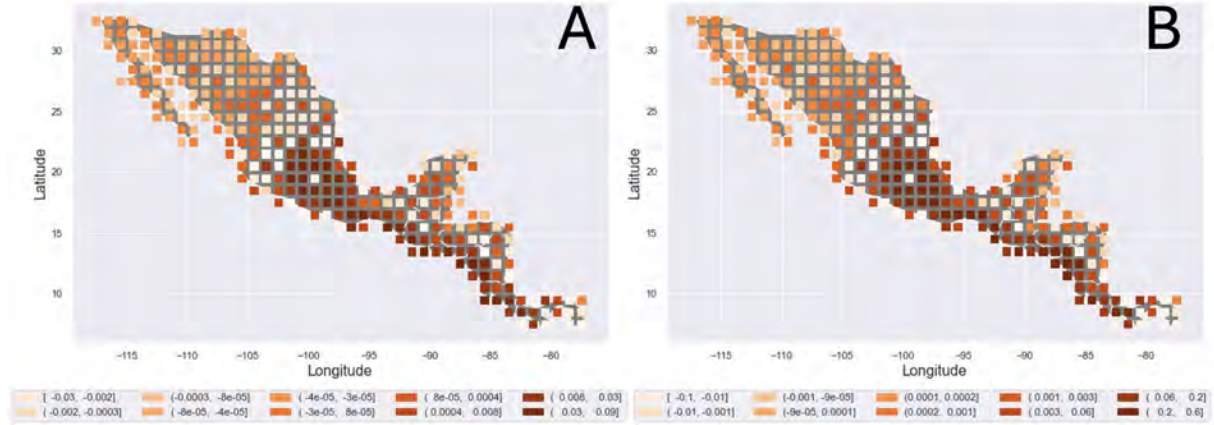
Figure 1.11: Impact on GDP per capita



Source: Author's Calculations.

Notes: Cell 100-year mean percentage difference between Counterfactual II (A) or Counterfactual III (B) with respect to the baseline. Color scale in deciles. High decile values are darker.

Figure 1.12: Impact on Utility

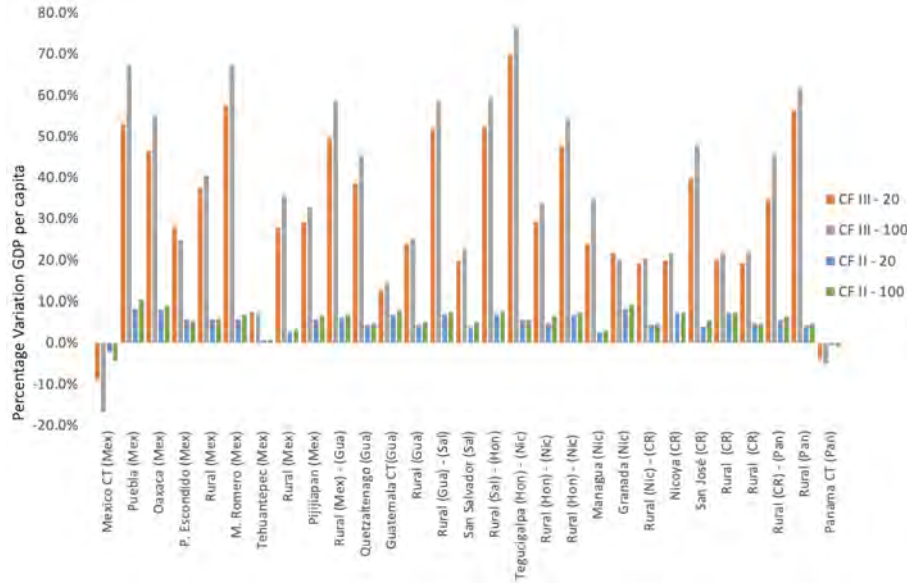


Source: Author's Calculations.

Notes: Cell 100-year mean percentage difference between Counterfactual II (A) or Counterfactual III (B) with respect to the baseline. Color scale in deciles. High decile values are darker.

Overall, the accumulation forces through productivity explain the positive effects in the cells and close neighbors of the Pacific Corridor. It is the opposite case for main cities such as Mexico City and Panama City, as shown in Figure 1.13 for the 29 cells affected directly by the project, where congestion effects due to population density dominate, showing adverse effects. Then, a person who lives in Mexico City will move if, due to a shift in productivity, the attractiveness of other locations is high enough to compensate for moving costs, given the specific preferences and initial values of amenities. The Pacific Corridor can create this shift in productivity, generating the reallocation of workers across the space.

Figure 1.13: Comparative Effects of the Project Cells



Source: Author's Calculations.

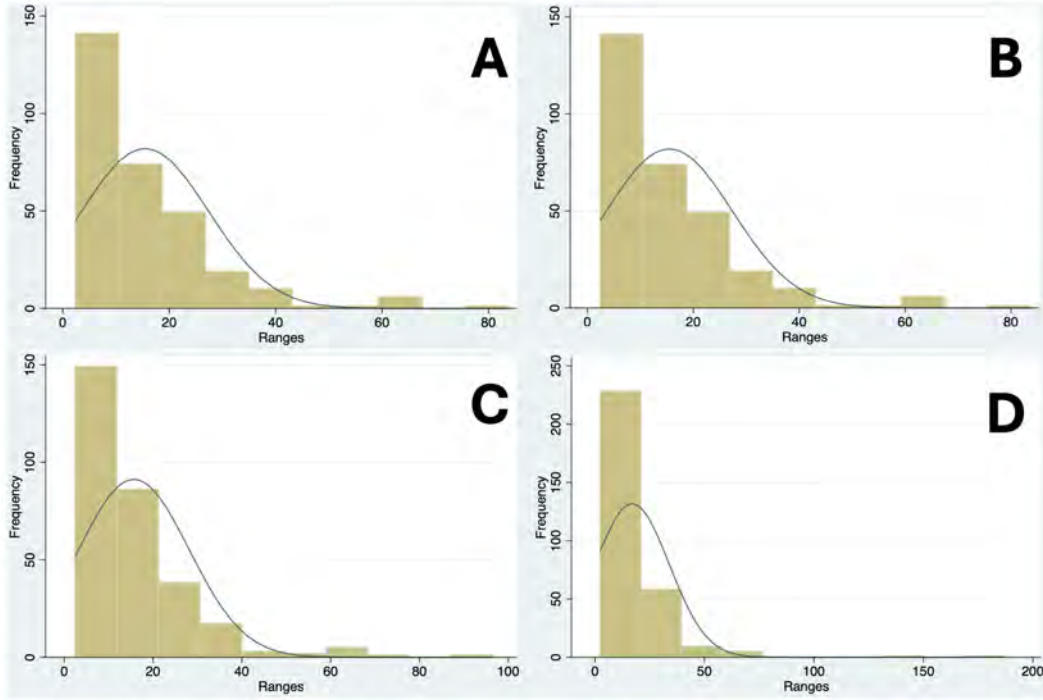
Notes: Cell 100 and 20-year mean percentage difference between Counterfactual II (CF II) and Counterfactual III (CF III) with respect to the baseline for the project cells.

According to these results, it seems plausible that remote areas connected to the Pacific Corridor could obtain positive shifts in productivity. However, if the distance to a location with high productivity increases, those spillovers weaken. Furthermore, if those remote areas lack amenities such as schools or hospitals, the population increase could easily offset the positive effect of the Pacific Corridor through the congestion forces. The results show a high concentration of positive impacts on Mexico City's neighbor cells. Therefore, building a road like the Pacific Corridor could create the desired productivity shift. Still, suppose the investment is limited to it, ignoring other needs such as each location's amenities. In that case, the benefits will be allocated towards cells with high initial values of amenities and productivity induced by population density. This result is aligned with [Banerjee et al. \(2020\)](#); everything else equal, proximity to transportation networks is the primary determinant of the positive effects of the investment in infrastructure. Chapter II explores the impact of lifting the time cost of border and customs controls over transportation.

1.5.1.1. Growth and Income Distribution

As discussed above, the shift in productivity, either positive or negative, is the driving force behind the set of results. Let's focus on the effects on GDP distribution across space and economic growth. Figure 1.14 shows the impact on the distribution of the GDP per capita using a histogram for the 302 cells of the region. Panel A shows the baseline income distribution by cell GDP per capita size clustered in deciles in the first year of the simulation. Panel B shows the same distribution in year 100. The shape of the distribution seems preserved. Panel C and D show the distribution in year 100 for counterfactuals II and III, respectively. Panels C and D show a bunching to the left of the distribution. This means that if the Pacific Corridor is built, in 100 years, there will be more cells in the low deciles of income and fewer cells in the higher ones. Panels C and D also show that those cells in the higher deciles get even higher GDP per capita levels. This result suggests a worsening income distribution due to the Project in the region.

Figure 1.14: GDP per capita distribution After 100 Years

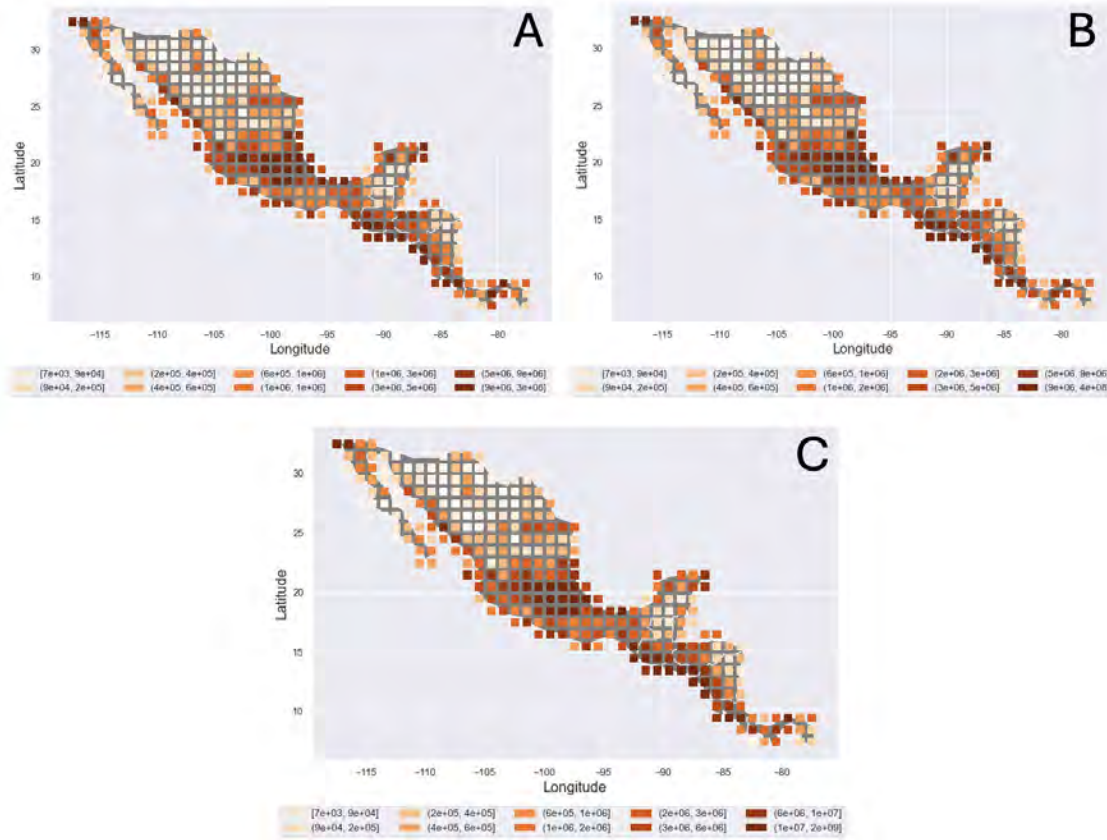


Source: Author's Calculations.

Notes: Histograms of the GDP per capita across 302 cells. Panel A: Baseline year 1. Panel B: Baseline year 100. Panel C: Counterfactual II year 100. Panel D: Counterfactual III year 100. The vertical axis shows the frequency of cells in each decile. The horizontal axis shows the ranges of the GDP per capita index with $GDP_{princeton} = 100$

Regarding the distribution across space, Figure 1.15 shows that in the long run, the spatial distribution is preserved, regardless of the Pacific Corridor. Both counterfactual's spatial distributions in Figure 1.15 resembles the initial distribution of population in Figure 1.7. According to the simulations, there is no shift or redistribution in the geographical distribution of income. Furthermore, given the change in productivity that enhances the agglomeration forces, the income distribution could concentrate, benefiting the high-income cells. Therefore, the project unaltered the GDP per capita geographical distribution.

Figure 1.15: GDP Geographic Distribution Impact

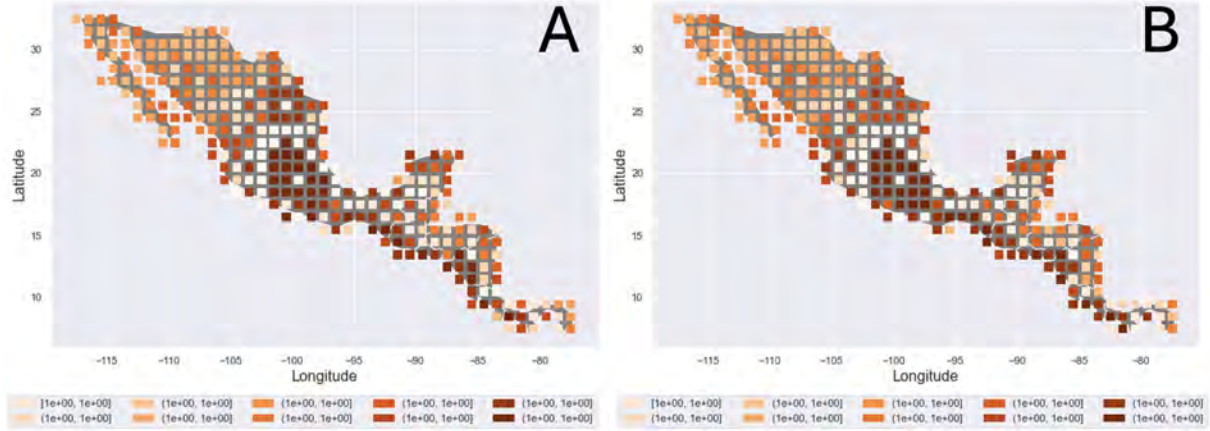


Source: Author's Calculations.

Notes: Cell level of GDP per capita year 100. Panel A: Baseline. Panel B: Counterfactual II. Panel C: Counterfactual III. Color scale in deciles. High decile values are darker.

Figure 1.16 plots the ratio of counterfactuals over baseline GDP per capita growth rates across the region. The differences are minor, even for the counterfactual III, which induces the highest cost reduction and shows the most significant impacts on GDP per capita and productivity. As before, the effect was concentrated in Mexico City's neighboring cells and the project's path. Then, the simulations show that the agglomeration effects of productivity positively impact growth, specifically in those previously highly productive areas and their surroundings through technology spillovers.

Figure 1.16: Economic Growth effects



Source: Author's Calculations.

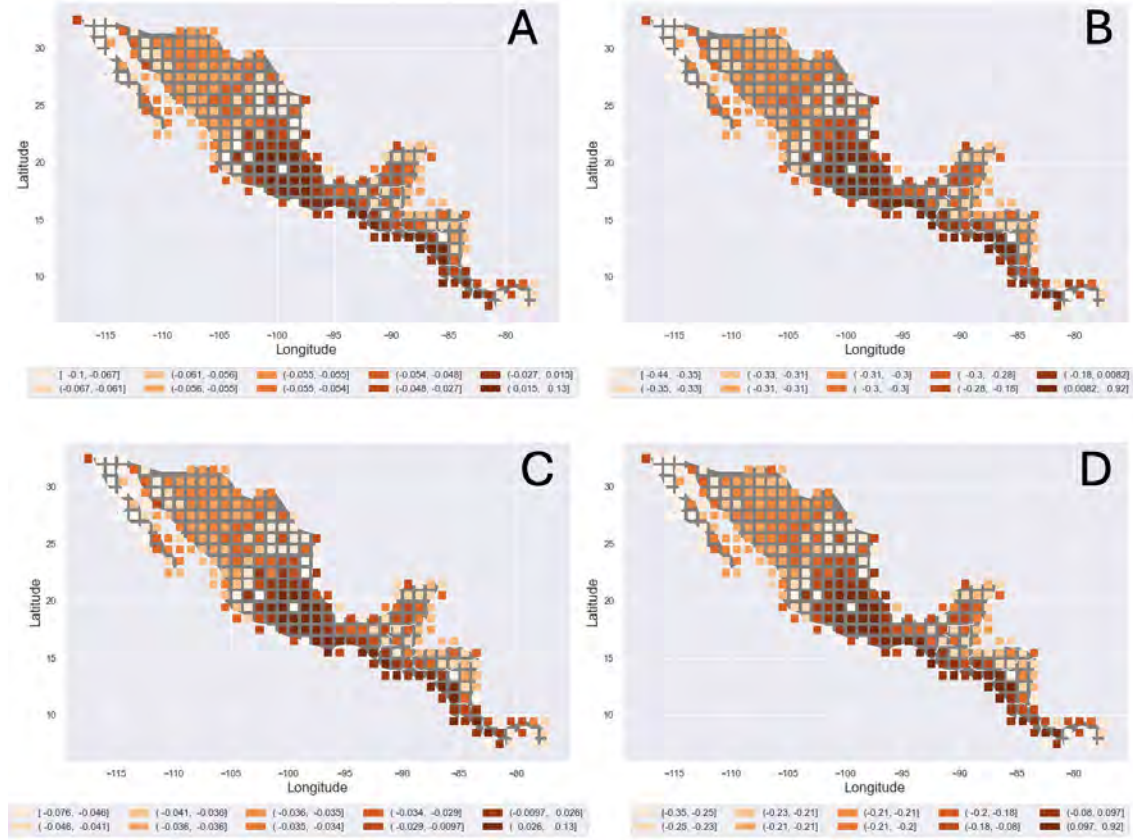
Notes: Average Cell GDP per capita growth rate ratio Counterfactual/Baseline. A: Counterfactual II. B: Counterfactual III. Color scale in deciles. High decile values are darker.

Following this section's results, if the objective of the infrastructure investment policy is to reduce inequality, then according to these simulations, that does not seem to be the case. The model shows the opposite due to the agglomeration forces of productivity. These results suggest that inequality is beyond the scope of this specific case and would not be improved by a road infrastructure project, given the initial population distribution and productivity.

1.5.2. Stage II: Restricted Simulations

As discussed above, Stage II focuses on the region, restricting the simulation to the 305 cells of the region. This exercise aims to check the consistency of the previous results. In the model, closing the world will reduce the interaction with overseas cells, restricting trade to the cells of their region. The nature of both counterfactual scenarios is preserved here.

Figure 1.17: Productivity and Population, Stage II

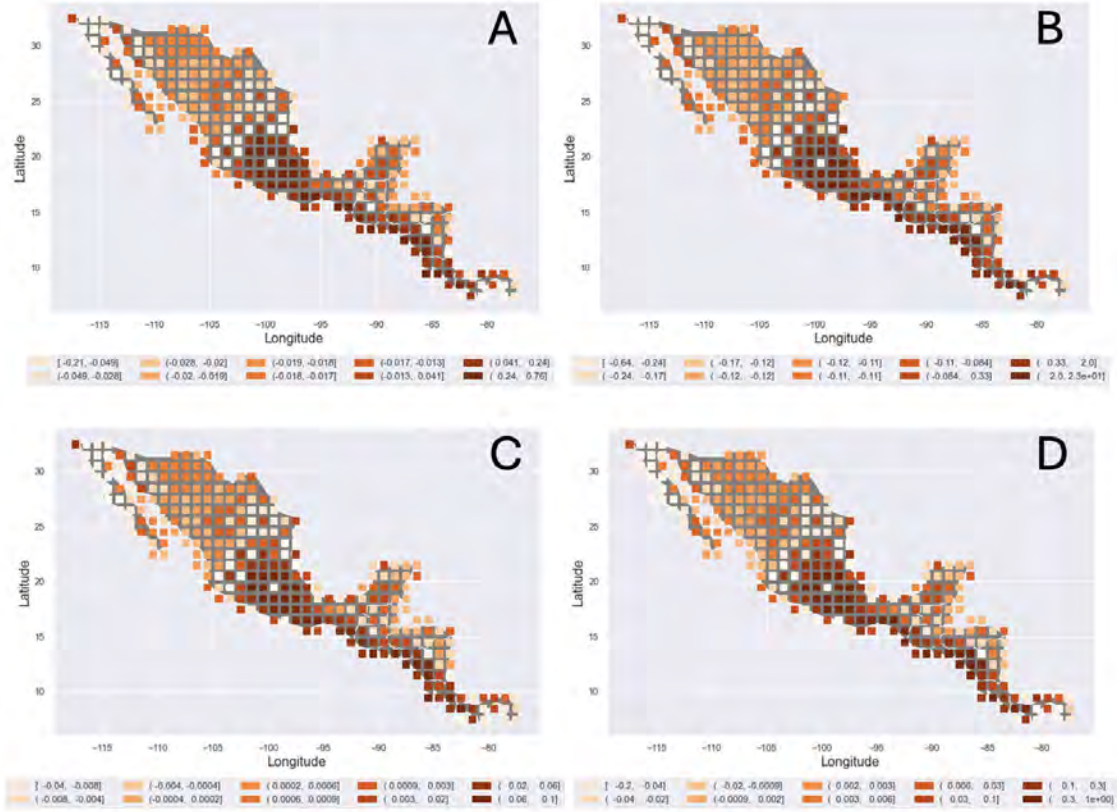


Source: Author's Calculations.

Notes: Cell percentage difference of the 100-year average of the variable with respect to baseline. Variables: Productivity in panels A and B, for Counterfactuals II and III, respectively. Population flows in panels C and D for Counterfactuals II and III respectively. The color scale in deciles. High decile values are darker.

Figure 1.17 shows the results for Productivity and Population flows, Figure 1.18 shows GDP per capita and Trade Shares, and Figure 1.19 shows the ones for utility. The patterns of the geographical distribution of the impact are preserved, compared to the world simulation shown above. However, the effect on productivity, population flows, and total trade shares is lower, the impact on the GDP is similar, and the effect on utility is higher than in stage one. These variations in the impact suggest that the agglomeration forces are not as strong as in stage one due to a limitation on the spillover effects. Thus, there is less congestion over amenities, increasing the utility, given a similar impact on the GDP.

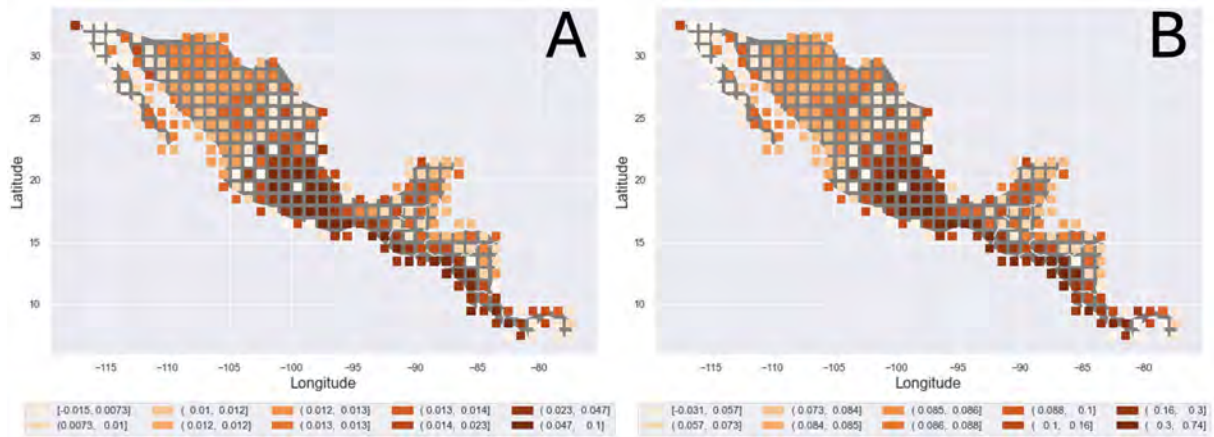
Figure 1.18: GDP per capita and Trade Shares, Stage II



Source: Author's Calculations.

Notes: Cell percentage difference of the 100-year average of the variable with respect to baseline. Variables: Trade Shares in panels A and B for Counterfactuals II and III, respectively. GDP per capita in panels C and D, for Counterfactuals II and III, respectively. Color scale in deciles. High decile values are darker.

Figure 1.19: Impact on Utility, Stage II



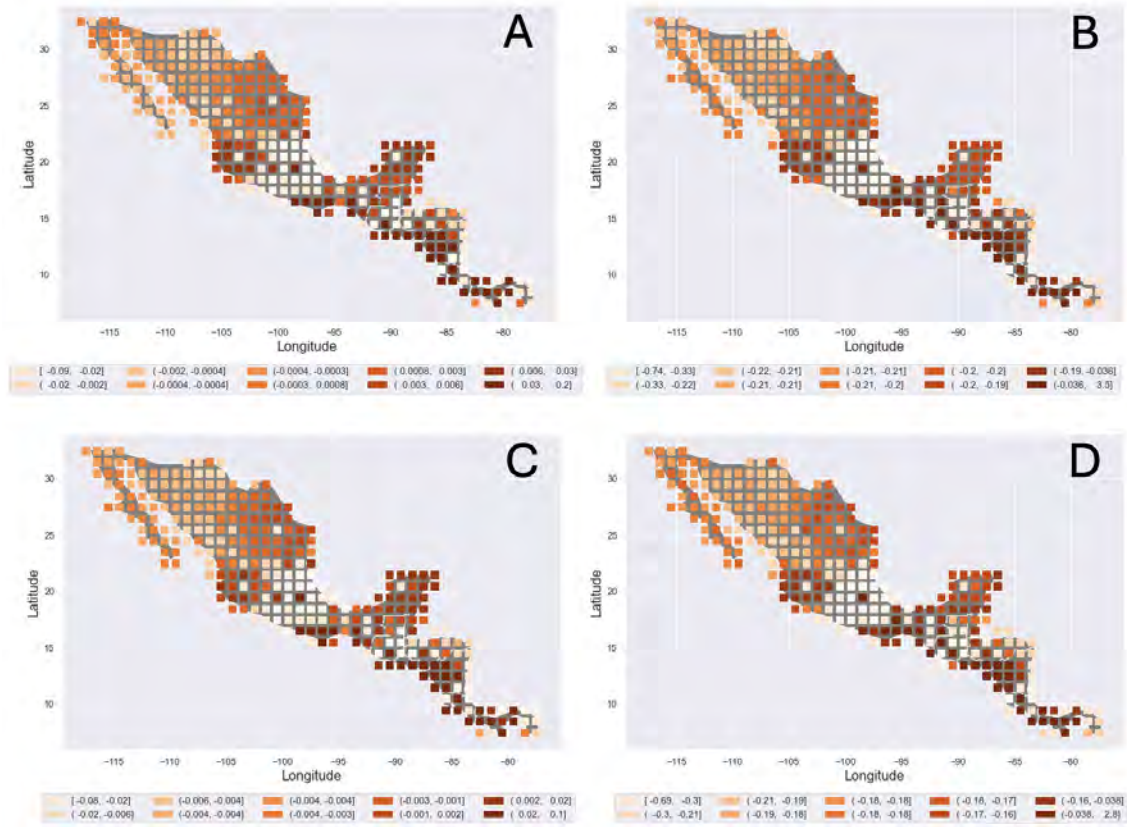
Source: Author's Calculations.

Notes: Cell 100-year mean percentage difference between Counterfactual II (A) or Counterfactual III (B) with respect to the baseline. Color scale in deciles. High decile values are darker.

1.5.2.1. Robustness check: Increasing the Cost of Water Transport

According to the IADB, the primary mode of transportation for trade across the region is through roads. Water shipments are less than 5% according to [Infante \(2012\)](#), given that 95% of regional trade uses the Pacific Corridor and its network. Water shipment is central to international trade. Thus, this feature can be added to the model by increasing the cost of water transport and then rerun the counterfactuals. Intuitively, the optimization process that chooses the least cost path using the Fast Marching Algorithm should now avoid waterways. A simple and ad-hoc rule to perform this exercise is setting $\varsigma_{water} = 2(\varsigma_{no_road}) = 3.9452$; The reason for this is that according to Table 4, the parameter ς_{water} shows a low participation of water in transport costs. The opposite is for ς_{no_road} . Intuitively, as estimated by [Allen and Arkolakis \(2014\)](#), shipping freight using a boat in the water is the cheapest mode of transportation. Conversely, a small road with limited specifications is the most costly way of shipping. The rule makes water transportation the most expensive mode, thus inducing the optimization to choose roads, as is the case for regional trade.

Figure 1.20: Productivity and Population, Stage III



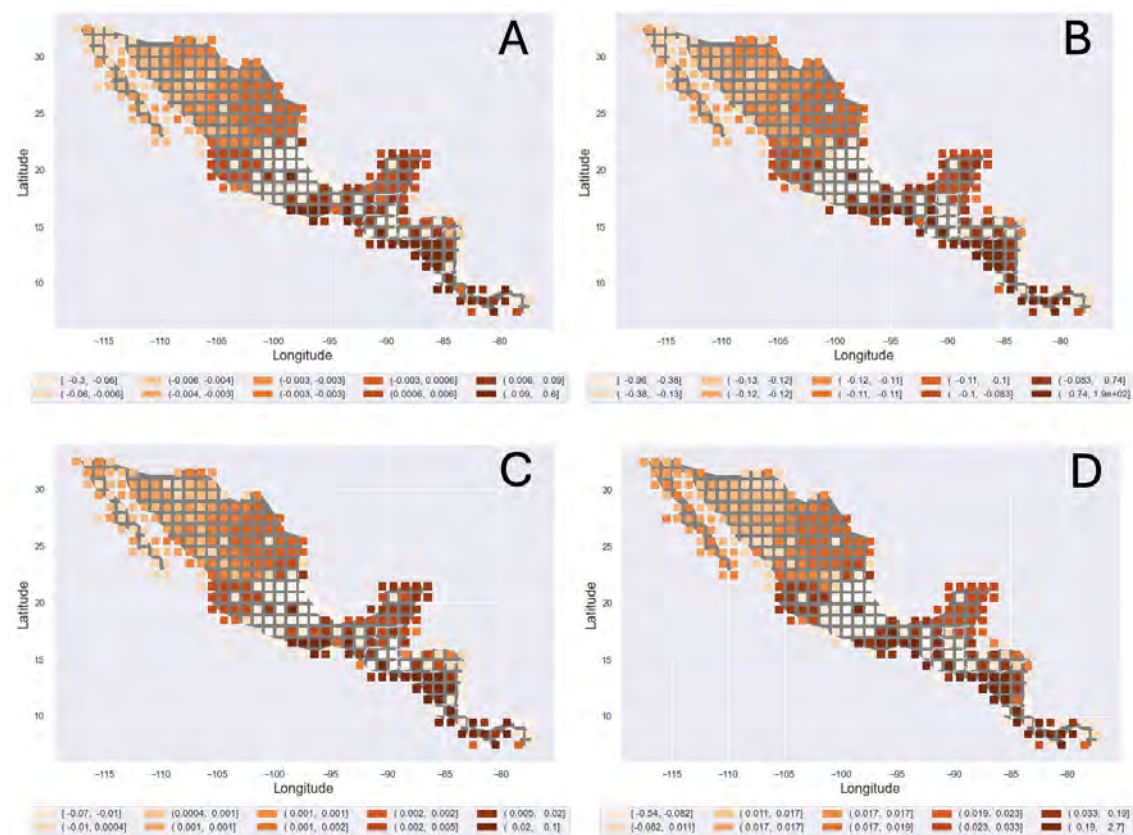
Source: Author's Calculations.

Notes: Cell percentage difference of the 100-year average of the variable with respect to baseline. Variables: Productivity in panels A and B, for Counterfactuals II and III, respectively. Population flows in panels C and D for Counterfactuals II and III respectively. Color scale in deciles. High decile values are darker.

Figures 1.20, 1.21, and 1.22 show the impact of the counterfactuals under the described scenario. The previous results in stages one and two hold along the path of the Pacific Corridor to the south of Mexico. However, the Mexico City neighbor gets the opposite results, with congestion forces dominating the agglomeration ones. These results show the importance of the transportation network beyond a particular transportation mode. Mexico City's neighbor possesses a complete network, including two of the most important sea ports of the country, Veracruz Port on the Caribbean Sea coast and Manzanillo Port on the Pacific Ocean coast. Then, unplugging those two essential parts of the network in the model negatively impacts productivity, redistributing the positive effects of the Pacific Corridor to the south. Therefore, the Mexico City neighbor's logistic advantages are central

to generating high productivity and the spillovers that benefit its surroundings, as suggested by the simulations.

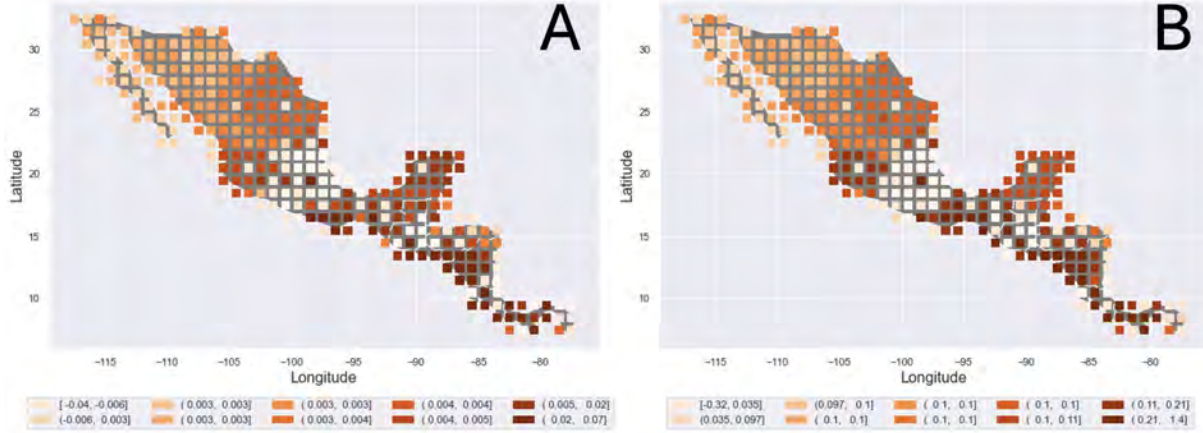
Figure 1.21: Trade Shares and GDP per capita, Stage III



Source: Author's Calculations.

Notes: Cell percentage difference of the 100-year average of the variable with respect to baseline. Variables: Trade Shares in panels A and B for Counterfactuals II and III, respectively. GDP per capita in panels C and D, for Counterfactuals II and III, respectively. Color scale in deciles. High decile values are darker.

Figure 1.22: Impact on Utility, Stage III



Source: Author's Calculations.

Notes: Cell 100-year mean percentage difference between Counterfactual II (A) or Counterfactual III (B) with respect to the baseline. Color scale in deciles. High decile values are darker.

1.5.2.2. Welfare and Annualized Returns

Following [Allen and Arkolakis \(2014\)](#) I perform a back-of-the-envelop calculation of the aggregate effects of the Pacific Corridor. Specifically, the results from the stage one exercise are used to compute the project's annualized rate of return. This calculation is as follows: first, individual cell outputs are aggregated using GDP per capita and population. For this purpose, I use the counterfactual II results given its characteristics discussed in section 1.4. Then, I calculate the Pacific Corridor average impact in utility across all cells belonging to each country. This result is shown in the second column of Table 1.5. Second, using aggregate GDP data from the World Bank, shown in column 3, I compute the monetary welfare impact shown in column 4, which is the product of the utility impact times the GDP. Table 1.5 also shows how big Mexico's economy is compared to other countries in the region. It also shows that El Salvador is obtaining the highest benefits from the Pacific Corridor project. Conversely, Panama obtains the least benefit from it.

Table 1.5: Country Welfare Impact

Country	Utility Impact	GDP	Monetary Welfare Impact
Mexico	0.52%	\$707.91	\$3,699
Guatemala	1.20%	\$19.29	\$228
Belize	0.03%	\$1.13	\$0.34
El Salvador	3.20%	\$11.78	\$378
Honduras	0.52%	\$7.19	\$38
Nicaragua	1.20%	\$5.11	\$61
Costa Rica	2.52%	\$15.01	\$378
Panama	0.44%	\$12.30	\$54
Total			\$4,836
Total*			\$1,137

Source: Column 3 World Bank (GDP Year 2000, US Billions). Column 4 Author Calculations, column 2 times column 3, US Millions.

Notes: Total is the summation of the impact value for all countries and Total* excludes Mexico.

Table 1.6 shows the calculations of the annualized returns. The annualized return is calculated: first, find the difference between the total monetary welfare impact value minus the annual maintenance and financial costs. Then, find the ratio between the result of the difference and the total investment amount. I calculate results with and without Mexico; the effect can be blurred in other countries, given its economic size. Using data from the IADB transportation unit of the maintenance and financial costs of the Pacific Corridor and the investment amount, the gap between annual income and the costs is around 549% for the region and 29% excluding Mexico. The annualized return of the investment is 75% for the region and 4,8% excluding Mexico. Then, the project has a positive rentability, a central element to obtaining the necessary financing. According to the IADB Transportation Unit, this return is two times bigger than the one calculated using CBA approaches the rate that excludes Mexico, and such difference is explained by the ability of the model to account for a set of indirect effects, as shown above.

Table 1.6: Costs, Investment and Annualized Returns

Annual Maintenance and Financial Costs	\$880
Total Investment amount	\$5,300
% Gap Annual Income vs Costs	549%
Annualized Return Rate	75%
% Gap Annual Income vs Costs*	29.20%
Annualized Return Rate*	4.85%

Source: Rows 1 & 2 IADB Transportation Unit. Rows 3 & 4 author's calculation.

Notes: Annualized return is $\frac{(\text{monetary welfare} - \text{annual maintenance costs})}{\text{Total Investment}} \times 100$

1.6. Conclusions

Infrastructure projects are expensive. Thus, it is crucial to understand the effects they can generate on the spatial distribution of the economy. In this chapter, I have used the dynamic spatial general equilibrium model of [Desmet et al. \(2018\)](#) to evaluate the impact of the Pacific Corridor in Central America. The simulations suggest the project's benefits are limited to a subset of cells in the neighbor's region. Agglomeration forces generated by the technology and productivity process tend to benefit places that are initially more productive than others, like Mexico City's area. As the distance between a cell and the Pacific Corridor increases, its benefits are null or negative. The shift in productivity leads to changes in the distribution of population, then induces changes in the GDP per capita, utility, and finally, changes in each cell's trade shares.

On its way to the south of Mexico, the cells affected by the Pacific Corridor projects tend to show positive benefits but are smaller than those of Mexico City's area. This suggests that in such places, the congestion effects on amenities could offset the agglomeration forces.' benefits, limiting the ability to attract the necessary investment to take advantage of the infrastructure. The neighbors Mexico City and Puebla capture most of the benefits. The advantageous initial conditions attract the most positive migration flows, concentrating the economic activity on that hub.

These results align with [Banerjee et al. \(2020\)](#) in the proximity to the infrastructure. Also, with the findings of positive effects over the GDP of [Fajgelbaum and Redding \(2022\)](#) and [Zhang et al. \(2020\)](#). Conversely, I do not find significant effects on growth, as [Sánchez and Méndez \(2000\)](#) or [Hong et al. \(2011\)](#). Other studies focused on the logistics performed by IADB associate consulting firms have found that San Salvador is the most benefited country of the region by positive increases in regional exports and usage of the Pacific Corridor to ship those exports. Conversely, Panama receives fewer benefits.³ Panama’s regional exports remain the same, and its Pacific Corridor usage is the least among the region’s countries. This result is aligned with the calculations of the welfare impacts in Table 1.5, as discussed above. Such studies using different methodologies and approaches provide external validity to this exercise.

This chapter has shown the capability of the model to simulate plausible counterfactual scenarios, generating results for a set of variables that allow policy recommendations and analysis. As the CBA, this model has limitations but also robust roots in theory and the tools to generate a wide variety of results that account for several indirect effects that are not considered in other methods. This proposed methodology should be used as a complementary tool for the existing techniques, as suggested by [Vickerman \(2007\)](#). The Pacific Corridor served as a first effort to test this approach, and this chapter is a first attempt to set the basis for the future use of this model in Impact Evaluations where data limitations prevent the use of the empirical methods or as a complement to them. This methodology delivers a wider variety of outputs than the CBA, though the possibility of creating counterfactuals as in the Impact Evaluation. In the future, new databases will allow the production of empirical tests of this methodology and other projects, large enough to be a good fit to test this model.

³Slott Consulting. “Operational Plan to Upgrade the Pacific Logistic Corridor in Mesoamerican Countries.” IADB 2018.

CHAPTER 2

Quantifying the Border Effect: A Simulation Approach

2.1. Introduction

The geographical economy literature has been trying to understand the role, impact, and consequences of political borders in trade, migration, and the overall geographical distribution of economic activity. Borders can be artificial or natural barriers that affect the distribution of economic activity ([Nagy \(2015\)](#)). This phenomenon has been widely documented using natural experiments, such as the creation of the European Union or the reunification of Germany. However, the effect of such barriers in regions where these borders have not changed in a long time, like Central America, is uncertain.

Central or Meso-America is a region with short and abundant borders and a lack of infrastructure to manage them. The region comprises seven countries, from Guatemala to Panama, and occupies an area of approximately a third of Mexico's surface size. This means eight national borders across the region. Currently, there are no trade agreements between them. Besides other transport and social infrastructure needs, the customs and border controls lack effective administration and infrastructure capacity. According to the Inter-American Development Bank (IADB), the most problematic border issue is not the tariffs but the time delay. This time delay happens because local transportation workers' unions don't allow foreign trucks to pass the border in an attempt to protect their jobs. Therefore, a shipment must be unloaded and re-loaded again at the border. In addition, the physical capacity of the border customs is not high enough to complete this process quickly, increasing the time delay.

The regional governments have recognized this problem. Therefore, they agreed to improve integration and trade by implementing an investment plan focused on road infrastructure and optimization of the border controls. This project is the “Puebla-Panama Plan” signed by the beginning of the twenty-first century. Unfortunately, its implementation is limited almost two and a half decades later. Table 2.1 shows the average border time delay for six countries using data from 17 of Central America’s most important customs and border controls, in terms of traffic, from a total of 47 border crossings. This data was collected by the Secretary for Central America Economic Integration (SIECA) using its own field surveys and official sources¹ and provided by the IADB.

Table 2.1: Average Border Time Delay Freight (Hours)

Country	Average Import Time	Average Export Time	Min Any	Max Any
Guatemala	15.50	12.60	1.00	24.00
El Salvador	2.30	2.75	0.90	16.00
Honduras	2.16	0.90	0.95	2.16
Nicaragua	3.60	2.25	1.00	6.00
Costa Rica	3.00	3.80	1.30	24.00
Panama	15.30	2.25	0.30	17.00
Total	41.86	24.55	5.45	89.16

Source: SIECA report “Estudio de Tiempos y Despacho (ETD) Regional 2021”. Highway Customs and Border Controls.

Compared to one of the US - Mexico border and customs controls, between San Diego (US) and Tijuana (Mexico), as shown in Table 2.2, the Central America, border time delay is more significant. For example, suppose a truck carries a freight shipment from North Dakota (US) to Mexico City (Mexico). Let’s assume that this truck drives in a straight line across the US to Mexico City over a distance of approximately 1850 miles. It passes through one border control, which delays its travel by about Forty-five minutes, averaging inbound and outbound shipments. Suppose a similar truck carries a shipment, driving in a straight line

¹“Estudio de Tiempos y Despachos Regional (ETD) 2021”. Highway Customs and Border Controls. This document is available on request.

from Mexico City to Panama City (Panama), over a distance of around 1500 miles. This truck will pass through 6 border controls, with a mean delay of 33 hours, averaging over import and export average times. This simple exercise implies that for a travel distance in Central America that is around 20% shorter than that between the US and Mexico, the border time delay is 44 times higher².

Table 2.2: Border Time Delay Freight (Hours)

<i>Type</i>	<i>Average</i>	<i>Min</i>	<i>Max</i>
Outbound	0.32	0.17	0.61
Inbound	0.58	0.10	1.07

Source: U.S. Department of Transportation.

The above example for regional trade also means that a shipment's travel costs should be higher in Central America compared to the US - Mexico shipments. According to [Allen and Arkolakis \(2014\)](#) and others, distance is a crucial explanatory variable for trade or travel costs. However, as shown above, distances in CA are smaller compared to the US - Mexico region. Then, the driving difference in this case is travel time. Intuitively, following [Allen and Arkolakis \(2022\)](#) speed, and ultimately travel time, explains travel costs. Border and customs controls in Central America are accountable for such time delays, in addition to road quality, availability of transportation modes, and distance. This finding can help explain the low intra-regional trade, besides trade agreements and each country's trade policy. According to the IADB, only 24% of the region's exports and 17% of imports are intra-regional. Thus, around one-fifth of the region's trade stays in the region, and 95% of it is transported using roads. Mainly the Pacific Corridor.³

²45 minutes = 3/4 hour. Then $33/(3/4) = 44$

³IADB Annual Transportation Unit Workshop. External consultant reports

Given the above findings, accounting for the border effects in the Impact Evaluation of the Pacific Corridor context is essential. In the previous chapter, I used the model of [Desmet et al. \(2018\)](#) to show how it can be used to perform an Economic Impact Evaluation. There, I focused exclusively on the effects of the Pacific Corridor infrastructure investment over the geographical distribution of the economic activity and the agent's decisions of where to live in Central America. However, the baseline scenario assumes a borderless surface, omitting its effect on trade costs. Therefore, this chapter will incorporate these border effects into [Desmet et al. \(2018\)](#) for a more realistic and accurate impact evaluation of this case. The existing literature shows that borders increase travel time and transportation costs, reducing trade flow across countries. How can these barriers affect this region's development? Will the Pacific Corridor have the expected benefits shown in the previous chapter if borders are accounted for? Which policy objective should be implemented, between building roads or making their border controls more efficient?

To measure the border effect, I expand the trade cost setup in [Desmet et al. \(2018\)](#) to include the borders. The intuition on this expansion is based on the framework of [Allen and Arkolakis \(2014\)](#), who provide the methodological tools to create positive walls within an iceberg transportation cost function. Then, I used a novel database from the IADB, which accounts for each pair of cells' origin and destination travel time. I exploit two travel time measurements, with and without border and customs time delay, to calibrate the parameter of interest. The objective of the calibration is to determine the model's optimal trade cost matrix replicates, on average, the observed travel time differences. After some additional adjustments that enhance the connection of the model to the actual features of Central America, the simulated optimal trade cost matrix replicates up to 89% of the variation of the observed travel time delay.

After the calibration process, the simulations show that a hypothetical scenario of eliminating all the borders can scale up the aggregate and per capita GDP levels by 1.80% on

average in a period of 100 years. This impact is more important than preserving the borders and, alternatively, building the Pacific Corridor is a scenario in which the aggregate GDP, on average, increases around 0.98%. However, if both scenarios are implemented, the combined impact increases the aggregate GDP by around 3.06% on average. Therefore, compared to Chapter I's conclusions, the Pacific Corridor's effect on GDP is attenuated, showing that borders can limit the benefits of such infrastructure. In addition, these results suggest that the role of the borders in Central America is a critical element that reduces the economic activity dynamic in the region. It is important to note that this is an extreme scenario, like recreating the US inter-state border dynamic, which implies a significant reduction of travel time costs, as illustrated in the example above. This impact comes with a concentration of economic activity in the most populated areas.

This research is related to the literature that studies the border effect. Since [McCallum \(1995\)](#) research on the US-Canada trade and the significative negative effect of the border on international trade, the literature has evolved to provide theoretical support to the empirical findings. For example, [Anderson and Van Wincoop \(2003\)](#) add economic structure to the empirical strategy, finding similar results than [McCallum \(1995\)](#) of negative effects in trade, but in a reduced magnitude. The most common setup in the literature involves using each country's GDP and measurements of remoteness, such as the distance across locations and dummy variables, to account for the fixed effect of the borders. For example, [Redding and Sturm \(2008\)](#) try to understand the effect of the division of Germany after World War II, and the afterward reunification over trade. They also use a theoretical framework based on the gravity equations of market access and a trade costs function defined in distance, finding a decline in population growth of the West German cities near the border. Similarly, [Brakman et al. \(2011\)](#) investigates the border effect of the enlargement integration of the European Union over time in cities and regions located near such vanishing borders. Their findings show a positive shift in population growth along the former border's cities. Adding road distance and travel time to their empirical strategy, [Braconier and Pisu \(2013\)](#) uses a

similar strategy to account for the border effect in Europe, finding negative effects for those two variables in nearby locations separated by a country border. [Santamaría et al. \(2021\)](#) attempts to capture the effect of trade on the European borders to measure the effectiveness of erasing their political borders. Their findings show that borders are equivalent to a tariff of 32.5%. [Nikolic and Chilosi \(2023\)](#) use this framework to understand the effect of the border between Serbia and the Austro-Hungarian Empire found increasing price gaps that vanished when the border disappeared.

This chapter is also related to the literature on transportation costs. In particular, the popular work of [Allen and Arkolakis \(2014\)](#) that sets a transportation cost structure based on both multimodal transportation matrix and their relative weight on costs depending on the bilateral trade across the US. [Desmet et al. \(2018\)](#) added accessibility to the multimodal transportation costs matrix. [Allen and Arkolakis \(2022\)](#) adapted their previous model to account for welfare effects when there are improvements in the quality of the road infrastructure, endogenizing the transportation costs. Given that the movement of goods from origin to destination occurs over multiple modes of transportation, [Fuchs and Wong \(2022\)](#) extended [Allen and Arkolakis \(2022\)](#) framework to account for multimodal transport networks and their impact on infrastructure investments, extending the routing-based formulation of transport cost to allow for multi and intermodal routing. One of their key contributions is the incorporation of time delays in the transportation nodes.⁴ Much of the application of this technique relies on the objective, and the data availability to calibrate or estimate the required parameters, for example [Nikolic and Chilosi \(2023\)](#) rely on [Allen and Arkolakis \(2014\)](#) to account for trade costs, on their research regarding border effects mentioned above.

Therefore, the contribution of this paper is to introduce the border effect within the High-Resolution spatial dynamic general equilibrium framework from [Desmet et al. \(2018\)](#). This contribution will extend the possibility of running counterfactual analysis and increase

⁴A node in this context is a point in the multimodal transportation network where a shipment needs to change from mode. For example, from road to water.

the simulation’s accuracy, improving the quality of the policy recommendations in the case of Central America. This chapter is divided as follows: In section 2.2, I discuss the concept of the iceberg transport costs, its relation to the border effect, and the specific features of [Allen and Arkolakis \(2014\)](#). Then, I show its implementation in [Desmet et al. \(2018\)](#) framework. Section 2.3 shows the calibration process and results. Section 2.4 analyzes the counterfactual exercise and its results. Section 2.5 concludes, and section 2.6 discusses future research.

2.2. Transport Costs and Border Effect: Theory

2.2.1. The Iceberg Costs

Iceberg trade, transport, or shipping costs are usually defined as a function that maps some characteristic of two geographical locations, where one is the origin and the other the destination, to express costs. Initially, it was interpreted as the real value amount of goods that the importer or consumer pays to get one unit of a good. This idea was proposed by [Samuelson \(1952\)](#) regarding physical units within a trade model. Then, [Krugman \(1991\)](#) and [Krugman \(1992\)](#) introduced the current version, where such costs are conceived as a continuously increasing function in the distance between origin and destination. The iceberg costs are usually employed due to their adaptability in the general equilibrium models. The function is often presented in an exponential or a multiplicative log-linear form. Their convex-with-distance delivered-price⁵ properties are a natural counterbalance to agglomeration economies of scale, as shown by [McCann \(2005\)](#), usually joining a gravity equation to determine a general equilibrium involving trade and other outputs.

The iceberg transportation costs do not fully reflect the practical transport rates and fee structure used by transportation firms. Even, after the incorporation of distance in the post-1991 transportation economics literature, their structure still misses essential items such as

⁵i.e., the higher the distance between a pair of origin and destination locations, the higher the price at the destination when delivered

freight volume and weight, tariffs, and tolls. However, as suggested by [McCann \(2005\)](#), given such incompatibility of such practical structure to the general equilibrium models, the economic geography models interpret the iceberg structure as capable of incorporating all forms of distance costs transactions. For example, trade, information costs, institutional barriers, tariff barriers, quality standards, and cultural and linguistic differences. For example, [Allen and Arkolakis \(2014\)](#) use language similarity of the origin and destination locations pairs as a control variable in the estimation of the parameters associated with their iceberg transportation costs, which depend mainly on distance. Even when the modeling of the transport costs still do not fully reflect reality, it has evolved to be closer by capturing some of the elements that were lacking at its beginnings.

Some of the most recent transportation economics literature, briefly shown above, has related such costs with the road instead of linear distance across locations, multimodal transportation, congestion, time, or speed. Furthermore, [Fajgelbaum and Schaal \(2020\)](#) developed a general equilibrium spatial model where trade costs are an outcome rather than a primitive, depending on the transportation network, infrastructure, and shipment characteristics. [Allen and Arkolakis \(2022\)](#) developed a general equilibrium spatial framework featuring endogenous transportation costs. This improvement allows individuals to choose a location and route to source each good, considering traffic congestion in the transportation network. Therefore, given a measurement of infrastructure, such congestion will modify the economic activity's equilibrium distribution across the geography.

2.2.2. Iceberg Costs and The Border Effect.

One of the first theoretical bridges linking the iceberg costs and the border effect was made by [Anderson and Van Wincoop \(2003\)](#) by introducing the trade cost factor between two locations r and s as $p_{rs} = p_r \varsigma_{rs}$. The first term is the price of region r goods for region s consumers, which equals the exporter's supply price times the trade cost factor ς_{rs} . The latter

could represent a set of different costs incurred by the exporter, such as information, design, legal, regulatory, and transport costs. Then, to account for the border effect, they define $\varsigma_{rs} = b_{rs}d_{rs}^\rho$, where $b_{rs} = 1$ if regions r and s are located in the same country. Otherwise, $b_{rs} = 1 + \alpha$, where α represents the tariff equivalent of the border barrier. d_{rs}^ρ stands for distance, with ρ as the elasticity of the trade costs factor to distance.

After [Anderson and Van Wincoop \(2003\)](#), the literature has employed similar strategies in some cases, with a direct link between iceberg transportation costs and the border effect. For example, to understand the spatial distribution of transport infrastructure, [Felbermayr and Tarasov \(2022\)](#) follow [Anderson and Van Wincoop \(2003\)](#) but modeling the iceberg transportation costs adding an aggregate infrastructure measurement. Then, they add border friction to the cost of delivering one unit of a product produced at a foreign location to a domestic location. The border effect is interpreted there as an ad valorem tax. [Coughlin and Novy \(2021\)](#) depart from an exponential trade costs function $\varsigma_{rs}^{1-\sigma} = \exp(\zeta BORDER_{rs}) dist_{rs}^\rho$, where $BORDER$ can either represent a domestic or international border to use the empirical dummy approach for borders. As in the previous cases, ς_{rs} represents the trade costs, and $dist_{rs}^\rho$ the bilateral distance. σ , ζ and ρ determine the sensibility of the log-costs to changes in $BORDER$ and $dist_{rs}$ respectively. To pinning down the border effect parameter ζ , the authors compare the trade flow across the border to the flow within the border. A Similar strategy is used by [Nagy \(2015\)](#) When examining the effects of the border on the geographical distribution of population after the border changes in Hungary in 1920, the iceberg transportation costs can be directly used to incorporate the border effect when studying their effect on trade, either for theoretical or empirical applications.

In another instance, the link is indirect; the iceberg cost is used there, but not as a direct tool to account for the border effect. When [Allen et al. \(2018\)](#) try to account for the impact on migration and labor of the border walls between the USA and Mexico, they use the exact iceberg transportation costs as in [Allen and Arkolakis \(2014\)](#) to measure trade costs. Then,

to estimate the bilateral trade frictions, they introduce the dummy variable in their empirical strategy, finding no effect on trade from the wall expansion. Trying to quantify the impact of more significant trade and transport integration in Africa, [Fontagné et al. \(2023\)](#) measures the transportation times between large cities in African countries and the rest of the world and integrates delays at sea or land ports and freight loading and unloading times. These times can be approximated by days to cross the border data. Then, the authors derive the shortest transport time between a pair of cities.

In summary, the iceberg costs are a standard and practical methodology to model transport costs, with the ability to incorporate a variety of them. The iceberg costs are mainly related to distance. But they can also account for speed, time, infrastructure, or congestion. The introduction of time-related variables such as speed, congestion, or travel time in the iceberg cost setup has been widespread recently, opening a new dimension to account for such costs. The iceberg costs framework has been used as a base to account for the border effect, both for empirical and theoretical applications, either directly or indirectly.

Given all the above discussion, in this chapter, I propose a direct incorporation of the border effect into the iceberg transportation cost within the framework of [Desmet et al. \(2018\)](#). Their trade costs are based in [Allen and Arkolakis \(2014\)](#) taking advantage of the multimodal features and adding accessibility to the infrastructure. I will use measurements of time delay available at the novel database from the IADB, in a similar spirit to [Fuchs and Wong \(2022\)](#) and [Fontagné et al. \(2023\)](#), but preserving the exogenous characteristics and structure of the trade costs matrix in [Desmet et al. \(2018\)](#), assimilating their nodes or unloading - loading times as borders here. I will start by analyzing the [Allen and Arkolakis \(2014\)](#) framework and then I will move to implement the border's extension in [Desmet et al. \(2018\)](#) to conduct a counterfactual exercise to the Central America case described above.

2.2.3. From Allen & Arkolakis (2014) to Desmet et al. (2018)

Allen and Arkolakis (2014) perform a quantitative and empirical analysis estimating the fraction of spatial inequality of income in the US due to variations in trade costs. Their framework relies on economic modeling using a gravity structure of international trade, labor mobility, and geographic micro-foundation for bilateral trade costs. Such micro-foundation assumes the existence of a topography of instantaneous trade costs over the surface that rely on each location's characteristics. Assuming that bilateral trade costs are the total expenses incurred by traveling from an origin to a destination along the least-cost route, it can be computed by accumulating the instantaneous costs, using the Fast Marching Algorithm⁶ to choose such an optimal path. This computation implies a unique mapping from instantaneous trade costs to bilateral trade costs in the space. The transportation networks can be incorporated by assuming that the instantaneous costs are lower where such infrastructure exists. Therefore, each trader can optimally choose the transportation mode from those available at each location, minimizing the shipping costs.

The implementation of the above characteristics is summarized as follows. Suppose there exists $m \in \{1, \dots, M\}$ modes of transport, a pair of origin $r \in S$ and destination $s \in S$, locations, with S representing the set of all locations. The bilateral geographical trade costs $GC(r, s)_{t,m}$ are represented by (2.1), the iceberg costs of a trader t shipping good from r to s using the mode m to minimize such costs. The mode-specific distances $d_m(r, s)$ capture the costs of traveling via different modes of travel. ς_m is the mode-specific variable cost. f_m is the mode-specific fixed cost concerning distance, and ν_{tm} is a trader-mode-specific cost. Intuitively, the exponential form shows that a given increase in distance results in a larger increase in the total geographic trade costs.

$$GC(r, s)_{t,m} = e^{(\varsigma_m d_m(r, s) + f_m + \nu_{tm})} \quad (2.1)$$

⁶Gabriel Peyre's Fast Marching Toolbox for Matlab.

This implementation of the geographic trade costs has two properties; first, geographic costs are symmetrical: Traveling over a particular point incurs the exact costs regarding the direction. Second, given the smoothness of the surface, nearby locations will face trade costs similar to those of all other locations. These two properties are convenient for simplifying the model and the computational effort. However, they are not necessarily accurate. It can be the case that traveling between two locations implies different travel times depending on the direction due to the geography⁷, or to other specific barriers⁸. In addition, two nearby locations can have different trade costs if they belong to different administrative areas. I stick to these properties in this chapter, but future research could relax such assumptions. To estimate the bilateral trade costs, a detailed set of geographical information⁹ is combined with mode-specific bilateral trade shares, inferring the relative cost of traveling using different modes of transportation, using a discrete choice framework to avoid endogeneity concerns. These parameters are used in [Desmet et al. \(2018\)](#) as discussed below.

Finally, [Allen and Arkolakis \(2014\)](#) suggest that incorporating borders within an iceberg, trade or transportation cost framework requires the following condition: *“Borders can be incorporated by constructing (positive measure¹⁰) “walls” between regions where the instantaneous trade costs are large; such “walls” can also be placed alongside roads or railroads so that they are only accessible at a finite number of entrance ramps or stations”*. These requirements are central to the intuition of the proposal of incorporating the border effects that I describe in the following paragraphs.

When [Desmet et al. \(2018\)](#) adapted [Allen and Arkolakis \(2014\)](#) framework to their purposes, the main parameters for Major Roads, Rail and Water, estimated by the latter, were augmented, introducing Other Roads, No Road, No Rail, and No Water. These additional

⁷Suppose a given place is located over a mountain and another in a valley. If the transportation mode is road, the speed of a vehicle depends on the direction given the geographical conditions.

⁸Like borders, administrative controls, tolls, etc.

⁹road, railroad, water & aerial networks

¹⁰*i.e. increasing the costs*

parameters preserve the original estimation features. As shown in Chapter I, initially, each cell r representing a location was characterized as having or not having access to each transportation mode. This is, for example $rail(r) = [1, 0]$, where having access to rails means $rail(r) = 1$, and no access is by default $rail(r) = 0$. This creates a multimodal transport cost matrix, computing the cost by the accumulation of the participation of each mode on them, weighting each by its corresponding accessibility measurement. This methodology resembles a Cobb-Douglas transportation cost technology that complies with the iceberg costs requirements. Then, following [Desmet et al. \(2018\)](#), the expression for the instantaneous transportation costs ς of passing through cell r is:

$$\begin{aligned} \varsigma(r) = & \left(\varsigma_{rail}^{rail(r)} * \varsigma_{no_rail}^{[1-rail(r)]} \right) * \\ & \left(\varsigma_{major_road}^{major_road(r)} * \varsigma_{other_road}^{[all_road(r)-major_road(r)]} * \varsigma_{no_road}^{[1-all_road(r)]} \right) * \\ & \left(\varsigma_{water}^{water(r)} * \varsigma_{no_water}^{[1-water(r)]} \right) \end{aligned} \quad (2.2)$$

Rearranging in logs terms:

$$\begin{aligned} \log \varsigma(r) = & (rail(r) \log(\varsigma_{rail}) + [1 - rail(r)] \log(\varsigma_{no_rail})) + (major_road(r) \log(\varsigma_{major_road}) + \\ & [all_road(r) - major_road(r)] \log(\varsigma_{other_road}) + [1 - all_road(r)] \log(\varsigma_{no_road})) + \\ & (water(r) \log(\varsigma_{water}) + [1 - water(r)] \log(\varsigma_{no_water})) \end{aligned} \quad (2.3)$$

Then, for a given location $r = r_0$, if there is a major road ($major_road(r) = 1$), a rail road $rail(r) = 1$ but, no other roads ($other_road(r) = all_road(r) - major_road(r) = 0$) and no water ways ($water(r) = 0$), the instantaneous costs for that cell [\(2.3\)](#) becomes:

$$\log \varsigma(r_0) = (\log(\varsigma_{rail})) + (\log(\varsigma_{major_road})) + (\log(\varsigma_{no_water}))$$

Or simply $\varsigma(r_0) = (\varsigma_{rail})(\varsigma_{major_road})(\varsigma_{no_water})$. This expression preserves the multiplicative nature of the iceberg costs. Then, given the higher resolution of the transportation mode access data available¹¹, aggregated to be compatible with the model's cell size. Now $rail(r) \in [0, 1]$ is the fraction of smaller cells within cell r that have access to the rail network. Following this argument, disaggregating the trade costs for each transport mode, define:

$$\varsigma(r) = \varsigma(r)_{rail} * \varsigma(r)_{roads} * \varsigma(r)_{water}$$

With:

$$\varsigma(r)_{rail} = \varsigma_{rail}^{rail(r)} * \varsigma_{no_rail}^{[1-rail(r)]}$$

$$\varsigma(r)_{roads} = \varsigma_{major_road}^{major_road(r)} * \varsigma_{other_road}^{[all_road(r)-major_road(r)]} * \varsigma_{no_road}^{[1-all_road(r)]}$$

$$\varsigma(r)_{water} = \varsigma_{water}^{water(r)} * \varsigma_{no_water}^{[1-water(r)]}.$$

Then, using rail as example, define $rail(r) = \left(\frac{[100]_{i=1} \sum rail(r_i)}{100} \right) \geq 0$. The denominator reflects the fact that there are a total of 100 subcells in each cell. With $rail(r_i) = 1$ if the subcell $i \subset r$ have access to railroads, 0 otherwise, we have that:

$$\log \varsigma(r)_{rail} = rail(r) \log \varsigma_{rail} + (1 - rail(r)) \log \varsigma_{no_rail}, \text{ then,}$$

¹¹Recall, as shown in chapter I, this data has a higher resolution at a $0.1^\circ \times 0.1^\circ$ level. It is available at www.natureearthdata.com

$$\log \varsigma(r)_{rail} = \left(\frac{[1 \ 00]i = 1 \sum rail(r_i)}{100} \right) \log \varsigma_{rail} + \left(1 - \left(\frac{[1 \ 00]i = 1 \sum rail(r_i)}{100} \right) \right) \log \varsigma_{no_rail} \quad (2.4)$$

Intuitively, if the number of subcells with access to rail increases, the weight into the costs of rails increases, and the weight of no rail shrinks. Similarly, with the other transportation modes. In a broad view, if for a given cell, the amount of access to railroads, roads and waterways exogenously increase, then the weight of such modes into the calculation of the instantaneous costs is increased. Using equation (2.3) and taking the partial derivative of the instantaneous costs for each transportation mode yields:

$$\frac{\partial \log \varsigma(r)}{\partial rail(r)} = \log \varsigma_{rail} - \log \varsigma_{no_rail} < 0 \text{ if } \log \varsigma_{no_rail} > \log \varsigma_{rail}$$

$$\frac{\partial \log \varsigma(r)}{\partial major_road(r)} = \log(\varsigma_{major_road}) - \log(\varsigma_{no_road}) < 0 \text{ if } \log \varsigma_{no_road} > \log \varsigma_{major_road}$$

$$\frac{\partial \varsigma(r)}{\partial other_road(r)} = \log(\varsigma_{other_road}) - \log(\varsigma_{no_road}) < 0 \text{ if } \log(\varsigma_{no_road}) > \log(\varsigma_{other_road})$$

$$\frac{\partial \log \varsigma(r)}{\partial water(r)} = \log(\varsigma_{water}) - \log(\varsigma_{no_water}) < 0 \text{ if } \log \varsigma_{no_water} > \log \varsigma_{water}$$

All these conditions depend on the value of the parameters that define each transportation mode. Taking the parameters chosen by [Desmet et al. \(2018\)](#) All the conditions can be verified and estimated by [Allen and Arkolakis \(2014\)](#) shown in Table (A.1) in the appendix. Therefore, increasing the accessibility of any transportation mode will reduce the instantaneous trade costs.

2.2.4. Adding the Border Effect in the Instantaneous Trade Costs

Recalling [Allen and Arkolakis \(2014\)](#), any proposal regarding accounting for the border effects should fit into the iceberg cost formulation. In addition, it should be a positive

amount that creates a wall, increasing trade costs. It should also account for trade costs if the cell contains a border and is not the origin or the destination. Alternatively, if the optimal path between two cells requires passing through the cell that contains a border, then the border effect should be accounted for. Given the mentioned conditions, it is possible to set a compatible way to implement such costs in the multimodal instantaneous trade costs matrix of [Desmet et al. \(2018\)](#). Suppose that the parameter ς_{border} accounts for the border effect in the region. Then, departing from equation (2.3), adding a variable for border:

$$\begin{aligned}
\log \varsigma_b(r) = & (rail(r)\log(\varsigma_{rail}) + [1 - rail(r)]\log(\varsigma_{no_rail})) + (major_road(r)\log(\varsigma_{major_road}) + \\
& [1 - other_road(r)]\log(\varsigma_{other_road}) + [1 - major_road(r) - other_road(r)]\log(\varsigma_{no_road})) \\
& + (water(r)\log(\varsigma_{water}) + [1 - water(r)]\log(\varsigma_{no_water})) \\
& + border(r)\log(\varsigma_{border})
\end{aligned} \tag{2.5}$$

With:

$$border(r) = \begin{cases} 1 & \text{if } r \text{ contains a border} \\ 0 & \text{otherwise} \end{cases}$$

And, $\varsigma_{border} \in (1, \infty)$

Then, ς_{border} represents the participation on costs of the border due to time delay on crossing it. Intuitively, the borders will be considered another infrastructure component determining the instantaneous costs of crossing a cell r . Taking the derivative of $\log \varsigma_b(r)$ with respect to border yields $\frac{\partial \log \varsigma_b(r)}{\partial border(r)} = \log \varsigma_{border} > 0$ which meets the “positive wall” condition. It also directly affects trade costs, as summarized in the literature above. It

does not directly affect the mobility of the population or the migration flows; it intends to introduce a relevant cost for trade specifically that so far is omitted.

Following [Desmet et al. \(2018\)](#) as shown in chapter I, the trade costs will affect the prices of the varieties produced in r and sold in s . Firms will observe the price shift, altering their maximization programs and probabilities to export. Then, the firm's optimal choice of how many workers to hire will activate the agglomeration forces of productivity. Those forces will generate a reallocation of population, altering each location's income, activating the congestion forces over amenities, and altering the attractiveness of a location. All these changes will determine the time sequence of equilibrium values of each location's productivity, net population flows, GDP per capita, utility, and total trade shares.

Finally, following the aggregation criteria for the transportation modes set by [Desmet et al. \(2018\)](#) to incorporating borders, as the accessibility of roads, etc., define $border(r) = \left(\frac{\sum_{i=1}^{100} border(r_i)}{100} \right)$. This equation represents the proportion of subcells containing border crossings. Then, as shown before, if there's an exogenous increase in infrastructure, say main roads, the instantaneous trade costs should diminish. Now, if there is an increase in border controls, the instantaneous costs should increase. This characteristic determines the weight of borders in the computation of the instantaneous trade costs. Intuitively, borders act as an adverse infrastructure, increasing trade costs and reducing commerce, as the literature on border effects summarized above shows.

2.3. Calibrating The Border Effect

The calibrating exercise aims to set a mapping between the data from travel time border delay and the trade costs matrix from [Desmet et al. \(2018\)](#), using its theoretical features to incorporate the border effect. Therefore, the calibration process departs from the equation (2.5) preserving the value of the parameters for road, rail, etc. The objective is to find a value of $\varsigma_{border} \in (1, \infty)$ that captures the variation in costs due to the travel time border

delay, the border effect, given the current information in $\varsigma_b(r)$ that comes from [Allen and Arkolakis \(2014\)](#) estimation. This establishes a link between such data and the multimodal and accessibility information in $\varsigma_b(r)$. The value of ς_{border} is not intrinsically relevant, what matters is that given such value, after choosing the least cost path using the Fast Marching Algorithm as shown in Chapter I, it generates a trade costs matrix $\varsigma_b(r, s)$ capable of replicating as much as possible the increase in travel time costs due to border delays.

The introduction of the border effect in terms of time follows the framework of [Fuchs and Wong \(2022\)](#) and [Fontagné et al. \(2023\)](#) using time delays at borders or transportation nodes as part of the transportation costs. For example, a transportation node is a location on a transportation network where a shipment should change its transportation mode, like a seaport. Then, the time it takes to unload a ship and place a freight shipment on a truck should be part of the costs. That part of the trade cost is not captured by distance or the accessibility to different transportation modes. Therefore, following such a framework, adapted for the Central America case, I assume that the travel time delay at borders should be accounted for in the transportation costs, as is the case for the transportation nodes. I also assume that such cost can be introduced in the equation (2.5) and that ς_{border} can account for the border effect. The first step to calibrate ς_{border} is to find a measurement for the travel time delay due to borders.

To measure the travel time border delay, I exploited a novel database from the IADB. This database consists of measurements of time travel by roads across Central America, including 1229 origin and destination municipalities from Guatemala to Panama. It was built by combining information from the Google Maps API and Open Street Maps to set a detailed map for all regional primary (paved) highway networks. It also uses geographical information from the United Nations Office for the Coordination of Humanitarian Affairs (OCHA) and the IADB Integration and Transport Hub. This database reports the border crossing time delay data from the SIECA report. The information was collected there using

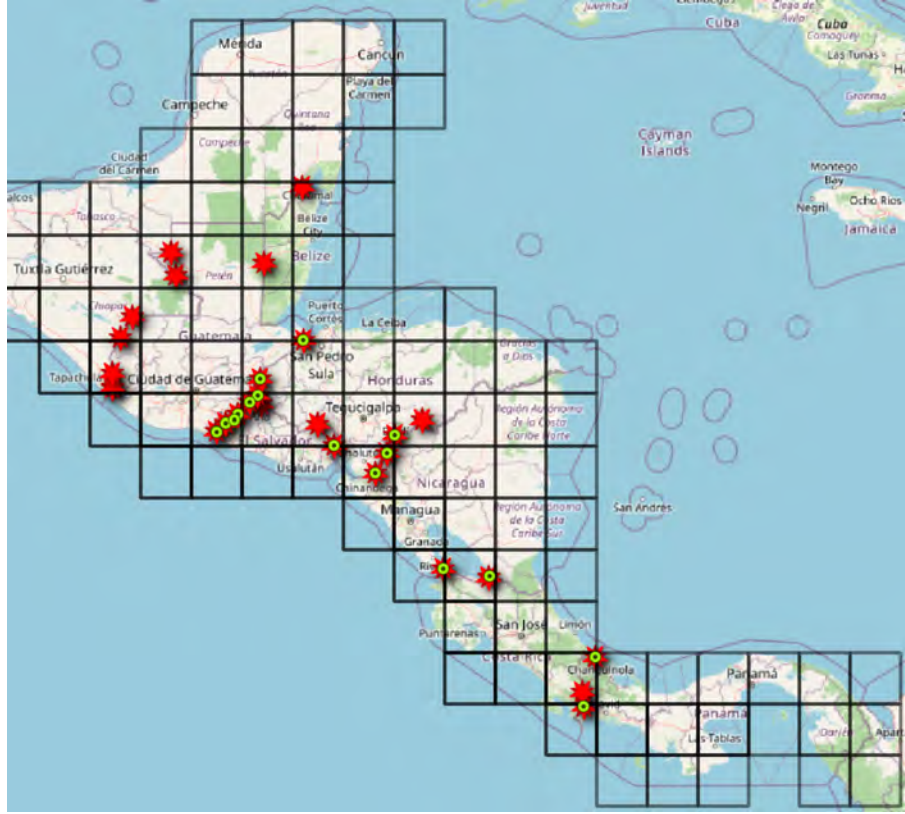
physical surveys in eight main customs controls freight transporters used. The information for the other nine border crossing points is imputed using the data from those initial eight and other official public reports available from each country. It is important to remark that according to the IADB transport unit officials, collecting data in certain areas of the region is difficult due to various factors, including staff security. In addition, some countries lack administrative support and funding to produce and provide such data. Until this research is elaborated, no better data source can measure the delay in border crossing travel time.

The procedure to measure the travel times consists of reproducing the actual transport network using a model embedded in the transportation software Visum.¹² The travel time from location r to s is calculated and calibrated to match Google Maps observed times and routes for 1229 origin and destination municipalities. This implies time travel measurements for 1.509.212 origin and destination pairs. Then, the border delay times are added with information from the “Regional Dispatch and Times Study, Results Report” provided by the IADB and briefly summarized in Table 2.1.¹³

¹²Visum is a commercial software used by transportation consultant firms. It can recreate multimodal transportation networks and is used for transportation planning.

¹³In Spanish: “Estudio de Tiempos y Despachos (ETD) Regional 2021.” SIECA

Figure 2.1: Location of the Included Border Crossing Controls



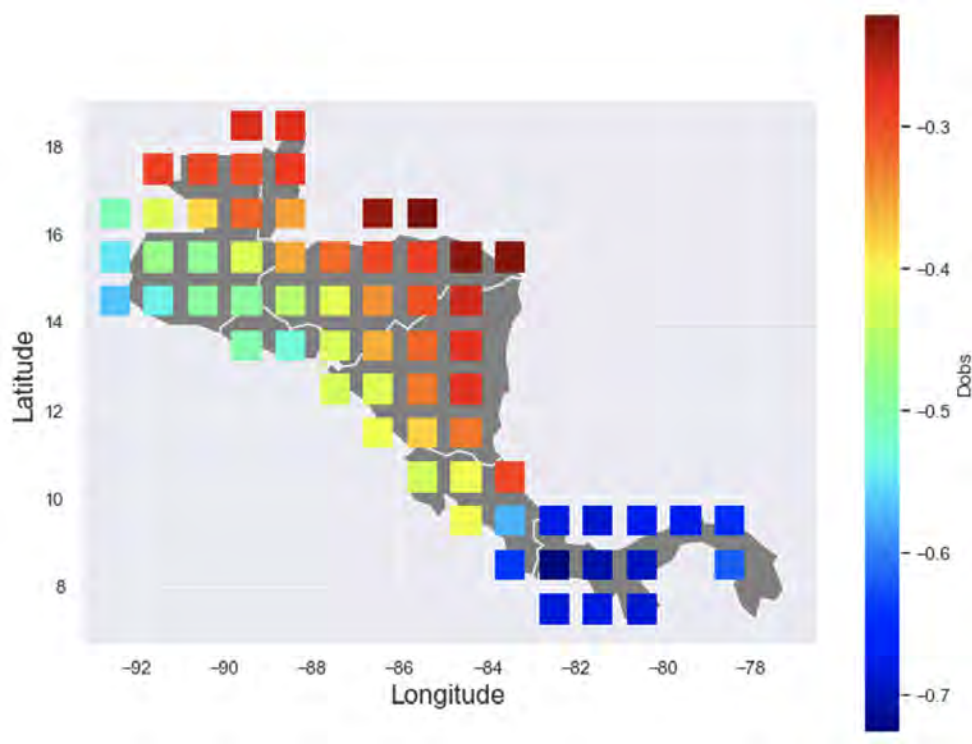
Source: SIECA database, processed in QGIS using Open Street Maps.

Notes: Red stars show an existing border crossing. Green dots show the subsample of those included in the IADB database that are relevant to this research.

The process of adding the borders consists of locating the 17 borders on the road network, as shown in Figure 2.1, and adding the travel time delay of each border to their initial calculations. Such time delay depends on the direction of the shipment, creating two measurements for each origin and destination pair. These two measurements depend on whether a shipment is an export, an import, or just crossing over a country to another destination. Then, to adapt such data for this research, the information is clustered in 63 cells of $1^\circ \times 1^\circ$ corresponding to the size and location of the model's grid, which restricts the simulation exercise to these 63 cells in Central America. The criteria for assigning each municipality to a given cell is the location's proximity to the closer cell's centroid. Each cell corresponds to a model's cell, representing each location r . Thus, the resulting database consists of 3906 origin-to-destination cell pairs.

I observe three measures of travel time (minutes) for each cell's origin and destination pair: travel time without borders, travel time from r to s with borders, and travel time from s to r with borders. Then, as pointed out in section 2.2, I assume symmetry in transport times. Therefore, I use an average of the last two measures to create a unique border travel time delay metric for each cell. These measurements define an observed matrix, $\varsigma^{obs}(r, s)$ of trade costs regarding travel times with two travel time measurements for each cell, one with border delays and one without. This matrix is comparable with the trade costs matrix from [Desmet et al. \(2018\)](#) regarding the cell's size and location in the region. Additionally, given that it consists of travel time observations, it can be assumed that it corresponds to optimal choices made by individuals when deciding their travel paths in the region.

Figure 2.2: Benchmark Observed Travel Time Reduction When Removing Borders



Source: SIECA database and Author's calculations.

Notes: Observed cell time percentage reduction if the border's travel time delay is eliminated in Central America.

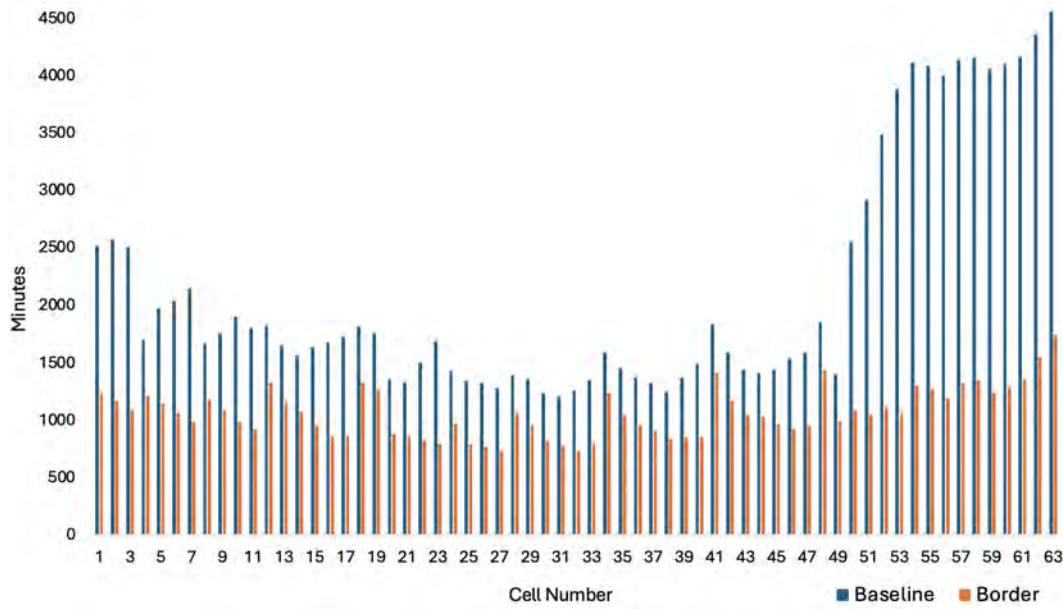
Figure 2.2 shows the cell's observed difference in travel times. The most significant reduction (Blue) occurs in the region's south, and mild reductions (green and yellow) are

observed along the Pacific coast where, according to the IADB, most freight shipments are moved. Most economic activity is close to the Pacific coast, where most capital cities are settled. The Caribbean coast has smaller reductions (orange to red). These regions are primarily natural reserves and natural parks. Figure 2.3 shows a bar chart comparing the average observed travel time with and without borders. The travel time reduction ranges from -22% to -73% minutes. This means reductions from 327 (5.5 hours) to 2817 (47 hours). These results align with the borders' location shown in Figure 2.1. Most border crossings are located close to the Pacific coast and are concentrated in Guatemala, El Salvador, and Honduras. This data and figures are the benchmark for the calibration exercise.

Using those measurements of time travel, I can define a benchmark for the calibration consisting of a weighted average of the time reduction due to removing the borders. Lets set $\zeta^{obs}(r, s)_b$ and $\zeta^{obs}(r, s)_{wb}$ as the matrices for the observed sixty-three cells containing travel time with and without border delay, respectively. Then, the benchmark value for comparison of the calibration exercise is defined as the percentage travel time reduction when removing the borders of the weighted average of all the region cells. As weights I use each cell's initial population from a database constructed and used by [Desmet et al. \(2018\)](#) to maintain coherence with the model and add relevance to those cells with more inhabitants in the calculations. Lets define $\bar{\zeta}^{obs}(r, s)_b$ and $\bar{\zeta}^{obs}(r, s)_{wb}$ as the weighted travel time averages with and without borders, respectively. Therefore, the benchmark value is defined as $\Delta_{b \rightarrow wb} \bar{\zeta}^{obs}(r, s) = ((\bar{\zeta}^{obs}(r, s)_b \bar{\zeta}^{obs}(r, s)_{wb}) - 1)$. Then, using the two measurements and the 3906 origin and destination pairs, $\Delta_{b \rightarrow wb} \bar{\zeta}^{obs}(r, s) = -49.29\%$. This means that, on average, travel time is reduced to approximately half when borders are removed.

To begin the calibration exercise with the model, I update the geographic information to calculate the instantaneous trade costs $\varsigma_b(r)$. The location of each border control included in this research is assigned to a subcell r_i of $0.1^\circ \times 0.1^\circ$, following the same aggregation process for the accessibility of modes explained above. Figure 2.1 illustrates the location

Figure 2.3: Benchmark Observed Travel Time Chart



Source: SIECA database and Author's calculations.

Notes: "Baseline" corresponds to the average travel time in minutes for each cell without borders and "Borders" to the corresponding time with borders.

of the border crossing controls with location information provided by the IADB. Then, I aggregate the cell's accessibility to borders according to $border(r) = \left(\frac{\sum_{i=1}^{100} border(r_i)}{100} \right)$. This added geography feature is measured similarly to the accessibility of transportation modes. Therefore, it is compatible with the model's requirements. With this updated geography database, the calibration exercise can proceed.

The calibration exercise aims to reproduce the benchmark established with the observed data using the model's trade costs matrix. Starting with equation (2.5), I assign a set of values to $\hat{\varsigma}_{border} \in (1, \infty)$ increasing stepwise and then computing the instantaneous trade costs matrix $\varsigma_b(r)$ for the 63 cells of the region. The other parameters are preserved to isolate the effect of the border. It is important to note that given the functional form of $\varsigma_b(r)$ the increases in the instantaneous trade costs due to increases in $\hat{\varsigma}_{border}$ are positive but marginally decreasing.¹⁴ This implies that for high values of $\hat{\varsigma}_{border}$ an additional increase

¹⁴Using the non linear version of equation (2.5), similar to equation (2.2), $\frac{\partial \varsigma_b(r,s)}{\partial \hat{\varsigma}_{border}} > 0$, and $\frac{\partial^2 \varsigma_b(r,s)}{\partial \hat{\varsigma}_{border}^2} < 0$.

will not generate a proportional change in $\varsigma_b(r)$. Then after calculating a set matrices $\varsigma_b(r)$ corresponding to different values of $\hat{\varsigma}_{border}$ the optimal path is calculated for each of them using the fast-marching algorithm. This generates a set of optimal trade costs matrices $\varsigma_b(r, s)$. Thus, to compare these simulations with the benchmark value, I averaged the 63 cells using their initial population, as I had done before for the observed ones. Then define $\bar{\varsigma}_b(r, s)_b$ and $\bar{\varsigma}_b(r, s)_{wb}$ as the simulated trade costs matrix with and without border effects, respectively. Therefore, similarly as before, define $\Delta_{b \rightarrow wb} \bar{\varsigma}_b(r, s) = ((\bar{\varsigma}_b(r, s)_b \bar{\varsigma}_b(r, s)_{wb}) - 1)$, the simulated average reduction in the optimal trade cost when borders are removed. Note that $\bar{\varsigma}_b(r, s)_{wb}$ is identical to the original set up in [Desmet et al. \(2018\)](#).

The critical part of this calibration exercise is choosing a value of $\hat{\varsigma}_{border}$ by comparing the benchmark value from the observed travel times with a similar outcome from the simulations. Implicitly, I'm assuming that both matrices, the observed and the simulated ones, are measures of trade costs that differ in the metrics each uses. Then, to set a selection criteria, define $\bar{\varepsilon}$ as the absolute difference between the simulated percentage change in the trade costs matrix $\Delta_{b \rightarrow wb} \bar{\varsigma}_b(r, s)$ and the benchmark value from the data $\Delta_{b \rightarrow wb} \bar{\varsigma}^{obs}(r, s)$. The goal is to find a value of $\hat{\varsigma}_{border}$ such that $\bar{\varepsilon} \rightarrow 0$ enough. The closeness to zero is arbitrary and is mainly due to the behavior of $\varsigma_b(r)$ as shown above, when $\hat{\varsigma}_{border}$ is increased and reaches high values. Intuitively, when the change in costs is irrelevant compared to the increase in the parameter, the increase stops. This adds a second layer to the criteria, $\Delta \bar{\varepsilon} \approx 0$. Equation (2.6) summarizes these criteria.

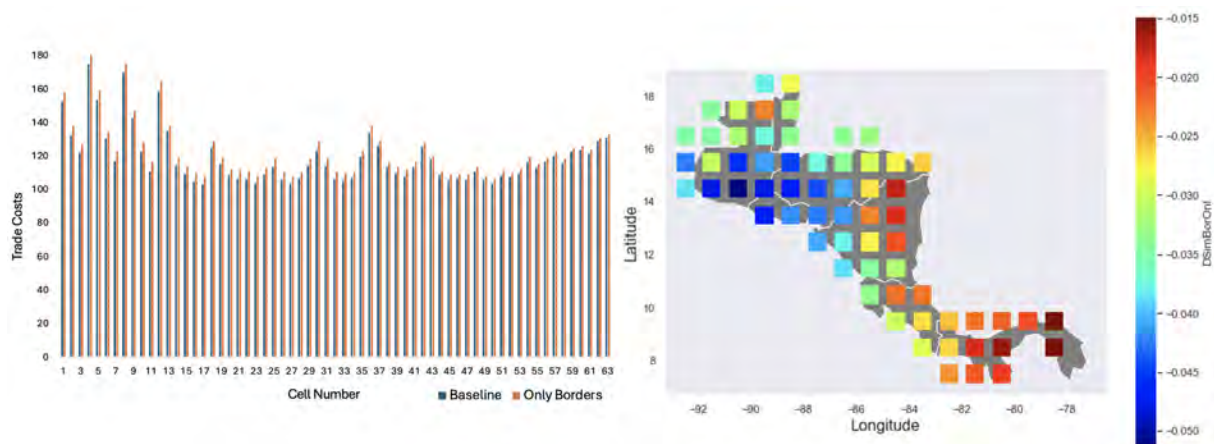
$$\bar{\varepsilon} = \left| \left| \Delta_{wb \rightarrow b} \bar{\varsigma}_b(r, s)_{border} \right| - \left| \Delta_{wb \rightarrow b} \bar{\varsigma}^{obs}(r, s)_{border} \right| \right| \rightarrow 0 \quad (2.6)$$

With $\Delta \bar{\varepsilon} \approx 0$.

The calibrating process updates the transportation costs matrix stepwise by increasing $\hat{\varsigma}_{border}$ until the criteria (2.6) is satisfied. The decreasing increases in the simulated trade costs

function imply the closeness to zero. The first calibration exercise preserves the parameters from Desmet et al. (2018) unaltered and only updates $\hat{\varsigma}_{border}$ until the criteria are reached. Figure 2.4 shows the simulated trade costs matrix results with and without border effect. The results show an effective reduction in trade costs for all the cells, with significant reductions occurring in El Salvador and its surrounding cells. This result is coherent with the density of border crossings in that area, as shown in Figure 2.1. Once the criteria are reached, the simulated trade costs matrix of this first calibration exercise generates a reduction in costs of -3.89% vs an observed reduction of -49.29%. The bar chart in Figure 2.4 shows a slight difference between the baseline and border scenarios. Compared to Figure 2.3, the pattern of trade costs in the chart is not similar to the pattern of travel times, and their correlation is around 0.07 with a non-significant t-test. In conclusion, the first exercise still does not capture the variation in travel time but correctly shows the effect on locations such as El Salvador. Therefore, additional adjustments are needed to improve the calibration.

Figure 2.4: First Calibration Exercise



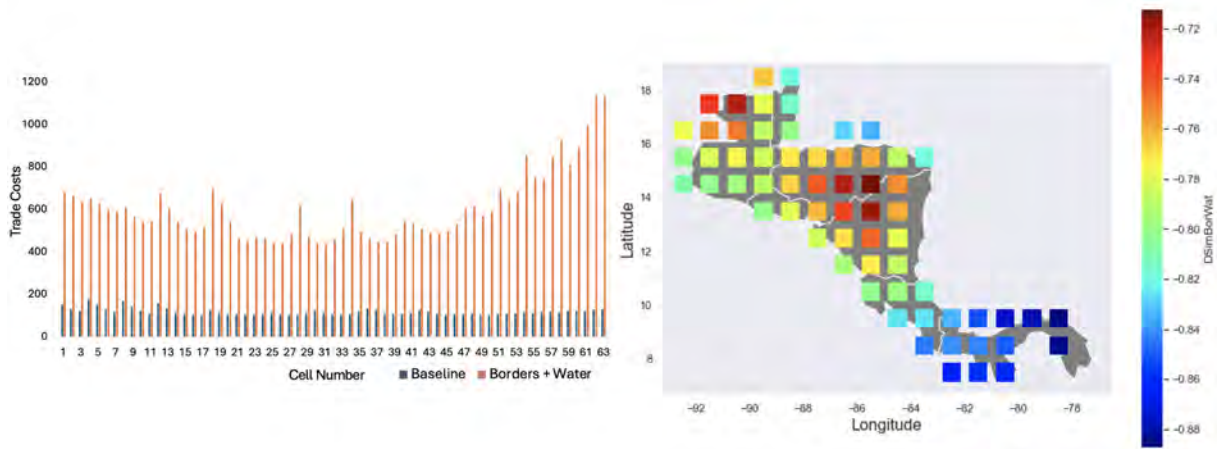
Source: Author's Calculation.

Notes: The bar chart compares the optimal value of trade costs (vertical axis), calculated by the model for each cell (horizontal axis) between the baseline scenario (without border effect) and the scenario with only border effect, as shown in Section 2. The heat map shows the percentage reduction in the optimal trade costs for each location when the borders are removed. Blue areas show higher reductions than green, yellow, or red areas, where the reduction is comparatively small.

To improve the trade costs calibration and push it towards the travel time benchmark, I use a similar approach as in the robustness exercises in Chapter I. The first calibration exercise preserved the parameters of Desmet et al. (2018). There, the cheapest way to move

across the cells is using waterways. Therefore, a possible reason behind the first calibration exercise results is that the optimal path avoids roads and uses waterways. However, such an argument is not realistic in Central America. As pointed out before, according to the IADB, approximately Roads move 95% of freight shipments, mainly the Pacific Corridor. Furthermore, some rail infrastructure exists in the region but is currently unused. These two reasons motivate the following calibration exercises.

Figure 2.5: Second Calibration Exercise



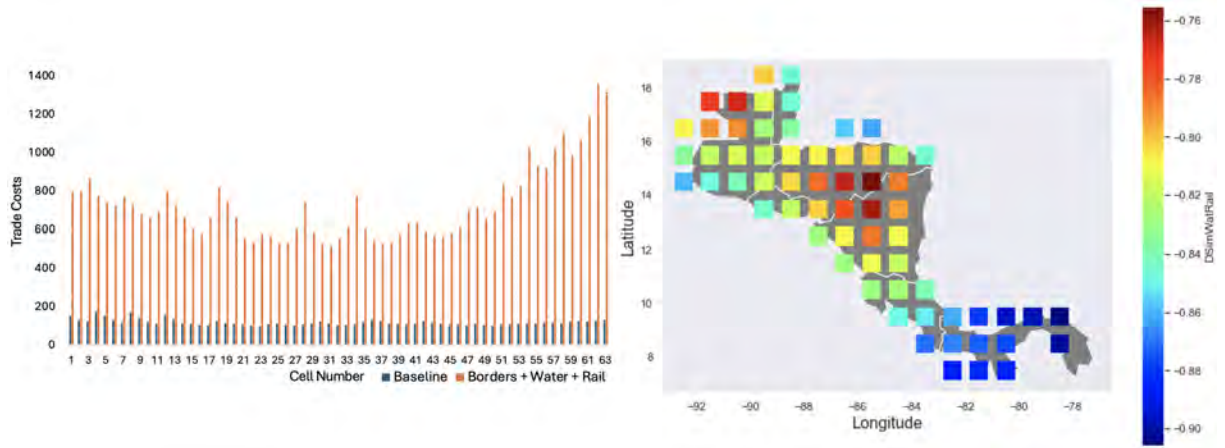
Source: Author's Calculation.

Notes: The bar chart compares the optimal value of trade costs (vertical axis), calculated by the model for each cell (horizontal axis) between the baseline scenario (without border effect) and the scenario with the border effect and an increase in the parameter for water (Border + Water). The implementation of the border effect is explained in Section 2. The heat map shows the percentage reduction in the optimal trade costs for each location when the borders are removed. Blue areas show higher reductions than green, yellow, or red areas, where the reduction is comparatively small.

The second calibration exercise consists of increasing the parameter associated with water (ς_{water}) as it was done in chapter I. The intuition is used to induce the algorithm to choose the least costly path that avoids waterways, enhancing the reality for the region. Thus, I follow the same simple rule as before $\varsigma_{water} = 2(\varsigma_{no_road})$ to set water as the most expensive transportation mode. Figure 2.5 shows the bar chart for the comparison of trade costs and the percentage variation of the trade costs across the space. This simulation enhancement generates a pattern in trade costs that looks similar to the benchmark. Furthermore, the spatial distribution of cost reductions is more accurate when compared to the benchmark. According to Table 2.3, the second calibration exercise generates an average decrease of 43.84%, only 5.4% lower than the benchmark. The correlation between the trade costs

generated by this exercise and the benchmark travel time with borders is around 89% and significant according to the t-test. Therefore, the costs simulated under this calibration can reproduce most of the variation in travel times due to borders. There's room to represent the region's reality by adjusting the rail mode parameters.

Figure 2.6: Third Calibration Exercise



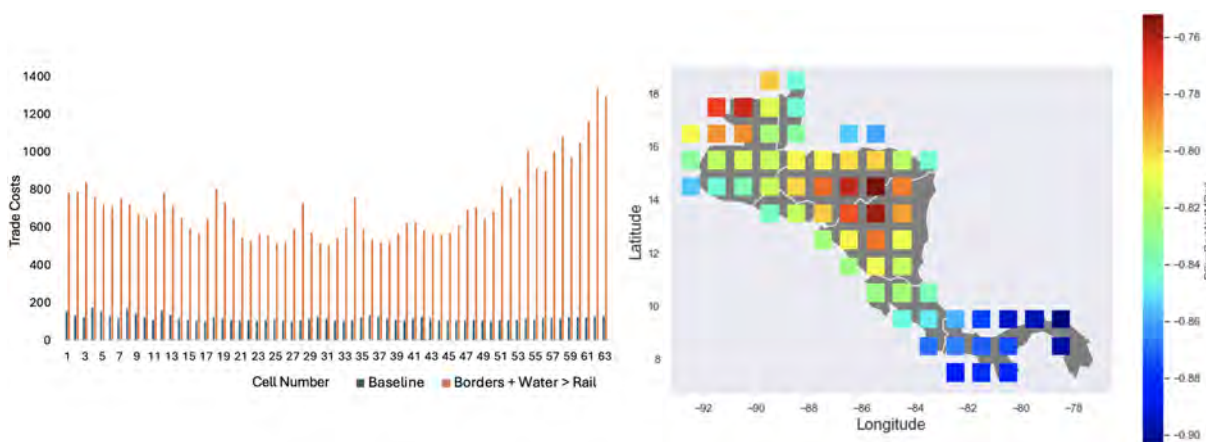
Source: Author's Calculation.

Notes: The bar chart compares the optimal value of trade costs (vertical axis), calculated by the model for each cell (horizontal axis) between the baseline scenario (without border effect) and the scenario with border effect and an increase in the parameters for water & rail (Border + Water + Rail). The implementation of the border effect is explained in Section 2. The heat map shows the percentage reduction in the optimal trade costs for each location when the borders are removed. Blue areas show higher reductions than green, yellow, or red areas, where the reduction is comparatively small.

The third and fourth calibration exercises try to introduce another characteristic of the region, the unused railroads. It is well known that railroads can contribute to developing areas and countries. However, in Central America, this transportation mode is unused. According to the IADB, a few rail lines exist in the region but are not used for passenger or freight transportation. Then, the third calibration used the same simple rule for waterways, such that $\varsigma_{water} = \varsigma_{rail} = 2(\varsigma_{no_road})$. The fourth calibration exercise imposes a higher cost on water, but according to the following rule: $\varsigma_{water} = 2(\varsigma_{no_road}) > \varsigma_{rail} = 1.5(\varsigma_{no_road})$. Therefore, increasing the cost of rail but letting water be the most costly transportation mode. Figures 2.6 and 2.7 summarize the third and fourth calibration exercises. The results are similar to those obtained by the second exercise. Both simulated trade costs generate high correlations of around 90% and are significant in both cases. However, both exercises

generate an average reduction of around 43.2%, slightly below the one from the second exercise.

Figure 2.7: Fourth Calibration Exercise



Source: Author's Calculation.

Notes: The bar chart compares the optimal value of trade costs (vertical axis), calculated by the model for each cell (horizontal axis) between the baseline scenario (without border effect) and the scenario with border effect and an increase in the parameters for water & rail (Border + Water > Rail). In this case, the parameter for water is greater than the parameter for rail. The implementation of the border effect is explained in Section 2. The heat map shows the percentage reduction in the optimal trade costs for each location when the borders are removed. Blue areas show higher reductions than green, yellow, or red areas, where the reduction is comparatively small.

Three calibration exercises achieved high and significant correlation levels, reproducing most of the observed travel time delay variation due to borders through the trade cost matrix. Tables 2.3 and 2.4 summarize such results, adding the minimum and maximum cell variation. The second exercise was chosen to run the counterfactual exercise because it reproduces most of the benchmark variation in the weighted average difference. The second calibration exercise introduced fewer changes than the third and fourth, generating the most gains in terms of the capability of reproducing the benchmark. The third and fourth exercises attempted to add more realistic features to the model. Nevertheless, they implied more arbitrary changes to the original parameters for a small gain than the second exercise. Thus, the choice of the second calibration follows a notion of frugality in introducing changes in the model's parameters and considerations regardless of the costs and benefits of each exercise.

Table 2.3: Calibration Exercise Output Summary

	<i>Benchmark</i>	<i>1</i>	<i>2</i>	<i>3</i>	<i>4</i>
<i>Weighted Average Difference</i>	-49.29%	-3.89%	-43.84%	-43.23%	-43.24%
<i>Minimum Cell Difference</i>	-22.03%	-1.48%	-25.41%	-25.99%	-25.98%
<i>Maximum Cell Difference</i>	-72.60%	-5.14%	-54.99%	-57.71%	-57.01%

Source: Author's Calculations.

Notes: Summary of the calibration exercises. Benchmark refers to the observed travel time costs. Columns 1 - 4 correspond to simulated outputs of the trade costs matrix for each calibration exercise. The first row refers to the percentage difference between weighted average travel time (benchmark) or trade costs with and without borders (1 - 4). The initial Cell population is used as weights. The second and third rows refer to the minimum and maximum percentage difference of the travel time (benchmark) or trade costs matrix with and without borders (1 - 4) at a cell level.

Table 2.4: Calibration Exercise Correlations

	<i>1</i>	<i>2</i>	<i>3</i>	<i>4</i>
<i>Correlation</i>	0.07	0.89	0.90	0.90
<i>T-Stat</i>	0.54	15.48	16.42	16.42
<i>Rejection</i>	No	Yes	Yes	Yes

Source: Author's Calculations.

Notes: Summary of the correlations from the calibration exercises. The correlations are calculated between the benchmark travel time with border and each of the simulated trade costs matrix with border effect for each calibration exercise (columns). T-Stat: Correlation T-Test, with the null hypothesis: Correlation = 0. Two tails test. Significance level = 0.05, critical value = 2, degrees of freedom = 61.

2.4. Results

After discussing the theory and the calibration, I now describe the counterfactual exercise and how it is implemented using [Desmet et al. \(2018\)](#) framework. As pointed out in the introduction, Central American integration has been a challenge. Since the “Puebla-Panama Plan” enactment, the discussion across countries, external agencies, and multilateral banks has centered on two primary interventions. The most popular is the Pacific Corridor. This highway, which motivated the counterfactual exercise in Chapter I, implicates a high investment of around 5.3 US billion dollars, and aims to upgrade Central America’s most important corridor to the level of a modern US interstate highway. The second intervention is the optimization of all the customs and border controls. The investment amount is unclear in this regard, but according to the IADB, it is several times lower than the Pacific Cor-

ridor investment value. The lower investment amount contrasts with the great difficulties of making agreements between countries and, as suggested before, numerous legal barriers, such as the laws protecting the local freight transporters. Using this framework, I simulate the implementation of those two interventions. These simulations use the improved trade costs calibration to generate a new baseline scenario for all the initial values of the model, as explained in section 1.3. Then, the counterfactual scenarios depart from this adjusted baseline.

These interventions initially generate three counterfactual scenarios, two where each one is implemented separately, and one where both interventions take place at the same time. The procedure consists of exploiting the new features of the trade costs matrix with border effect and run the model to analyze the impact of each of those scenarios over the region's productivity, GDP per capita, population flows, and trade shares.

The counterfactual exercise one is the complete elimination of the borders. As shown above, this implies a reduction in travel time of around 49.2%. Therefore, I can exploit the selected calibration (exercise 2) in Section 2.3 to simulate this intervention and compare the baseline scenario with borders against the one without borders. This exercise is possible in theory but not that much in reality. It implies transforming Central America into a country similar to the US, where state borders exist but don't create comparable distortions in travel time. The results below must be interpreted as the potential outcome of an actual agreement or investment project that could reduce the border effect.

The counterfactual exercise two consists of using the new baseline scenario to redo Chapter I's Exercise III, a fixed increase in the accessibility of main roads, shown in section 1.4.2. The choice of this scenario is based on the realistic modification it generates on the geography of the model, as discussed in the previous chapter. The selected calibration gives the new baseline (border baseline), including the border effect. Then, as in Chapter I, I run the model using the new baseline and introduce the Pacific Corridor by updating the accessibil-

ity of main roads for each cell affected by the project. This exercise refines the simulations in Chapter I by adding the border effect.

The counterfactual exercise three consists of the possibility that both policy interventions happen simultaneously. Such simulation aims to recreate an ideal scenario of integration and investment across the region. Intuitively, the most significant policy push to the region could boost trade by significantly reducing travel time costs. This will eliminate the border delays and introduce a highway, allowing faster and shorter trips. The period for all the counterfactual exercises is One hundred years to capture the long-run effect of each variable. After running the model and collecting the output, the results are presented as the percentage variation of each cell's average over 100 years. These percentage variations are shown in heat maps over the surface of Central America.

Before proceeding to discuss the results, let's briefly refresh [Desmet et al. \(2018\)](#) framework. It focuses on how people choose their preferred location to live and work. Those choices are affected by variables such as their utility, derived from consumption, the amenities available at each location, and their income level. The firms optimally allocate resources (workers) for goods production and innovation. An exogenous shock such as the Pacific Corridor or the elimination of borders will directly affect the prices of the goods produced by a firm in a specific location and sold abroad by reducing trade costs. Then, the firm's optimal allocation of inputs can change, and it will face better prices (less distorted by the trade costs), thus increasing its profits and participation in trade. Such an increase in profits will generate an additional allocation of workers to produce goods and innovate, expanding the demand for workers and productivity. This effect also increases the GDP per capita of the location, ultimately growing its attractiveness in terms of utility. The shift in productivity works as an agglomeration force, attracting agents to the most productive locations. The congestion effects over the amenities oppose this force; the more population in a particular location, the less access to amenities. All these effects reach an equilibrium, generating a

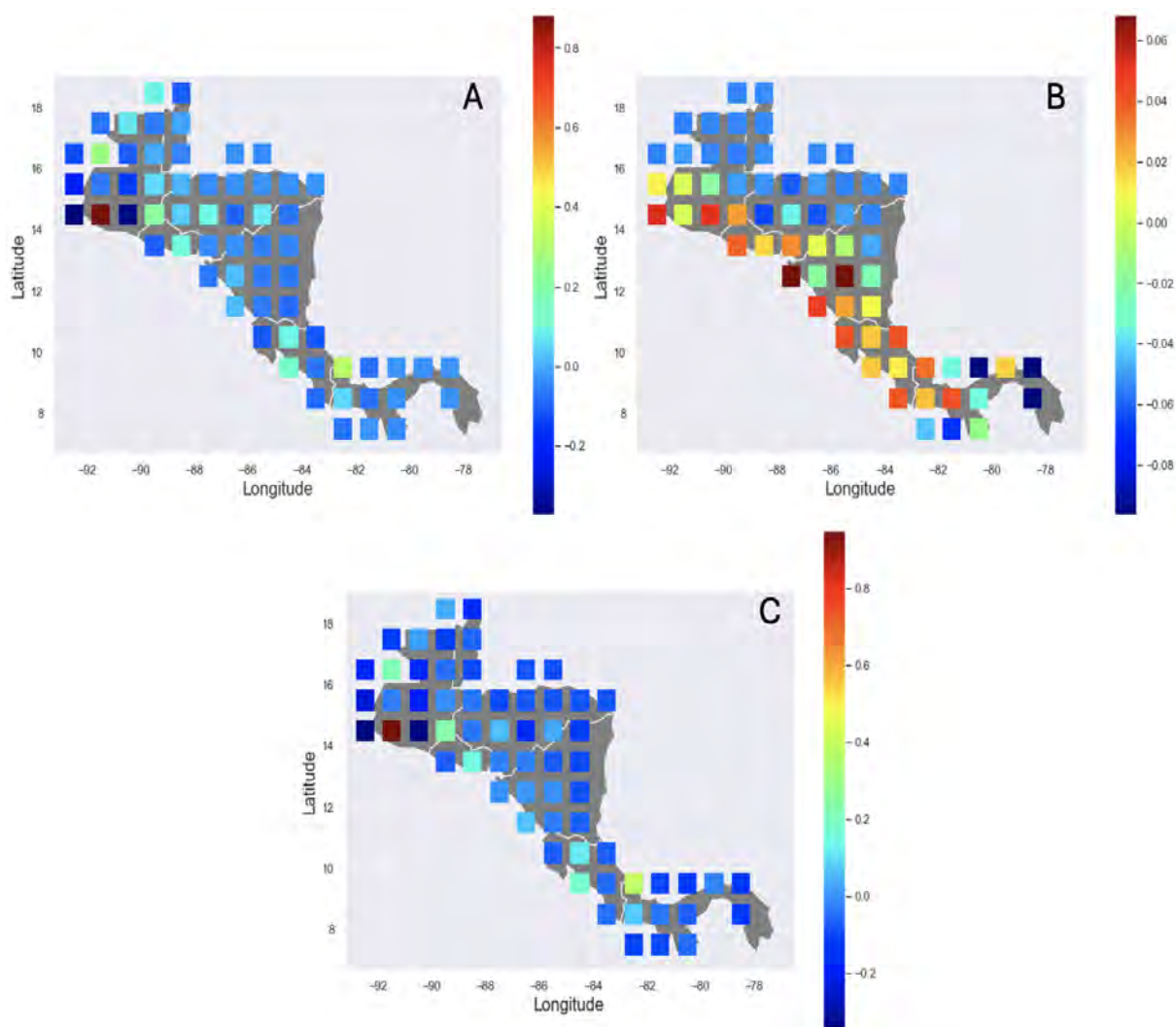
new distribution of the population, productivity, GDP per capita, utility, and trade shares across the space.

Following this intuition, the three counterfactual scenarios will reduce trade costs by eliminating the borders, increasing access to main roads, or both. Then, the firms' prices in the affected areas will be reduced proportionally in each location where it is sold. This will give those firms that benefited from reducing trade costs an advantage against their competitors, increasing their sales. This first push can alter the profit maximization program of such firms. With the increased benefits, they will hire more workers to produce their goods and innovate in quality. This generates a second push because this innovation investment increases this location's productivity. Furthermore, given the possibility of generating spillovers, the productivity of the neighbor is also increased, and the effect of this increase will go over time, as described in the firm's technology theory in Chapter I, section 1.3.

The impact on productivity is summarized in Figure 2.8. Panel A shows the counterfactual exercise 1. Most of the cells have a null to small positive effect on productivity, with a high concentration in Guatemala City's cell. Some cells in the neighborhood of Guatemala City show negative impacts on productivity. This trade-off between Guatemala City and its neighborhood could be explained by the high concentration of population in the first, implying stronger accumulation forces that reallocate population there. Those cells containing border customs controls as shown in Figure 2.5, have a positive effect as expected by the calibration of the trade costs matrix. Panel B shows the counterfactual exercise 2. The map clearly shows the increase in productivity due to implementing the Pacific Corridor along the Pacific coastline. However, the impact size comparing panels A and B is significant. This result suggests that the travel time delays due to borders are more important than the Pacific Corridor in terms of the size of its effects on the region's productivity. Nevertheless, the impact of panel A is mainly concentrated in one cell, while the effect of the Pacific Corridor is broader across the region. Finally, Panel C shows the impact of the counterfactual exercise

three. There, the effects are driven by the border elimination, resembling the results in Panel A. This suggests that the border elimination impact is dominant in terms of productivity compared to those of the Pacific Corridor Implementation. It is worth noticing that the initial locations with more productivity, given the population density, also drive the results. Most of the inland cells of Central America are located in mountain ranges. There, the effects tend to be small or negative. Conversely, the capital cities tend to be on the Pacific coastline, with primarily flat geography. There, the impact is positive and significant.

Figure 2.8: Productivity Under the Three Counterfactuals

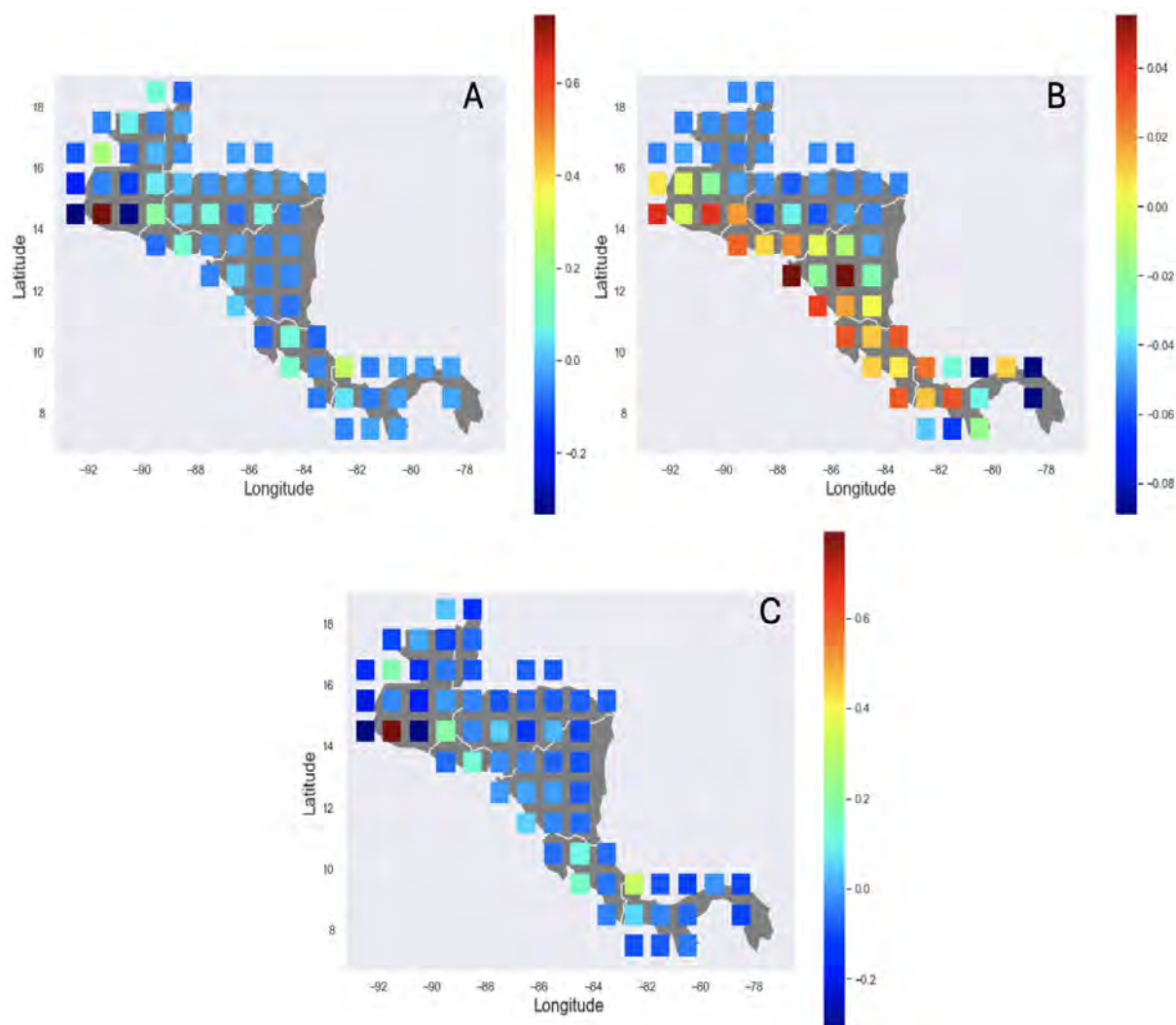


Source: Author's Calculations.

Notes: Heat maps displaying the 63 cells simulated in Central America. Panels A, B, and C show the results of the simulation's output of the percentage change in the cell's 100-year average productivity $\tau(r)$ (Shown in Chapter I) for counterfactuals 1 (remove borders only), 2 (build the Pacific Corridor only), and 3 (remove borders and build the Pacific Corridor), respectively.

Following the model's intuition, the impact on population is explained by the agglomeration forces of productivity. The more productive a place is, the more opportunities for employment and better wages. Figure 2.9 shows the impact on the distribution of population. Each agent will observe the productivity change and move to those places, searching for better wages and income. The agglomeration forces will increase the population concentration in those locations where productivity grows. Conversely, those places where the impact of productivity is negative will show a negative flux of inhabitants. Therefore, the patterns on panels A, B, and C follow a similar shape to those from Productivity. This implies a higher concentration in urban areas under the counterfactual exercises, particularly in Guatemala City. This finding is critical if the region's objective is to reallocate the population to urban areas rather than boosting remote areas to prevent migration to the cities.

Figure 2.9: Population Net Flows Under the Three Counterfactuals



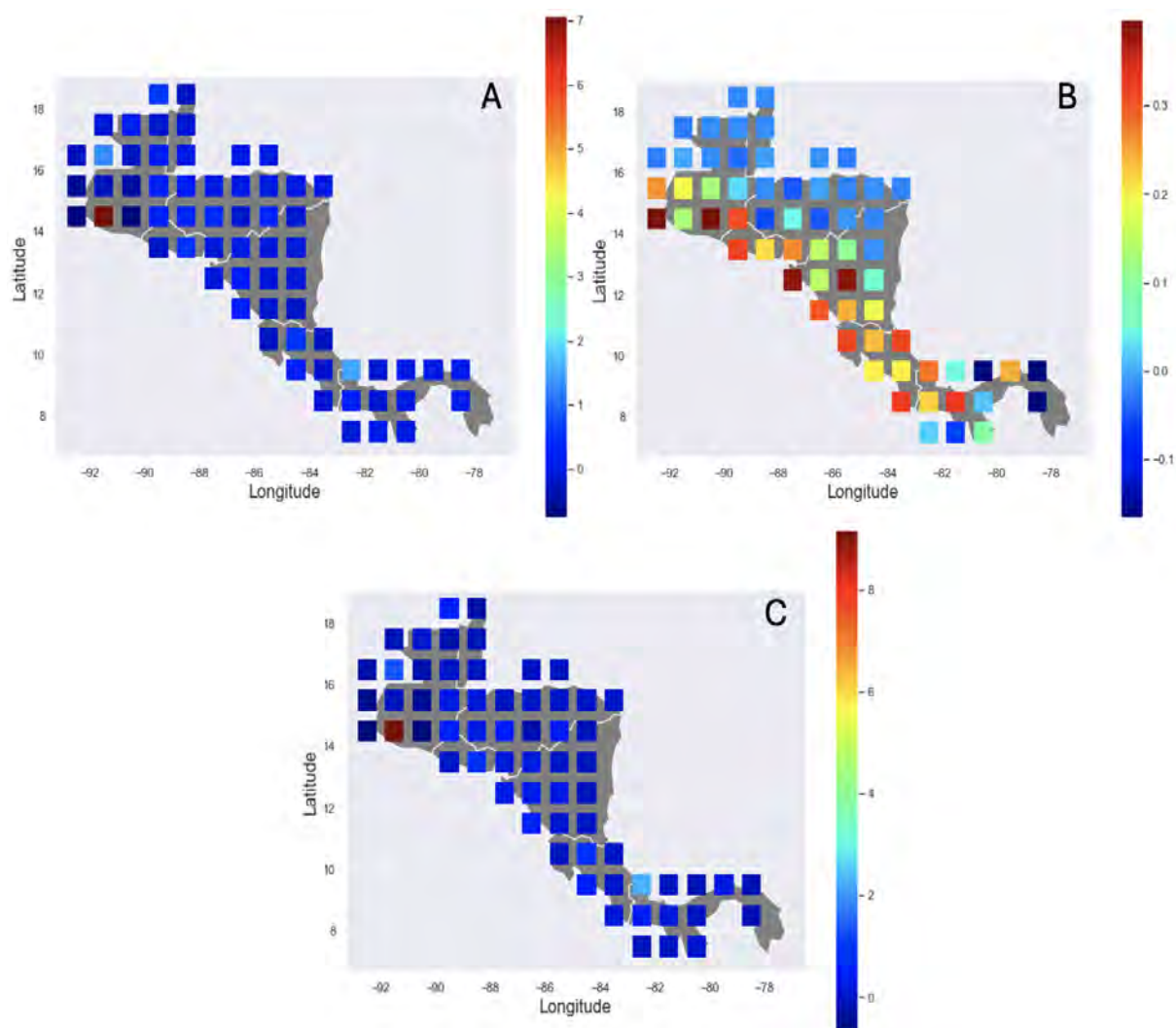
Source: Author's Calculations.

Notes: Heat maps displaying the 63 cells simulated in Central America. Panels A, B, and C show the results of the simulation's output of the percentage change in the cell's 100-year average of the net population flows for counterfactuals 1 (remove borders only), 2 (build the Pacific Corridor only) and 3 (remove borders and build the Pacific Corridor), respectively.

The double shock on prices, first from the reduction in trade costs due to the elimination of borders, the construction of the Pacific Corridor or both, and then for the increases in productivity boost trade. Given that productivity shocks can reduce firms' marginal costs, as shown in Chapter I, section 1.3, the firms of places with increased productivity can sell at a lower price, increasing their opportunities to sell their products in other locations. Therefore, local sales and exports should increase. Figure 2.10 shows the impact on Central America;

in this case, the impact size is remarkable between counterfactual exercises 1 and 2 in panels A and B. This suggests that in terms of the integration of the economies, the focus should be on reducing the border effect. This does not indicate that the Pacific Corridor cannot positively impact trade, but reducing the border time delays seems to have a more significant effect. Additionally, the counterfactual exercise three in panel C suggests that the two policy interventions are complements, given that the join simulation gets higher impact sizes than the previous two. But again, the benefits for Guatemala City (the only red square in panels A and C) are remarkable.

Figure 2.10: Trade Shares Under the Three Counterfactuals



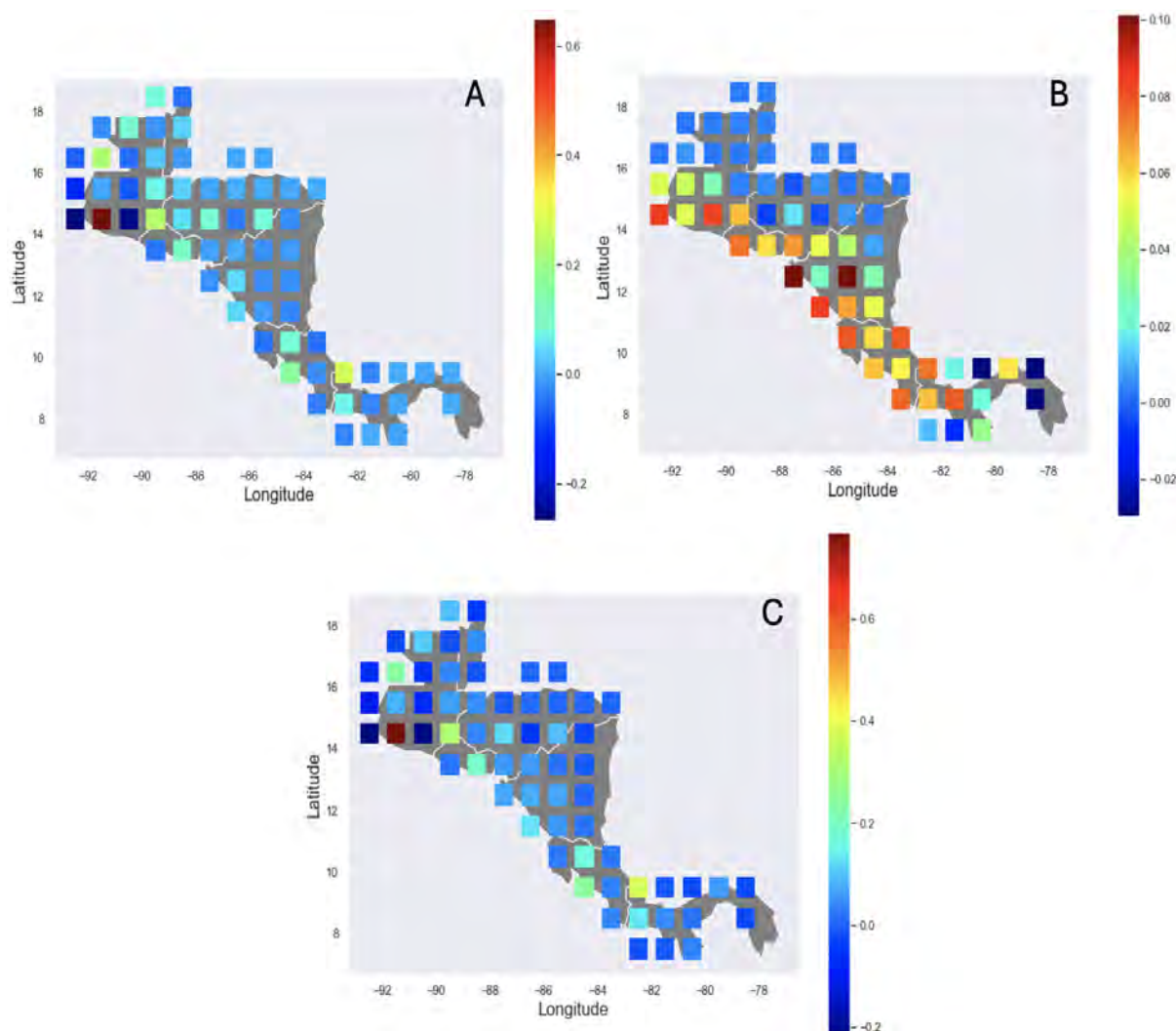
Source: Author's Calculations.

Notes: Heat maps displaying the 63 cells simulated in Central America. Panels A, B, and C show the results of the percentage change in the simulation output of the total sum of trade shares for counterfactuals 1 (remove borders only), 2 (build the Pacific Corridor only) and 3 (remove borders and build the Pacific Corridor), respectively.

For those locations where the increase in productivity activated the agglomeration forces, attracting population and increasing its trade shares, the real GDP per capita rises, too. Figure 2.11 shows the impact on the real GDP per capita across the region. The patterns are similar to those for productivity, population, and trade. A remarkable effect occurs here again; panel C shows an impact more prominent than the ones in panels A and B. This implies that implementing both policies works as complements in the case of the GDP

per capita. This is explained by combining three elements: increased productivity, positive population flows, and increased trade shares. However, this result implies a reduction of the GDP per capita in other locations, such as those dark blue points inland in Guatemala, and null to minor effects in the blue cells in Honduras and Nicaragua. The concentration on urban areas boosts the GDP per capita there but at the cost of reducing it in low-productive places.

Figure 2.11: Real GDP per Capita index Under the Three Counterfactuals

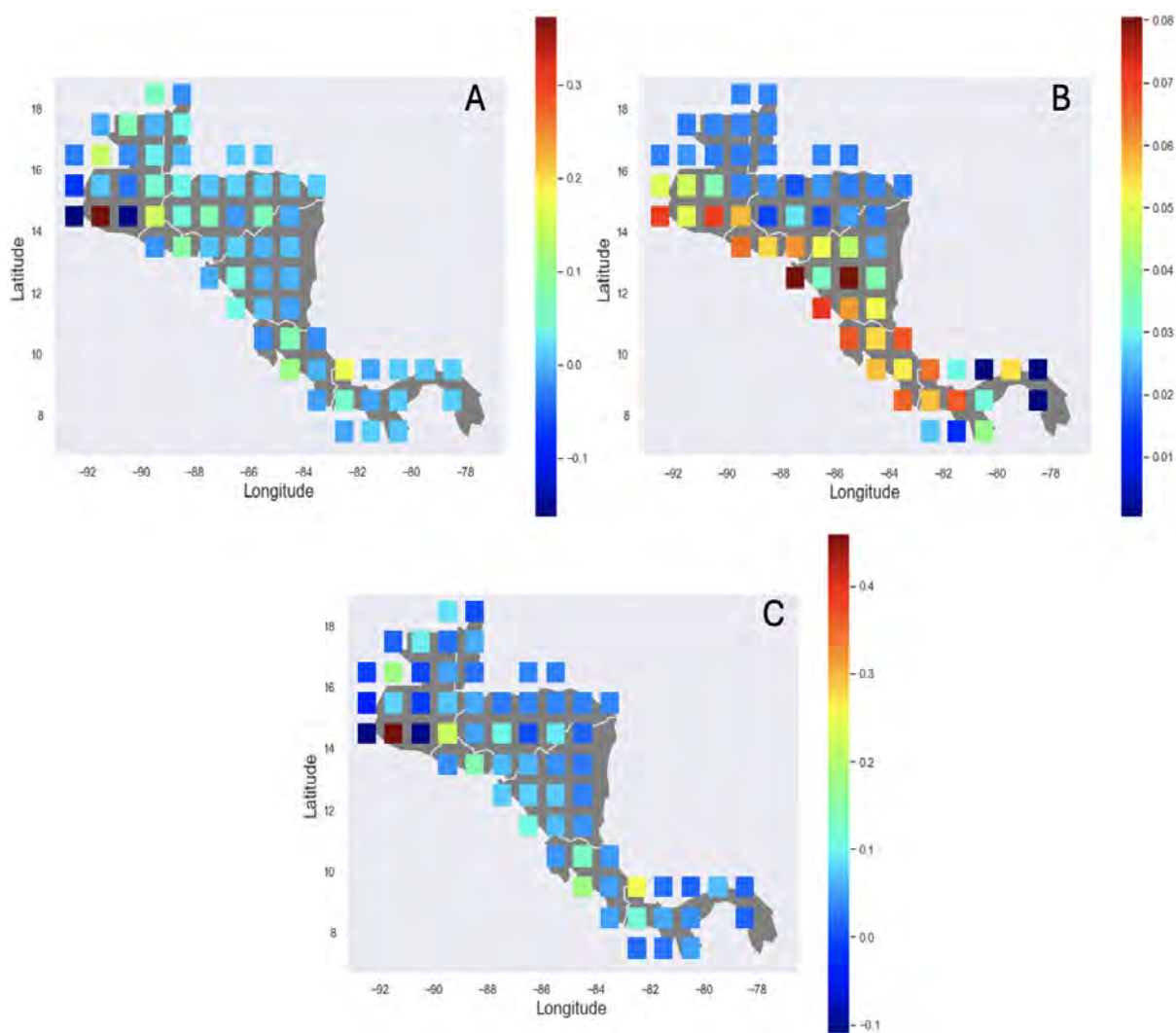


Source: Author's Calculations.

Notes: Heat maps displaying the 63 cells simulated in Central America. Panels A, B, and C show the results of the simulation's output of the percentage change in the cell's 100-year average of the Real GDP per capita Index with Panama City cell = 100 for counterfactuals 1 (remove borders only), 2 (build the Pacific Corridor only), and 3 (remove borders and build the Pacific Corridor), respectively.

Finally, given the increase in the GDP per capita, the attractiveness of such places increases, as shown in Figure 2.12. The attractiveness depends on the capability of buying consumption goods, the GDP per capita, and the accessibility to amenities. As in the case of the GDP, combining both interventions, generates the highest impact. Urban areas usually grant more accessibility to amenities. This explains that the Pacific coast receives most of the benefits. Nevertheless, the concentration patterns simulated by the model imply stress over the existing amenities. If these interventions are implemented, the governments should be aware of this possibility and work to prevent the congestion effect over the amenities.

Figure 2.12: Utility Under the Three Counterfactuals



Source: Author's Calculations.

Notes: Heat maps displaying the 63 cells simulated in Central America. Panels A, B, and C show the results of the simulation's output of the percentage change in the cell's 100-year average of the Utility for counterfactuals 1 (remove borders only), 2 (build the Pacific Corridor only) and 3 (remove borders and build the Pacific Corridor), respectively.

Summarizing, the impact of borders is remarkably higher than that of the Pacific Corridor. This finding is aligned with the simple example and the data in the introduction. The magnitude of the travel time border delay is considerable, implying significant effects when those costs are eliminated from the geography. This also suggests that the cost reduction generated by the Pacific Corridor is not as high as the one from the elimination of borders. This result is aligned with the objectives of the “Puebla-Panama Plan.” One of the

main concerns is the difficulty of regional economic integration and logistics of the complex network of border crossings and the lack of adequate infrastructure. This combination of characteristics generates high travel time delays, as shown in Table 2.1.

The Pacific Corridor generates positive effects along the locations on its way. However, the simulations show that its benefits are smaller than those generated by eliminating the border effect. The ideal scenario of implementing both interventions shows slightly higher impacts than the sole interventions in counterfactual exercises 1 and 2. Finally, in this case, the simulation results suggest that even with an improved transport infrastructure like the Pacific Corridor, its effects will be limited due to the travel time border delay.

Finally, Table 2.5 shows the aggregate percentage change results for total real GDP, total productivity, and total utility computed using the population results under each counterfactual exercise. Due to the elimination of the travel time border delay in counterfactual exercises one and three, as seen in Figure 2.8, the agglomeration force generates a positive increase in total productivity clustered in Guatemala City, however, the aggregate average change in total productivity is small and negative. This suggests that on average, at an aggregate level, none of the policies will increase productivity. However, given the concentration of population in the most productive areas, as shown in Figure 2.9, and the significant shift in trade, the aggregate GDP change is positive, as seen in Table 2.5 row 2. At aggre-

Table 2.5: Aggregate Impact

Variable	<i>Counterfactual 1</i>	<i>Counterfactual 2</i>	<i>Counterfactual 3</i>
<i>Total Productivity</i>	-0.35%	-0.29%	-0.61%
<i>Total Real GDP</i>	1.80%	0.98%	3.06%
<i>Total Utility</i>	1.51%	1.62%	103.29%

Source: Author's Calculations.

Notes: Column labels, counterfactuals 1 to 3. Rows: Percentage change in the 100-year average of the aggregate variables. Each variable is defined, following [Desmet et al. \(2018\)](#), as seen in Chapter I. Total Productivity: $[\tau_t(r)\bar{L}_t(r)^\alpha]^{1/\theta}$, with $\tau_t(r)$ fundamental productivity and $\bar{L}_t(r)$ population per unit of land. $\alpha = 0.06$, $\theta = 6.5$. Total real GDP: $GDP_t(r)_{per\ capita} * \bar{L}_t(r)$. Total Utility: $u_t(r) * \bar{L}_t(r)$.

gate levels, the significant impact is simulated when both interventions take place, the minor impact is generated by the counterfactual exercise two.

The total utility also increases, but in a different magnitude depending on each counterfactual. In the first exercise, the increase is less than the GDP, suggesting that the agglomeration forces are generating some congestion effects over amenities. In the second case, the increase is more significant than the GDP, implying that the congestion forces are not as strong as in the first case. This result also suggests a more evenly distributed impact, as shown by Figure 2.12 Panel B. Thus, the agglomeration is not as highly concentrated as eliminating borders. In the third case, the balance between the agglomeration forces that increase the GDP and the more evenly distribution of the effect by constructing the Pacific Corridor in aggregate duplicates the value of utility. This result is remarkable for the welfare of the region. Future exercises can consider a reduction in such costs due to the decrease in border travel time delays of a smaller size. However, the study of the extreme cases suggests that the most problematic issue in Central America is its borders and that a considerable investment in infrastructure like the Pacific Corridor will not be as effective as expected if the border travel time delay is not attenuated. Future data on additional transportation time delays could improve the measurement of such transportation costs, thus improving the calibration of the border effects.

2.5. Conclusions

The results in this chapter show the importance of borders in achieving effective integration across the region. According to the simulations, the PC has a positive but smaller effect on such a goal than the border improvement. Conversely, the potential elimination of the border travel time delay due to customs and border controls could have a greater impact on the regional economy, fueling GDP per capita and trade. These results are aligned with [Fontagné et al. \(2023\)](#) for the African integration, with comparable sizes on the impacts of the border.

The simulations suggest the importance of the travel time border delay for the region. Thus, the expensive investment required to build the Pacific Corridor will not be as effective as expected if no policy is devoted to improving the border and customs controls. In addition, the expected GDP and trade gains will concentrate the population in urban areas with high productivity. Is that the intended shift in population? If the region's development involves attracting the population to urban areas, this intervention will do as intended. But, if that is not the intended shift, other policies are needed to achieve such goals.

The calibration exercise provided an improved trade costs matrix capable of replicating a significant quantity of the variation of the observed travel time border delays. Introducing this adaptation to the region enhances the accuracy of the results in Chapter I regarding the Pacific Corridor. The impact of such infrastructure is lower after the introduction of borders but still positive in terms of the GDP. However, this result doesn't include Mexico; therefore, it is not fully comparable. Future improvements in the IADB database will permit the addition of new borders and refinement of the calibration process. The iceberg transportation costs, as modeled by [Desmet et al. \(2018\)](#), can be expanded to include other features of the transportation technology.

APPENDIX A

Additional Parameters of the Model

Table A.1: Parameters from Desmet et al. (2018)

TABLE I PARAMETER VALUES	
Parameter	Target/Comment
1. Preferences: $\Sigma_i \beta^i u_i(r)$, where $u_i(r) = \bar{a}(r) \bar{L}_i(r)^{-\lambda} (\int_0^1 c_i^e(r)^e d\omega)^{1/\rho}$ and $u_0(r) = e^{\beta_0(r)}$	
$\beta = .965$	Discount factor
$\rho = .75$	Elasticity of substitution of 4 (Bernard et al. 2003)
$\lambda = .32$	Relation between amenities and population
$\Omega = .5$	Elasticity of migration flows with respect to income (Monte et al. 2018)
$\psi = 1.8$	Deaton and Stone (2013)
2. Technology: $q_i^e(r) = \phi_i^e(r)^{\eta} z_i^e(r) L_i^e(r)^{\theta}$, $F(z, r) = e^{-T_i(r) z^{\frac{1}{\theta}}}$, and $T_i(r) = \tau_i(r) \bar{L}_i(r)^{\alpha}$	
$\alpha = .06$	Static elasticity of productivity to density (Carlino et al. 2007)
$\theta = 6.5$	Trade elasticity (Eaton and Kortum 2002; Simonovska and Waugh 2014)
$\mu = .8$	Labor or nonland share in production (Greenwood et al. 1997; Desmet and Rappaport 2017)
$\gamma_i = .319$	Relation between population distribution and growth
3. Evolution of productivity: $\tau_i(r) = \phi_{i-1}(r)^{\theta \eta} [\int_s \eta \tau_{i-1}(s) ds]^{1-\eta} \tau_{i-1}(r)^{\eta}$ and $\psi(\phi) = \nu \phi^{\xi}$	
$\gamma_2 = .993$	Relation between population distribution and growth
$\xi = 125$	Desmet and Rossi-Hansberg (2015)
$\nu = .15$	Initial world growth rate of real GDP of 2%
4. Trade Costs	
$\hat{c}_{rail} = .1434$	Allen and Arkolakis (2014)
$\hat{c}_{no_rail} = .4302$	
$\hat{c}_{major_road} = .5636$	
$\hat{c}_{other_road} = 1.1272$	
$\hat{c}_{no_road} = 1.9726$	
$\hat{c}_{water} = .0779$	Elasticity of trade flows with respect to distance of $-.93$ (Head and Mayer 2014)
$\hat{c}_{no_water} = .0779$	
$\hat{\mathbf{T}} = .393$	

Source: Taken from Desmet et al. (2018)

BIBLIOGRAPHY

- Allen, T. and Arkolakis, C. (2014). Trade and the topography of the spatial economy. *The Quarterly Journal of Economics*, 129(3):1085–1140. [4](#), [6](#), [19](#), [22](#), [23](#), [41](#), [44](#), [50](#), [51](#), [53](#), [54](#), [55](#), [56](#), [57](#), [58](#), [59](#), [62](#), [65](#)
- Allen, T. and Arkolakis, C. (2022). The welfare effects of transportation infrastructure improvements. *The Review of Economic Studies*, 89(6):2911–2957. [6](#), [50](#), [53](#), [55](#)
- Allen, T., de Castro Dobbin, C., and Morten, M. (2018). Border walls. Technical report, National Bureau of Economic Research. [56](#)
- Anderson, J. E. and Van Wincoop, E. (2003). Gravity with gravitas: A solution to the border puzzle. *American economic review*, 93(1):170–192. [52](#), [55](#), [56](#)
- Andrade Hernández, J. M. and Lugo Delgadillo, M. (2018). Qué tan factible es aumentar el acervo de infraestructura en México: una propuesta de inversión de largo plazo. [4](#)
- Asturias, J. (2020). Endogenous transportation costs. *European Economic Review*, 123:103366. [6](#)
- Banerjee, A., Duflo, E., and Qian, N. (2020). On the road: Access to transportation infrastructure and economic growth in China. *Journal of Development Economics*, 145:102442. [6](#), [34](#), [47](#)
- Bernal, R. and Peña, X. (2011). *Guía práctica para la evaluación de impacto*. Ediciones Uniandes-Universidad de los Andes. [1](#)

- Braconier, H. and Pisu, M. (2013). Road connectivity and the border effect: Evidence from europe. [52](#)
- Brakman, S., Garretsen, H., van Marrewijk, C., and Oumer, A. (2011). The positive border effect of eu integration. [52](#)
- Coughlin, C. C. and Novy, D. (2021). Estimating border effects: The impact of spatial aggregation. *International Economic Review*, 62(4):1453–1487. [56](#)
- Davis, H. C. (1990). *Regional economic impact analysis and project evaluation*. UBC Press. [1](#)
- Desmet, K., Nagy, D. K., and Rossi-Hansberg, E. (2018). The geography of development. *Journal of Political Economy*, 126(3):903–983. [2](#), [4](#), [6](#), [11](#), [13](#), [14](#), [15](#), [17](#), [18](#), [19](#), [21](#), [22](#), [24](#), [29](#), [46](#), [51](#), [53](#), [54](#), [57](#), [59](#), [60](#), [62](#), [63](#), [64](#), [68](#), [69](#), [71](#), [72](#), [76](#), [78](#), [88](#), [90](#), [91](#)
- Donaldson, D. (2018). Railroads of the raj: Estimating the impact of transportation infrastructure. *American Economic Review*, 108(4-5):899–934. [3](#)
- Eaton, J. and Kortum, S. (2002). Technology, geography, and trade. *Econometrica*, 70(5):1741–1779. [14](#), [17](#)
- Fajgelbaum, P. and Redding, S. J. (2022). Trade, structural transformation, and development: Evidence from argentina 1869–1914. *Journal of Political Economy*, 130(5):1249–1318. [6](#), [47](#)
- Fajgelbaum, P. D. and Schaal, E. (2020). Optimal transport networks in spatial equilibrium. *Econometrica*, 88(4):1411–1452. [55](#)
- Felbermayr, G. J. and Tarasov, A. (2022). Trade and the spatial distribution of transport infrastructure. *Journal of Urban Economics*, 130:103473. [56](#)
- Fontagné, L., Lebrand, M. S. M., Murray, S., Santoni, G., and Ruta, M. (2023). Trade and infrastructure integration in africa. *Available at SSRN 4672520*. [57](#), [65](#), [89](#)

- Fuchs, S. and Wong, W. F. (2022). Multimodal transport networks. Technical report, Working Paper. [53](#), [57](#), [65](#)
- Hallegatte, S., Rozenberg, J., Maruyama Rentschler, J. E., Nicolas, C. M., and Fox, C. J. E. (2019). Strengthening new infrastructure assets: a cost-benefit analysis. *World Bank Policy Research Working Paper*, (8896). [5](#)
- Hong, J., Chu, Z., and Wang, Q. (2011). Transport infrastructure and regional economic growth: evidence from china. *Transportation*, 38(5):737–752. [5](#), [6](#), [47](#)
- Infante, I. (2012). Corredor mesoamericano de integracion. integrando mesoamerica por el pacifico. *BID-INTAL*. [7](#), [22](#), [41](#)
- Jedwab, R. and Storeygard, A. (2022). The average and heterogeneous effects of transportation investments: Evidence from sub-saharan africa 1960–2010. *Journal of the European Economic Association*, 20(1):1–38. [3](#)
- Jones, H., Moura, F., and Domingos, T. (2014). Transport infrastructure project evaluation using cost-benefit analysis. *Procedia-Social and Behavioral Sciences*, 111:400–409. [5](#)
- Krugman, P. (1991). Increasing returns and economic geography. *Journal of political economy*, 99(3):483–499. [54](#)
- Krugman, P. (1992). *Geography and trade*. [54](#)
- Maparu, T. S. and Mazumder, T. N. (2017). Transport infrastructure, economic development and urbanization in india (1990–2011): Is there any causal relationship? *Transportation research part A: policy and practice*, 100:319–336. [6](#)
- McCallum, J. (1995). National borders matter: Canada-us regional trade patterns. *The American economic review*, 85(3):615–623. [52](#)
- McCann, P. (2005). Transport costs and new economic geography. *Journal of Economic Geography*, 5(3):305–318. [54](#), [55](#)

- McCarthy, P. and Zhai, Z. (2019). Economic impact analysis of gdot short line railroad infrastructure investment in georgia. *Research in Transportation Economics*, 77:100728. [4](#)
- Nagy, D. K. (2015). Border effects and urban structure. [48](#), [56](#)
- Nikolic, S. and Chilosi, D. (2023). Vanishing borders: Ethnicity and trade costs at the origin of the yugoslav market. *Available at SSRN 4333166*. [53](#)
- Perkins, P., Fedderke, J., and Luiz, J. (2005). An analysis of economic infrastructure investment in south africa. *South African Journal of Economics*, 73(2):211–228. [4](#)
- Redding, S. J. and Sturm, D. M. (2008). The costs of remoteness: Evidence from german division and reunification. *American Economic Review*, 98(5):1766–1797. [52](#)
- Samuelson, P. A. (1952). The transfer problem and transport costs: the terms of trade when impediments are absent. *The Economic Journal*, 62(246):278–304. [54](#)
- Sánchez, F. and Méndez, J. N. (2000). *Geography and economic development: a municipal approach for Colombia*. Centro de Estudios Sobre Desarrollo Economico, Universidad de los Andes. [5](#), [47](#)
- Santamaría, M. A., Ventura, J., and Yeşilbayraktar, U. (2021). Borders within europe. Technical report, National Bureau of Economic Research. [53](#)
- Vickerman, R. (2007). Cost-benefit analysis and large-scale infrastructure projects: State of the art and challenges. *Environment and Planning B: Planning and Design*, 34(4):598–610. [5](#), [11](#), [47](#)
- Wardman, M., Neki, K., and Humphreys, R. M. (2023). Meta-analysis of the value of travel time savings in low-and middle-income countries. [5](#)
- Zhang, X., Hu, Y., and Lin, Y. (2020). The influence of highway on local economy: Evidence from china’s yangtze river delta region. *Journal of Transport Geography*, 82:102600. [6](#), [47](#)